TÉCNICO LISBOA

Optimal design and economic analysis of a grid-connected PV systems, operating under Net Metering or Feed-In-Tariff support mechanisms – case study of a warehouse in Poland.

Ryszard Górnowicz

Thesis to obtain the Master of Science Degree in

Energy Engineering and Management

Supervisor: Prof. Rui Castro

Examination Committee

Chairperson: Prof. Duarte de Mesquita e Sousa

Supervisor: Prof. Rui Manuel Gameiro de Castro

Members of Committee: Prof. João Filipe Pereira Fernandes

December 2019

I declare that this document is an original work of my own authorship and that it fulfils all the requirements of the Code of Conduct and Good Practices of the *Universidade de Lisboa*.

Acknowledgements

I would like to truly thank my supervisor, Prof. Rui Castro, under whose supervision I have undertaken this thesis. Without his advice, guidance and support it would have been difficult to give shape to this work.

I would also like to express a special gratitude to all the lecturers, programme coordinators and staff of Instituto Superior Técnico in Lisbon, Silesian University of Technology in Gliwice and InnoEnergy Master' school for providing me with the unique experience of undertaking the double-degree master programme, and developing the highly valued and in-demand skills and knowledge in the field of sustainable energy and energy engineering. The last two years were truly invaluable and unforgettable experience for me.

Finally, I would like to thank my family and friends who have always supported me during this time and in all my endeavours.

Abstract

The thesis focuses on cost effective design of the grid-connected rooftop photovoltaic (PV) system. The work is based on the case study of a warehouse located in Poland. The work aims to find the optimal system configuration, indicated by the highest Net Present Value (NPV) of an investment, for the scenario of Net-Metering (NM) and Feed-In-Tariff (FIT) support mechanisms. PVsyst software was used to simulate performance of various system sizes, tilts of the modules, as well as types and capacities of PV panels and inverters. Financial analysis was performed for each variant, by treating PV generation data in economic evaluation model. Since the benefits of a PV system derive from minimization of electricity imports from the grid, it was necessary to determine the building's electricity demand, using the bottom-up method. Preliminary analysis, based on generic components, allowed to estimate the optimal size of the system. Detailed simulations of the selected modules and inverters were later conducted in the specified ranges. Results of the simulation showed that the support mechanism has a substantial impact on the optimal size of the installation. For the analysed case, the system capacity optimized for NM was nearly twice bigger, than for FIT one. Comparing installations with the same nominal powers, the NM support system proves to be more beneficial than FIT, as it generates significantly larger NPVs. The sensitivity analysis showed that the three parameters most affecting the NPV of the systems studied were: electricity prices, the building's electricity demand and capital expenditures.

Keywords

Economic assessment, Electricity demand estimation, Feed-In-Tariff, Net-Metering, Net Present Value PV design optimization

Resumo

A tese foca-se no projeto técnico-económico de um sistema fotovoltaico ligado à rede, instalado no telhado de um armazém, na Polónia. O trabalho visa encontrar a configuração ideal do sistema fotovoltaico, avaliada através do Valor Atual Líquido (VAL), para dois cenários, baseando o sistema em tarifas bonificadas ou *net-metering* . O software PVsyst foi usado para simular o desempenho de sistemas com várias dimensões, inclinações dos módulos, bem como tipos e capacidades de painéis e inversores fotovoltaicos. Para cada opção estudada, os dados de geração fotovoltaica foram incluídos no modelo de avaliação económica. As curvas de consumo electrico do edifício foram estimadas usando um método *bottom-up*, uma vez que os benefícios de um sistema fotovoltaico derivam da minimização das importações de eletricidade da rede. A análise preliminar, baseada em componentes genéricos, permitiu estimar a faixa onde a dimensão ideal do sistema se situaria. Simulações detalhadas dos módulos e inversores selecionados foram posteriormente conduzidas nas faixas especificadas pela análise preliminar. Os resultados da simulação mostraram que o mecanismo de suporte tem um impacto substancial na dimensão ideal da instalação. Para o caso analisado, o sistema otimizado para *net-metering* tem uma dimensão quase duas vezes maior. Comparando instalações com as mesmas potências nominais, o sistema de suporte *net-metering* mostra-se mais benéfico do que a tarifa bonificada, pois gera VALs significativamente maiores. A análise de sensibilidade mostrou que os três parâmetros que mais afetam o VAL dos sistemas estudados foram: preços da eletricidade, procura de eletricidade do edifício e investimento.

Palavras-chave

Avaliação econômica, Estimativa de consumo eletrico, Medição de rede, Otimização do projeto fotovoltaico, Valor presente líquido, Tarifa de alimentação

Table of Contents

Acknowledgements v
Abstract vii
Resumo ix
Table of Contents xi
List of Figures xiii
List of Tables xiv
List of Symbols xv
List of Software xvii
1 Introduction 1
1.1 Motivation 2
1.2 Aims and methodology outline 3
1.3 Thesis structure 4
2 Literature overview 5
3 Renewable energy in Poland 10
3.1 Analysis of the current energy system structure 11
3.2 Legislation and perspectives 12
3.3 Electricity prices and average cost of the PV system 13
4 Theoretical background and methodology 15
4.1 Solar geometry 16
4.2 Electricity demand and load profiles estimation method 17
4.3 Irradiation calculation method 17
4.3.1 Transposition model 18
4.3.2 Determination of a shading loss 19
4.4 PV module calculation method 20
4.5 PV string sizing method 22
4.6 Economic assessment 24
4.6.1 Description of the model for economic assessment 25
5 Case study – background and preliminary analysis 29
5.1 Site analysis 30
5.1.1 Location 30
5.1.2 Meteorological data 30
5.1.3 Building parameters 31
5.1.4 Far and near shading 32
5.2 Building's electricity demand 32
5.2.1 List of appliances and their use 32

5.2.2 Load profiles 33
5.3 Preliminary design 38
5.3.1 Optimal tilt 39
5.3.2 Source of energy to cover the demand 40
5.3.3 NPV and IRR vs. PV system capacity 41
5.3.4 Annual cost structure 42
5.4 Components selection 43
5.4.1 PV modules 43
5.4.2 Inverters 44
5.5 Specific design 45
5.5.1 Effects of snow cover on soiling loss and albedo 45
6 Results and discussion 46
6.1 Results of the detailed simulations conducted in the ranges from the preliminary design 47
6.1.1 Results for the system ranges working under the NM 47
6.1.2 Results for the system ranges working under the FIT 49
6.2 Optimal system for the NM support mechanism 51
6.3 Optimal system for the FIT support mechanism 54
6.4 Comparison of energy profiles 57
6.5 Comparison of produced and consumed energy 59
6.6 Comparison of cashflows and discounted payback time 60
6.7 Sensitivity analysis 61
6.7.1 Sensitivity analysis of the system optimised for NM 61
6.7.2 Sensitivity analysis of the system optimised for FIT 63
7 Conclusions and recommendations 65
References 68
Annex 72
A.1 Full characteristics of selected PV modules and inverters 73
A.2 Visualization of the shadding simulations 75
A.3 PV systems layout on the building's roof 76
A.4 PV systems simple diagrams 77

List of Figures

Figure 1.1 Methodology outline 3
Figure 3.1 Share of installed capacities in the Polish energy mix, based on data for 2018. 11
Figure 3.2 Average price for a crystalline silicon PV system in a capacity range of 10-50 kWp. 14
Figure 4.1. Solar angles 16
Figure 4.2 Equivalent circuit of a 1-diode 5-parameter model. 20
Figure 5.1 Site location. 30
Figure 5.2 Site visualization 31
Figure 5.3 Average daily electricity consumption – profiles of all months 36
Figure 5.4 Monthly average hourly power demand – selected months 36
Figure 5.5 Annual average hourly power demand by building section 37
Figure 5.6 Annual average hourly power demand by appliance type 37
Figure 5.7 Average daily electricity demand 38
Figure 5.8 Optimal tilt of the PV panes 39
Figure 5.9 Breakdown of energy sources covering up the demand vs. system capacities - FIT 40
Figure 5.10 Breakdown of energy sources covering up the demand vs. system capacities – NM 40
Figure 5.11 NPVs of various PV system's capacities and support models 41
Figure 5.12 IRRs of various PV system's capacities and support models 41
Figure 5.13 Annual cost structure of different PV system capacities – case of NM 42
Figure 5.14 Annual cost structure of different PV system capacities – case of FIT 43
Figure 6.1 NPV vs. system capacities - for NM support scheme 47
Figure 6.2 IRR vs. system capacities - for NM support scheme 48
Figure 6.3 DPP vs. system capacities - for NM support scheme 48
Figure 6.4 LCOE vs. system capacities - for NM support scheme 49
Figure 6.5 NPV vs. system capacities - for FIT support scheme 49
Figure 6.6 IRR vs. system capacities - for FIT support scheme 50
Figure 6.7 DPP vs. system capacities - for FIT support scheme 50
Figure 6.8 LCOE vs. system capacities - for FIT support scheme 51
Figure 6.9 Monthly values of electricity balances – NM 53
Figure 6.10 Monthly normalized production per installed kWp for and a temperature - NM 53
Figure 6.11 Performance Ratio - NM 54
Figure 6.12 Monthly values of electricity balances - FIT 56
Figure 6.13 Monthly normalized production per installed kWp for and a temperature 57
Figure 6.14 Performance Ratio - FIT 57
Figure 6.15 Energy profile of the facility - NM 58
Figure 6.16 Energy profile of the facility – FIT 58
Figure 6.17 Comparison of the energy produced from the PV system during 25 years of operation 59
Figure 6.18 Comparison of the energy consumption during 25 years of operation 59
Figure 6.19 Cashflows for the PV system optimised for NM 60
Figure 6.20 Cashflows for the PV system optimised for FIT 60
Figure 6.21 Sensitivity analysis on NPV for the system optimised for NM 61
Figure 6.22 Sensitivity analysis on DPP for the system optimised for NM 62
Figure 6.23 Sensitivity analysis on NPV for the system optimised for FIT 63
Figure 6.24 Sensitivity analysis on DPP for the system optimised for FIT 63
Figure A.2.1 Visualization of shading for the system optimized for NM 75
Figure A.3.1 Top view with dimensions of the PV system optimized for NM 76

List of Tables

Table 3.1 Breakdown of electricity costs for a C11 tariff plan 13
Table 5.1 Monthly weather data values for the city of Miszewo 31
Table 5.2 List and specification of electrical appliances 33
Table 5.3 Part of a load demand table for an average working day in April 35
Table 5.4 Shortened characteristics of the selected PV panels 44
Table 5.5 Shortened characteristics of the selected inverters 44
Table 5.6 Monthly values of albedo and soiling from snow 45
Table 6.1 Optimal PV system for NM support scheme - Configuration 51
Table 6.2 Optimal PV system for NM support scheme – Performance results 52
Table 6.3 Optimal PV system for FIT support scheme - Configuration 55
Table 6.4 Optimal PV system for FIT support scheme -- Performance results 56
Table A.1.1 Full characteristics of the selected PV panels 73
Table A.1.2 Full characteristics of the selected inverters 74

List of Symbols

α_s	solar altitude angle, °
β	tilt of the PV module, °
γ	surface azimuth angle, °
γ_s	solar azimuth angle, °
δ	declination, °
δs	ground reflexion factor
η	rated efficiency of the PV modules, %
θ	angle of incidence, °
θ_z	zenith angle, °
$\mu_{(Isc)}$	short-circuit current temperature coefficient, A/°C
$\mu_{(Voc)}$	open-circuit voltage temperature coefficient, V/°C
ω	hour angle, °
a	ideality factor
A	generator area of the PV module, m^2
AM	air mass
CAPEX	capital expenditures, EUR
C_{bos}	balance of system cost per installed Wp of the PV system, EUR/Wp
$c_{e.save,n}$	annual mitigated cost of electricity purchase in the n^{th} year, EUR
c_{gross}	gross investment cost per installed Wp of the PV system, EUR/Wp
c_{inst}	installation cost per installed Wp of the PV system , EUR/Wp
c_{inv}	inverter cost per installed Wp of the PV system, EUR/Wp
G_{Tb}	bream component of irradiance on a tilted plane, W/m^2
G_{Td}	diffuse component of irradiance on a tilted plane, W/m^2
G_{Tr}	reflexion component of irradiance on a tilted plane, W/m^2
H	average solar irradiation, kWh/m^2
I	current supplied by the PV module, A
I_0	reverse saturation current, A
I_D	diode current, A
$I_{e.sold,n}$	annual income from the sold surplus electricity in the n^{th} year, EUR
I_L	photocurrent, A
I_{mp}	current at maximum power point, A
IRR	Internal Rate of Return, %
I_{sc}	shotr-circuit current, A
k	Boltzmann's constant = 1.381×10^{-23}, J/K
LCOE	Levelized Cost of Electricity, EUR/MWh
n	year of the investment
N	lifetime of the project, years
NM	Net Metering
N_{max}	maximum number of modules in a series
N_{min}	minimum number of modules in a series
NPV	Net Present Value, EUR
O&M	operation and maintanance

C_{inv}	cost of the inverter, EUR
c_{mount}	mounting structure cost per installed Wp of the PV system, EUR/Wp
$c_{pur,n}$	annual cost of electricity purchased in the n^{th} year, EUR
c_{PV}	PV panels cost per installed Wp of the PV system, EUR/Wp
c_{trans}	transportation cost per installed Wp of the PV system, EUR/Wp
D	annual degradation factor, %/year
DPP	Discounted Payback Period, years
$E_{avail,n}$	annual amount of available electricity from the PV system in the n^{th} year, kWh/year
$E_{consPV,n}$	annual amount of electricity consumed from the PV system by the user in the n^{th} year, kWh/year
$E_{dem,n}$	annual electricity demand at n^{th} year ,kWh/year
E_g	material's energy bandgap, eV
$E_{inj,n}$	annual amount of electricity injected to the grid in the n^{th} year, kWh/year
$E_{pur,n}$	annual amount of purchased electricity in the n^{th} year ,kWh/year
$E_{rec,n}$	annual amount of electricity recovered from the grid in the n^{th} year ,kWh/year
FIT	Feed-In-Tariff
G	global irradiance on a horizontal plane, W/m^2
G_b	bream component of irradiance on a horizontal plane, W/m^2
G_d	diffuse component of irradiance on a horizontal plane, W/m^2
G_{eff}	effective irradiance on a tilted plane, W/m^2
G_r	reflexion component of irradiance on a horizontal plane, W/m^2
G_{ref}	reference incidence irradiance, 1000 W/m^2
G_T	global irradiance on a tilted plane, W/m^2
OPEX	operating expenditures, EUR
P	generated power, W
$p_{e.pur,fix}$	fixed price of the electricity, EUR/kWh
$p_{e.pur,var}$	variable price of the electricity, EUR/kWh
$p_{e.sold}$	price at which the grid operator buys the surplus electricity, EUR/kWh
PR	performance ratio
PV_{cap}	installed capacity of the PV system, Wp
q	charge of the electron = 1.602×10^{-19} ,C
r	discount rate, %
R_b	geometric factor
R_s	series resistance, Ω
R_{sh}	shunt resistance, Ω
T	ambient temperature
$tax_{e.sold}$	income tax on the sold surplus of electricity, %
T_c	cell temperature, K
V	voltage at the terminals of the PV module, V
$V_{invDC,max}$	maximum input DC voltage of the inverter, V
$V_{invDC,min}$	minimum input DC voltage of the inverter, V
$V_{invMPP,max}$	maximum MPP tracking voltage of the inverter, V
$V_{invMPP,min}$	minimum MPP tracking voltage of the inverter, V
V_{mp}	voltage at maximum power point, V
V_{oc}	open-cicruit voltage, V

List of Software

Meteonorm 7.1	for acquiring the weather data
SkechUp Pro	for building a 3D model of the building and the environment
PV*SOL premium 2019	for simulating shading on the PV field
PVSyst v6.79	for simulating PV performance and detailed sizing

Chapter 1

Introduction

This chapter present author’s motivation for undertaking the topic of this thesis, as well as gives a brief overview of the aims and scope of the work.

1.1 Motivation

Human society faces major challenges to keep up with the growing need for energy, and it finally became obvious to the world's governors that necessity for the major transitions in the global energy sector is undeniable. According the World Energy Outlook 2018, published by the International Energy Agency (IEA), and the model of New Policies Scenario, it is predicted that the energy demand will increase by at least 25% in the next 20 years, requesting more than 2 trillion EUR each year to finance the necessary investments in the new energy supply, as well as the reinforcement of the energy transportation and distribution of the electric system [1].

At the forefront of this transition are renewable energy technologies, which are by far the fastest growing energy sector. Their development is accelerated by four key factors: growing energy demand caused by the population growth and improving living standards, obligations to reduce the greenhouse gases emissions which are contributing to the climate change, the need for diversification of energy sources in a view of scarcity of resources, and finally by most countries' urge for limiting their dependency on fossil fuel imports [2].

One of the energy sources that seems particularly appealing is solar energy. On average, solar power reaching the earth's surface is of about 90 000 TW. It has been estimated that out of it around 1000TW is technically recoverable. In comparison, current global energy consumption is of roughly 18 TWh and in 2050 it is predicted to reach about 30 TWh [3]. This makes solar a virtually limitless energy resource, which offers reliable energy production with low embodied carbon emissions. It cannot be seen though as a cure-all solution that will resolve the globe's energy demand on its own, but it certainly has a potential to make a significant contribution together with other RES as a part of a low carbon mix of energy sources. Even though energy generated from the sun radiation is intermittent, as it fluctuates with cloud cover, solar declination and elevation, there is a strong connection between generation from the solar energy and the commercial energy use. In most regions, the peak of solar-based energy output falls in the middle of the regular business opening hours.

Construction of the grid-tie solar photovoltaic systems may be seen like a simple job. The system is composed of a number of photovoltaic modules, that are connected to an inverter, which is later linked to a building's electrical grid through a switchgear and energy meter. Regardless of this apparent straightforwardness, designing a PV generation system that is efficient, reliable, safe in operation, compliant with the regulations and economically optimized is a complex and not always well executed task [4]. Simulating correctly the performance of the PV system requires employing a number of inter-related models, such as the ones describing solar geometry, estimating available solar radiation, computing electrical properties of a solar cell and an inverter. Frequently, external data, like historic meteorological data, information from the manufacturer's datasheets must be combined with the above mentioned algorithms. The amount of input, general complexity and level of uncertainty in each of the models, may influence the accuracy of the calculations, and for this reason a thorough analysis should be made to avoid false conclusions. Moreover, due to this reason, selection of the equipment should be based on a multi-criteria evaluation of all key parameters, e.g. price, performance, warranty conditions,

aesthetics. It is important to carry out all the design steps with precision and sufficient detailedness, in order to unlock the full potential of the technology and minimise the investment risk for the system owner.

The author's personal motivations for this work were to increase his knowledge on solar PV technology, and get familiarised with the design procedures as well as the commercially used software, in order to become more proficient and prepared for professional challenges in this field.

1.2 Aims and methodology outline

Decarbonization of a built environment in a cost effective manner is a complex challenge, that many of the public and private investors are confronting when planning to equip their buildings with renewable energy technologies. As the answer to this problem, this master thesis aims to:

- simulate various grid connected PV generation system capacities, tilts of the panels as well as the types and sizes of PV panels and inverters for a warehouse based in Poland,
- find the optimal system configuration, which returns the highest financial benefit, expressed by the Net Present Value (NPV) of an investment,
- investigate how the optimal configuration changes, depending on the direction in which Polish regulations regarding support mechanism of micro-PV systems will change. The two possible regulatory outcomes are either the continuation of the Feed-In-Tariff support model or the adoption of a new Net-Metering support mechanism.

The results and conclusions from this work are hoped to serve as a guidance and a decision support framework for evaluating this technological investment.

Visualization of the methodology framework is illustrated by the figure 1.1

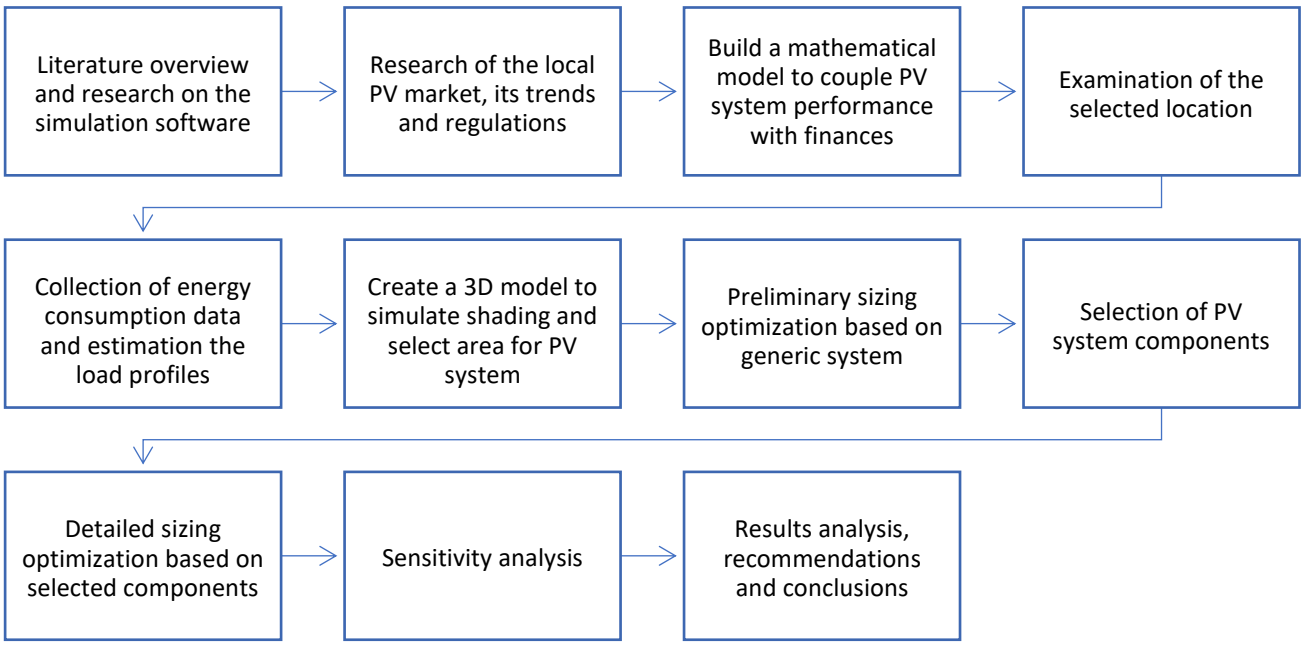

Figure 1.1 Methodology outline

The thesis will begin by reviewing the previous works, methods and models connected to designing and simulating the performance of PV systems. Alongside, a study of the necessary simulation software will be done. To understand better the context, research of the market and local regulations will be performed later. In order to find the optimal configuration of the PV system, a model coupling PV performance with economics will be created.

Once it is done, an investigation of the analysed location will begin, which would include finding meteorological data for the region, properties of the building and estimation of its electricity needs. The next step of the is the local vision, based on which a 3D model of the facility and its surrounding will be constructed for simulations of shading.

Next, a preliminary study will be conducted, in which by simulating the performance of generic components, estimation of the optimal capacity, for two possible policy scenarios, will be made. Afterwards, selected PV modules and inverters will be used in detailed modelling of the system. Results of those simulations will indicate the configuration of the PV generation system, optimized for each of the regulatory support mechanisms.

By the end of the thesis, results of the optimization will be subjected to a sensitivity analysis. Lastly, a chapter summarizing the work, obtained results and conclusions will be produced.

1.3 Thesis structure

The following work consists of 7 chapters. The introductory chapter is followed by the 2nd chapter, which presents a review of the literature related to PV installations. It addresses topics such as estimation of building's electricity demand, assessment of economic attractiveness, approaches to optimize a PV system, and the impact of snow cover on the performance of the PV modules. The 3rd chapter gives an overview of the situation of renewable energy in Poland and discusses the current legislation, as well as the perspectives regarding support mechanism of micro-PV installations. The chapter also presents the breakdown of electricity process and the average costs of the grid-tie PV generation system on the Polish market. The 4th chapter describes the theoretical issues related to solar energy, physical models, and methods used to simulate the work of the PV system and evaluate its economic performance. At the beginning of the 5th chapter background information about the studied facility and its location is presented. The chapter also includes a preliminary analysis that discusses appraising of the building's electricity demand and load profiles, optimization of PV modules tilt, and estimation of the system's optimal size. Lastly in this chapter, components selection and assumptions for the specific simulations are covered. Chapter 6th presents results of detailed simulations of all selected modules and inverters and highlights the optimal configurations of the PV generation systems for both Net-Metering and Feed-In-Tariff support mechanisms. The chapter describes in details the performance of both optimal systems and presents their parallel comparison. Lastly, 7th chapter summarizes the thesis and draws conclusions, and recommendations for the future actions.

Chapter 2

Literature overview

The second chapter presents a review of the literature related to PV installations. It addresses issues such as estimation of building's electricity demand, assessment of economic attractiveness, optimization methods of the PV system, and the impact of snow cover on the performance of the PV modules.

In the recent years, investments in a grid-connected, rooftop PV systems, which are meant to reduce building's electricity imports from the grid, are booming. Such systems generate their value from the displacement of electrical energy or sales of the surplus generated electricity. Thus, to assess the financial attractiveness of the PV installation, it is necessary to estimate the current and future electricity demand of the examined building, which can be a challenging task. Provided that the building is already in operation and has a building management system or is equipped with the smart metering devices, the task of finding the electrical load should in principle be easier, as the electricity consumption data can be accessed easily. Several methods addressing modelling and predicting the electricity load profiles in such cases can be found in the literature. Barak and Sadegh [5] treat all analysed buildings as a black-box, and based on their present energy consumption profiles they forecast the future demand by applying artificial intelligence algorithms. Gruber et al. [6] describe how a residential energy consumption can predicted by combining data recorded by smart-metering devices with a statistical forecasting methods. Even though very precise, the above mentioned sophisticated methods require access to the electricity consumption data, which unfortunately is very often scarce or not available at all. In case of the absence of such system, present energy bills can be used to assess the energy needs and produce an estimate of daily electricity consumption. However, if the building has not yet been constructed, which is a case of this work, the task of estimating the electricity demand becomes more challenging. This is due to the incomplete and imperfect information regarding the electrical equipment that is going the be used in the building, as well as the unknown work and behaviour patterns of the building users. To answer this problem, the literature points out that the most common method of estimating the load profiles, when the consumption data is not accessible, is the bottom-up approach. The study of Chuan et al. [7] describes this method, in which facility's load is estimated based on a detailed list of electrical appliances, their electrical requirements and the consumption patterns. Analysis done by Swan and Ugursal [8] indicate that in order to achieve a good accuracy of the model, an investigation of a behavioural patterns regarding the use of electrical devices is highly recommended. Such analysis can be done through personal interviews of specific questionnaire. Both Sepher et al. [9] and Paatero [10] compared the measured energy profiles with the ones estimated with the bottom-up approach, and suggested that this method proves to be the best choice when load profiles need to be modelled from scratch.

Since the photovoltaic system considered in this work is to be located in Poland, the impact of snow cover on the operation of photovoltaic modules has been reviewed. Heidari et al. [11] analysed how a snowfalls can influence the system's performance, and highlights the importance of taking into account seasonality of the weather, and in particular the effect of snowfall, when modelling the systems operating in cold climates. The study showed that the snow cover may significantly limit the solar radiation reaching the surface of the PV cells, which in turn results in dampening the electricity generation. On the other hand, Andenæs et al. [12] analyzed that due to the high reflectance of the snow, the reflected component of irradiance may increase, improving the performance of the photovoltaic system. Even a thin layer of snow pack will result in increasing the albedo - being the ratio of the amount of reflected irradiation to the amount of incidence irradiation – to the values between 0,7 and 0,9, in contrast to the standard 0,2 for the cases of no snow. In case the snow cover is present only on the ground, and the

PV panels are clear, the electricity generation is expected to be slightly bigger. The situation however changes dramatically when also the PV cells are cover in snow. According to the research done by Perovich [13] even the relatively slight snow cover will reduce the electricity generation form PV panels to nearly nothing. The study claims that the first 2 cm of snow sheet are the most impactful on soiling loss, as they may reduce the light transmittance by as much as 90%. A snow cover of 10 cm will block around 95% of visible light and 99% of infrared one, halting the PV electricity generation completely. Paper produced by Andrews et al. [14] argues that snow covers are also very problematic due to the potential shading of PV cells, which depending on the circumstances may be uniform or partial. The uniform shading caused also for instance by cloud coverage, will just slightly reduced the performance of the PV system. Partial shading is however much more critical to the operation of the PV system, as it triggers complex fluctuations in the balance of electric currents inside the conductive elements of the cells. Even though solar PV manufacturers put by-pass diodes in the electrical circuits linking individual cells to mitigate the impacts of partial shading, the performance of electricity generation can be greatly aggravated. Unfortunately, snowfall accumulation on the PV modules is greatly affected by the wind speeds, ambient temperatures, inclination from the horizontal, properties of the surface, as well as recently changing climate, making the modelling of the snow cover an extremely difficult task.

The leading issues faced by those who consider purchasing a PV system is the economic viability of such system. Over the last years number studies have been conducted to assess the financial attractiveness of equipping buildings with this technology. Orioli et al. [15] and Bernal-Augustin with Dufo-Lopez [16] studied the economic and environmental benefits of a grid-tied PV system using several financial indicators. Both suggested that the economic convenience of the PV system is best estimated by the means of a Net Present Value and a Discounted Payback Period. Their works analysed also the influences of different economic parameters, such as energy sale price, costs of initial investment and maintenance, as well as inflation on the profitability of the investment. Audenaert et al. [17] uses the cash flow projection method to evaluate the economic feasibility of investing in PV systems by companies, which are subjected to much higher corporate energy tariffs.

One of the factors that influence the economic viability of the investment are the regulations supporting development of the PV distributed generation systems. Dusonchet et al. [18],[19] presented an overview of main support policies in the European countries. The findings highlighted that the support models have a strong impact on profitability of the investments, however their efficiencies depends greatly on the details of each country's national law. Depending on the country, different regulations are in force. García-Álvarez et al. [20] analysed the energy policies promoting distributed PV in EU and indicated that Feed In Tariffs, which is the most predominant support mechanism in EU, under which 70% of the self-consumption PV systems operate, has a positive, but not significant impact on the development of this technology in the EU region. Poullikkas [21] made an comparative economic evaluation of the Net Metering (NM) and Feed-In-Tariff (FIT) support mechanism, and researched how the profitability of the system changes, depending on the installed capacity. The study points out that due to the grid storage option of NM, the optimal size of the installation will be bigger than for FIT. The comparison revealed that the NM support model is financially more appealing, than FIT for the PV owners. When analysing installations of the same capacity, study of Christoforidis et al. [22] shows that PV systems working

under NM achieve lower LCOE. Moreover, they are likely to generate higher savings, which leads to a quicker pay-off, than the system operating under FIT mechanism. The study concludes that the type of support mechanism has a significant impact on profitability of the system. A review of the international support policies, done by Pereira da Silva et al. [23], highlighted that however the NM policy may support best the ones owning the PV systems, the model is not flawless. Due to the larger optimal sizes of the PV installations and the possibility of storing surplus electricity produced in the power grid, the systems working in the NM model will have lower net energy imports from the grid, and consequently lower transmission fees. This in turn means, that the growing grid costs will buried mostly by the non-photovoltaic consumers.

The gains of having a photovoltaic system result from the reduction of electricity imports from the grid or additionally from the sale of generated electricity surplus. Both benefits depend on the amount and coverage of electricity generated by solar modules in relation to the electricity demand in the building. For this reason, a notable volume of literature focuses on the optimization of production, system sizing and operating conditions of the system. Mehleri et al. [24] describes the optimal tilt angle and orientation of the fixed-tilted PV modules at the any given location. The approach taken in this study maximizes the amount of global solar irradiance reaching the PV cells. The same topic has been also studied by Rowlands et al. [25], though the approach was different. Optimal tilt angles were found in respect to the highest global solar irradiance and later in respect to the maximum revenue generated by the solar system. It has been noticed that those angle are not the same, implying that the highest output performance doesn't always go together with the highest economic benefit. While designing the system it is crucial to know which one is prioritized.

The big dilemma when designing a PV system is determining the distance between the rows. If the rows are too close, the losses from mutual shading may by significant. On the other hand, if the displacement of arrays is too big, the space of installation will be used inefficiently. Several approaches to this issue have been discussed in the literature. Malara et al. [26] describes a classical approach, which assumes that the PV array should deliver energy even on the shortest day of the year, which for the northern hemisphere is during the winter solstice. Using solar diagram pathways a minimum solar altitude angle is found, and using trigonometric relationships, row distance which does not cause any shading is calculated. This method is the most conservative and the least space-efficient. The more efficient version of this method, calculates the row spacing with the assumption, that during winter solstice the modules will receive 4h of sunshine around the noon, meaning there will be no mutual shading between 10AM and 2PM. Based on those assumptions Bany et al. [27] developed a series of equations calculating the optimal row distance of the modules that are mounted on the stepped height. Copper et al. [28] proposes to calculate the arrays spacing using a vector analysis method for a non-horizontal and non-ideally oriented installations. Castellano et al. [29] came up with a model that computes the optimum use of space by analysing together the impacts of mutual-shadowing for each hour of the year, forecasted PV production and energy demand of the building. Ioannou et al. [30] proposes a methodology that ties together row spacing, PV generated electricity, and financial performance to optimize the design in respect to the highest economic benefit.

Another difficulty is connected with an optimal sizing of the system. Mondol et al. [31] studied the optimal array and inverter sizes for the grid-connected systems. As a leading criterion the highest system output and system outputs per specific system cost were optimized. The study found that the optimal PV/inverter power ratio ranges from 1.1 to 1.3. Notton et al. [32] also researched the optimum PV/inverter sizing ratios, though maximizing the annual system's efficiency. Results were in line with the ones of Mondol et al.. Gong et al. [33] describe the optimization method of a large scale rooftop PV installation in which the nominal power of system is based on maximal utilization of PV produced energy and minimal electricity imports from the grid. The model proposed by Ren et al. [34] optimizes the capacity of the PV system operating under FIT with regard to the minimal annual cost of energy. The method accounts for the investment and maintenance costs, cost of electricity purchased from the grid and revenues for the energy injected to the grid. Finally, the model developed by Kornelakis et al. [35] used particle swarm optimization algorithm to define the optimal size of the grid-connected PV system in respect to the highest NPV of the system. The proposed methodology computes also the discounted payback time and the internal rate of return as additional economic parameters.

Chapter 3

Renewable energy in Poland

This chapter gives an overview of the situation of renewable energy in Poland. Current legislation, as well as the perspectives regarding support mechanism of micro-PV installations are discussed. The chapter also presents the breakdown of electricity process and the average costs of the grid-tie PV generation system on the Polish market.

3.1 Analysis of the current energy system structure

As can be seen on the Figure 3.1, Polish energy system still relies very strongly on fossil fuels. Based on a data from the Energy Regulatory Office [36] at the end of 2018, the total installed capacity in Polish power system equalled 45 GW, out of which 70% was based in coal fire power plants. The capacity of renewable energy installations connected to power grids was 8.7 GW. The largest share in the Polish renewable sector comes from wind energy, making for nearly 70% of renewable energy sources (RES) installed power. Second is hydropower energy with an installed capacity of 1 GW. Energy from biomass and biogas have similar contributions, of around 2%, to the national mix. The smallest share comes from solar energy. Total installed capacity of utility scale PV plants and individual micro-installations barely reaches 600 MW. In terms of the share in the electricity production, the numbers for solar are even less gracious, as its contribution is of 0.2%

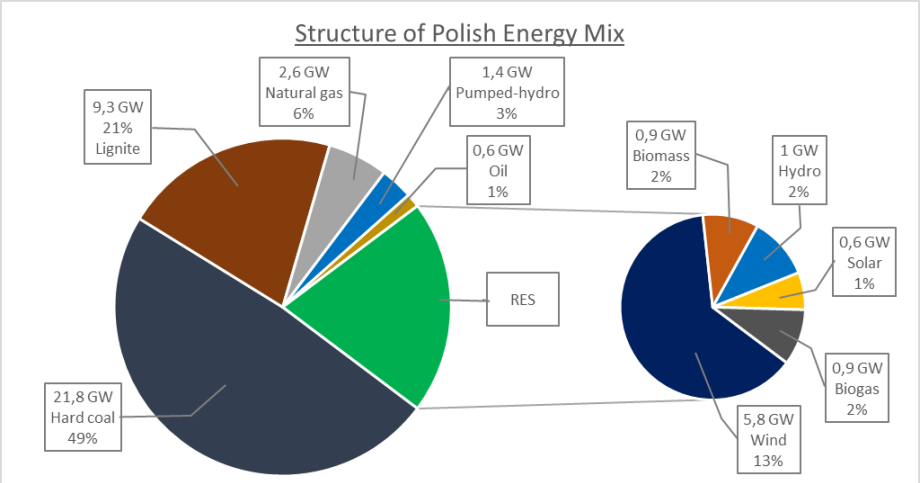

Figure 3.1 Share of installed capacities in the Polish energy mix, based on data [36] for 2018.

According to the think tank “Forum Energii”, the poor condition of RES in Polish market is owed to a very strong coal lobbies and low political will to expand the RES portfolio. At present, the prospect of support mechanisms for RES is determined only until the end of 2020. This is unfavourable for investment planning and is connected above all with the government's ad hoc activities aimed at Poland's fulfilment of EU commitments related to obtaining a 15% share of renewable energy in 2020 (including in the electricity, heating and transport sectors) in the national final consumption gross energy [37]. In the latest report of National Institute of Renewable Energy it is highlighted that the foremost difficulty for investors in solar sector is obtaining promise of financing. Banks see shortcomings of the legal environment in which renewable energy operates, they are: lack of a broader perspective in state policy, short-term and not always thought-out regulations, legal instability and growing legislative uncertainty. Without achieving the common sense of direction for RES, the banks will remain unwilling to take the risk of financing further projects planned for implementation [38].

3.2 Legislation and perspectives

In Poland, electricity produced from RES is promoted through several support mechanisms. The most important are tenders, organized in a form of a one stage bid format, that guarantee the tender's winner a minimum purchasing price for the next 15 years. Other support models for RES include net-metering, feed-in tariff and a feed-in premium, however the latter support is only suitable for small biogas and small hydro power plants technologies [39]. Polish government is also incentivizing producers of electricity from RES by tax exemptions on the sale and consumption of electricity [40]. Furthermore, a structure of low interest rate loans and subside mechanisms are offered by the National Fund for Environmental Protection and Water Management (NFOŚiGW) to support the purchase and mounting of RES installations.

In 2014, Polish government introduced into the national legislation a definition of a "prosumer", by whom are classified owners of micro-installations who are producing electricity from RES to cover their own needs, who import electricity from the grid when needed. At the same time, a support model for boosting investments of decentralized micro-PV installations was announced, under the same name – Prosumer. In 2016, Polish Ministry of Energy made an amendment on the "Act of Renewable Energy Sources from 20 February 2015", which is still valid today. The most important takes from the updated energy law provision, for the owners of micro-PV installations are [41]:

- A new definition of a micro-installations has been introduced: "a micro-installation is a system of renewable energy sources with a power capacity not grated than 50 kW, connected to the grid with a voltage power lower than 110 kV",
- The terms and conditions for accounting the electricity generated from RES have been changed to a **Net-Metering** support scheme. This means that owners of micro-installations are permitted to virtually store the surplus of produced energy and collect it later at the reduced amount. For the installations with the capacity up to 10 kWp, for each 1 kWh injected into the grid, the prosumer will receive 0,8 kWh. In case of the micro-installations between 10 and 50 kWp the ratio is 1 to 0.7. The injected surplus energy can be recovered from the grid within 365 days from the moment of injection – for example the energy injected on 1st of March 2020 can be recovered only until 1st of March 2021. Recovery of energy is done in a First In-First Out method.
- The connection to the grid of micro-installations with a capacity up to 50 kW is free of charge (Art. 3 No. 20b Energy Law, referring to RES-Act definitions),
- The subsidy for the purchase and installation of micro-RES installations from the National Fund for Environmental Protection and Water Management (NFOŚiGW) can cover up to 15% of the total investment. In case of micro-PV, the support can only be qualified if the cost of the system doesn't exceed 6000zł (1400EUR) per each installed kWp.
- The PROSUMENT programme and its benefits are available for single and multi-family houses, and housing co-operatives.

The last point is especially important, as due to the imposed restriction, the beneficiary group has been limited only to individual customers and housing communities. This means that from 2016, all of the

enterprises that wanted to install a PV system, with a capacity lower than 50kW, were not falling into the definition of the Prosumer. As a result they neither could use the system of net-metering for accounting the produced electricity, nor apply for the state subsidies and tax reliefs. According to the adopted amendment, entrepreneurs can at the moment count on **Feed-In-Tariff** support scheme, which allows them to sell the surplus electricity "at a price equal to 100% of the average electricity sales price on the competitive market in the previous quarter announced by the President of Energy Regulatory Office" [42]. This unthought energy law, has been condemned many times by state officials and public opinion. It is believed that this legal provision has significantly slowed down the pace of micro-PV systems development and installations in Poland.

However, according to the latest information released by the Polish Press Agency on 30th of May 2019, this situation will most likely change, as the Standing Committee of the Council of Ministers confirmed to fix the programme, by expanding the prosumer's status for small and medium-sized enterprises. This amendment will be of great importance, as it would enable them to use much more beneficial Net Metering support mechanism for accounting the surplus electricity from their PV systems. The amendments to the current law provision are expected to come into force around fall of 2019 [43].

3.3 Electricity prices and average cost of the PV system

For small and medium companies, Polish Distribution System Operators (DSO) offer an energy tariff called C11, which composes of various fixed and variable costs. For the studied facility, a DSO Energa S.A will be providing electricity and the breakdown of C11 tariff costs [44] is presented in the table 3.1:

Table 3.1 Breakdown of electricity costs for a C11 tariff plan [44]

Fixed costs	PLN/year	EUR/year
Transmission fee	137.40	32.71
Network fixed charge	95.94	22.84
Trade fee	65.42	15.58
Subscription fee	9.68	2.30
Sum of all fixed costs	**308.44**	**73.44**
Variable costs	PLN/kWh	EUR/kWh
Active energy	0.577	0.137
Network variable fee	0.217	0.052
Quality fee	0.083	0.020
Fee for RES development	0.052	0.012
Sum of all variable costs	**0.929**	**0.221**

One of the very important components of the preliminary design is cost estimation. Over the last years the prices of the components plunged significantly making the investments in micro-installations more accessible and financially appealing. According to the report of the German's Fraunhofer Institute the

average total cost of the PV system of a capacity between 10 and 50 kWp, based on the crystalline panels, ranges from 900 to 1100 €/kWp [45]. It is observed that this range is quite alike within European countries, with small variations resulting from different labour costs and contractor's margins. The below pie chart represents the average breakdown of cost for a Polish market. [46]

It can be seen from figure 3.2 that the cost of PV modules is the biggest expense, accounting for nearly half of the capital spending. Second biggest cost is associated with contractor's margin which covers the part of engineering, permitting and inspection. Cost of the inverter is around 1/3 of the PV modules price. Installation labour together with cost of support structure (racking) for PV modules, cost of electrical balance of the system (BOS) and transportation build up to around a quarter of the total investment cost.

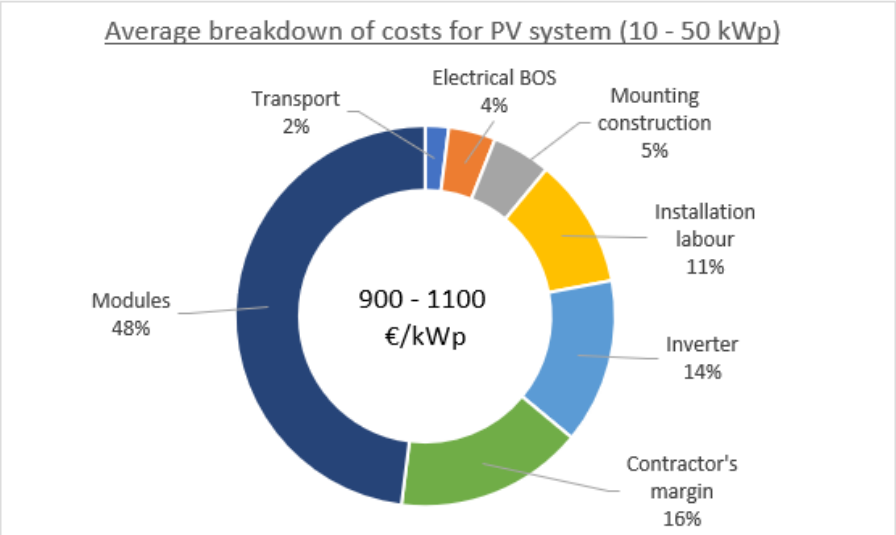

Figure 3.2 Average price for a crystalline silicon PV rooftop system in a capacity range of 10-50 kWp.

Chapter 4

Theoretical background and methodology

In order to design and analyse the performance of the PV generation system, a set of long and time-consuming calculations must be made. To perform the simulations in an efficient manner, commercially available software, namely PVsyst, will be utilized in this master thesis. To bring clarity to the work and obtained results, this chapter will describe in a concise way the theory, physical models that are implemented behind the mentioned software, and an economic evaluation model that was created by the author for the given study.

4.1 Solar geometry

As the Earth revolves around the Sun and rotates around its own axis, its position in respect to the Sun changes constantly. Consequently, for the observer standing on Earth, Sun's trajectory varies throughout the year. To define this dynamic relationship and precisely describe Sun's position at any time, a set of solar angles were introduced [47]. Most important of those include:

δ – Declination, being the angle between the sun's position at solar noon and the equatorial plane. The angle varies between $-23.45^\circ \leq \delta \leq 23.45^\circ$, and takes positive values towards north.

θ – Angle of incidence, is the angle among the beam radiation on the surface and the normal to that surface.

θ_z – Zenith angle, is the angle measured between the incidence of beam radiation on a horizontal surface and the vertical.

α_s – Solar altitude angle, is the angle measured between the incidence of beam radiation on a horizontal surface and the vertical. It is a complement of the zenith angle.

γ_s – Solar azimuth angle, the angular shift from the south of the projection of the beam radiation on the horizontal plane. Displacements west of south are positive and east of south are negative.

γ – Surface azimuth angle, is the angular displacement of the projection of the normal to the surface on a horizontal plane from the local meridian. Surface facing south is regarded as 0°, east takes negative, and west positive values; $-180^\circ \leq \gamma \leq 180^\circ$.

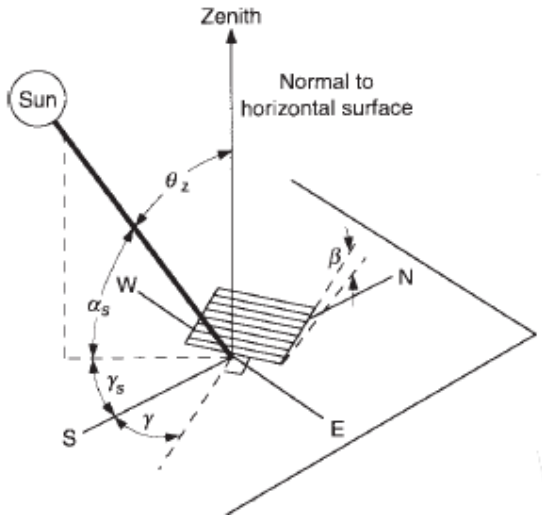

Figure 4.1. Solar angles [48]

β – Tilt, describes the angular relationship between the plane of the surface under study and the horizontal. $0^\circ \leq \beta \leq 180^\circ$. Values of $\beta > 90^\circ$ indicate that the surface faces downward.

ω – Hour angle, is the angular shift of the sun east or west from the local meridian because of the Earth's rotation around its axis. Each hour counts for 15°, and solar noon is respected as 0°. Morning hours take negative and afternoon hours positive values.

4.2 Electricity demand and load profiles estimation method

Prior to designing the PV generation system, the first thing one needs to do is determine the buildings electricity consumption. As the building is not yet in operation, a bottom-up method of estimating the demand and creating the load profiles has been adopted.

The first step in this approach is to create a detailed table with all the electrical appliances to be found in the facility. The table should contain types, quantities and power ratings of the electrical devices. A breakdown of electricity requirements should be made for those, which operating state – working or stand-by mode – vary.

The next step is to determine how frequently, at what hours and for how long the individual equipment is to be used. To gather this data and obtain a reasonable approximation, a series of interviews should be conducted with the users of the building. Once the data is collected, the individual electricity demands should then be placed on a 24-hour timeline, with 30 min or 1h timestep. In order to estimate the demand for the whole year, the timeline needs be expanded and, ideally, adjusted for each day of the year. However, due to the often incomplete and imperfect information regarding the electrical equipment that is going the be used in the building, as well as the randomness of work and behaviour patterns of the building users, the bottom-up method introduces a simplification, assuming that energy consumption of the individual days of the specific month does not differ significantly. This means that instead of modelling each day independently, a monthly estimates are conducted. As the building's electricity demand is assumed to be similar for the working days of the week an "average working day of the month" is created, for each month separately. Similarly, the consumption profile can be assumed similar through the weekends, resulting in the creation of an "average weekend day of the month". This results in modelling separately 12 average working days and 12 average weekend days – one of each per each month. By taking 5 times the average working day of the specific month and adding to it twice the average weekend day of the specific month weekly profiles are created. Monthly profiles are assembled from the weekly profile. This operation is later repeated for each month separately, enabling the production of a 24-hours energy demand timeline profile for each day of the year.

4.3 Irradiation calculation method

To simulate the performance of a tilted PV panels, it is necessary to know the effective incident irradiance G_{eff} that falls on the PV cells. The value is obtained in the following sequence [48]:

- First, the hourly values of horizontal global irradiance G (composed of beam G_b and diffuse G_d irradiances) expressed in W/m^2, are obtained from the available meteorological data,
- By using one of the transposition models, the horizontal irradiance data is transposed to the incident irradiance on a sloped plane. At this stage the plane irradiance consists of the beam G_{Tb}, diffuse G_{Td} and ground reflected G_{Tr} components,
- Next, the computed components are altered by the calculations of a near shading,

- Lastly, the values of irradiances are corrected by the Incidence Angle Modifier (IAM) factor, which corresponds to the decrease of irradiance reaching the PV cell due to the reflections on the module's glass cover. Typically, the loss due to reflection is of around 5%, however they are already included in the stated modules efficiency.

In this way an effective irradiance G_{eff} on the PV panel surface is computed, and with it a corresponding effective irradiation I_{eff} over a given time period, expressed in kWh/m^2.

4.3.1 Transposition model

To estimate the incidence irradiance on a tilted surface, PVsyst software utilizes a Perez transposition model [49]. The model assumes gains from three components - beam, diffuse and ground reflected (albedo) irradiance, and calculates them separately.

The computation of a beam component $G_{Tb,}$ involves just a pure geometrical transformation, using the geometric factor R_b, expressed by the below equality.

$$R_b = \frac{G_{Tb}}{G_b} = \frac{cos\theta}{cos\theta_z} \quad \text{(Eq.1)}$$

where:

R_b = geometric factor [-]

G_{Tb} = bream component of irradiance on a titled plane [W/m^2]

G_b = bream component of irradiance on a horizontal plane [W/m^2]

θ = incidence angle [°]

θ_z = zenith angle [°]

The diffuse irradiance is evaluated in the Perez model in details, dividing it into 3 sections.

$$G_{Td} = G_d \left[(1 - F_1) \left(\frac{1 + cos\beta}{2} \right) + F_1 \frac{a}{b} + F_2 sin\beta \right] \quad \text{(Eq.2)}$$

where:

G_{Td} = diffuse component of irradiance on a titled plane [W/m^2]

G_d = diffuse component of irradiance on a horizontal plane [W/m^2]

F_1, F_2 = brightness coefficients [-]

a, b = variables describing circumsolar diffuse [-]

β = tilt of the PV module [°]

First is the isotropic diffuse, which receives uniformly the irradiance from the sky domain. The second one is a circumsolar diffuse, which is concentrated around the sun and comes in form of a forward scattering of solar radiation. The last one is the diffuse received from around of the horizon. Variables *a* and *b* help descried the circumsolar diffuse and are defined as:

$$a = \max(0, cos\theta), \qquad b = \max(cos85, cos\theta_z) \quad \text{(Eq.3)}$$

F_1 and F_2 are empirically found brightness coefficients describing the sky conditions. They are dependent on the zenith angle θ_z, clearness of the sky and its brightness [50].

The last part of the Perez model is connected to ground reflectance component. As the inclined plane

has a view factor to the ground $F_{c\text{-}g}$ = (1-cosβ)/2, the irradiance reflected from the surrounding is computed by multiplying it by the ground reflexion factor ρ_g and the horizontal global irradiance G.

$$G_{Tr} = G\delta_s\left(\frac{1-cos\beta}{2}\right) \quad \text{(Eq.4)}$$

where:

G_{Tr} = reflexion component of irradiance on a titled plane [W/m^2]

G = global irradiance on a horizontal plane [W/m^2]

δ_s = ground reflexion factor [-]

The set of above equations combined together constitutes a working version of the Perez model. Using the below equation, allows to transpose the value of horizontal irradiance to the one reaching the surface tilted at any studied angle.

$$G_T = G_bR_b + \left[G_d(1-F_1)\left(\frac{1+cos\beta}{2}\right) + G_dF_1\frac{a}{b} + G_dF_2 sin\beta\right] + G\delta_s\left(\frac{1-cos\beta}{2}\right) \quad \text{(Eq.5)}$$

where:

G_T = global irradiance on a tilted plane [W/m^2]

4.3.2 Determination of a shading loss

Both PVsyst and PV*SOL treat individually the three irradiance components [49][51]:

- For the beam component, a shading factor, dependant on the sun position, is determined. The analysis is done in a purely geometric manner. For every hour, traces of visual shades are defined on the studied PV field. If they overlap the active surface of the module, a shading factor defined as the fraction of the shaded PV panel active area to its total area is defined,
- Determination of the shading loss on the diffuse component, is based on the assumption that the diffuse is isotropic, meaning that the PV cell receives irradiance from every direction of the sky. For this reason the diffuse shading factor is computed as an integral over the entire sky dome for every hour, and is independent on the sun's position,
- Shading loss on the ground reflexion component is determined through integrating the reflected irradiance from the obstacles that are near to the PV field. The computed shading factor is independent on the sun's position.

When applying those computations to the hourly simulations, two kinds of shading losses are observed. First is the linear shading loss, which is calculated from the above shading factors and treated as the attenuation of irradiance on the module. Due to this simplification, the linear loss give a rough reflection of effects of shading on the PV system. The second effect describes the losses in a much more sophisticated way, as it takes into account the electrical effects that occur in the shaded panel. Under the partial shading the output of PV module can be significantly reduced, as due to the uneven irradiance, its performance will be driven by the PV cell producing the lowest current. This impact can be reduce by the activation of a by-pass diodes that are inside the module. Since it requires a detailed 3D model of the location, exact placement of the PV panels and the accurate layout of their electrical system, calculation of the electrical shading losses are very complex and will not be calculated here.

4.4 PV cell calculation method

To simulate performance of the PV module, PVsyst uses a well-established 1-diode 5 parameter model, whose equivalent circuit is shown in figure 4.2 [49]. Assuming that the cells are identical, the model can be used to describe an individual cell, a full module, or an array composed of several modules [52].

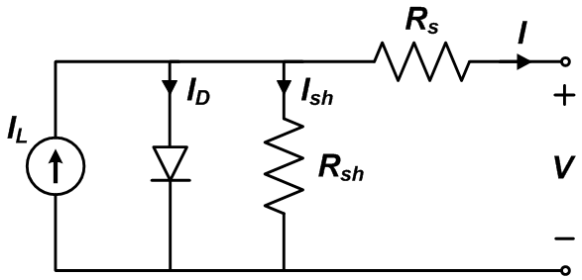

Figure 4.2 Equivalent circuit of a 1-diode 5-parameter model. Source: [48]

At a fixed solar irradiance and temperature, the I-V characteristic of the model is written as [53]:

$$I = I_L - I_D - I_{sh} = I_L - I_0 \left[exp\left(\frac{q(V + R_s I)}{akT} \right) - 1 \right] - \frac{V + R_s I}{R_{sh}} \quad \text{(Eq.6)}$$

where:

I = current supplied by the PV module [A]

I_L = photocurrent [A]

I_D = diode current [A]

I_0 = reverse saturation current [A]

V = voltage at the terminals of the PV cell [V]

R_s = series resistance [Ω]

R_{sh} = shunt resistance [Ω]

k = Boltzmann's constant = 1.381 x 10^{-23} [J/K]

q = charge of the electron = 1.602 x 10^{-19} [C]

T = cell temperature [K]

a = ideality factor [-]

All five parameters $I_L, I_0, R_s, R_{sh},$ and a are obtained through measurements and computations of voltage and current characteristics of a module at a reference conditions and data provided by the manufacturer, and are functions of either cell temperature of absorbed irradiation. Therefore, for any operating conditions, they will be determined with respect to their values in the reference state. Reference measurements are done in Standard Test Conditions (STC), in which reference incidence irradiance G_{ref} = 1000 W/m^2, reference cell temperature $T_{c,ref}$ = 25°C and the air mass AM = 1.5 [54].

To determine the 5 parameters, 5 different equations describing them must be solved. The method is to use 3 known points on the I-V curve – (0,V_{oc}), (I_{sc},0) and (I_{mp},V_{mp}) –, a condition at the MPP in which the derivative of power with regard to the voltage is equal to zero, and the open-circuit voltage temperature coefficient [47].

First one relates to the open-circuit condition, at which the current is zero and open circuit voltage is that

$$I_{L,ref} = I_{0,ref}\left[exp\left(\frac{V_{oc,ref}}{a_{ref}}\right) - 1\right] + \frac{V_{oc,ref}}{R_{sh,ref}} \quad \text{(Eq.7)}$$

where:

$V_{oc,ref}$ = open-circuit voltage at reference conditions [V]

Second condition describes the short-circuit current for the condition when voltage is zero.

$$I_{sc,ref} = I_{L,ref} - I_{0,ref}\left[exp\left(\frac{I_{sc,ref}R_{s,ref}}{a_{ref}}\right) - 1\right] - \frac{I_{sc,ref}R_{s,ref}}{R_{sh,ref}} \quad \text{(Eq.8)}$$

where:

$I_{sc,ref}$ = short-circuit current at reference conditions [A]

Next, measured reference values of current and voltage at the maximum power point can be substituted into the Equation 6, resulting in

$$I_{mp,ref} = I_{L,ref} - I_{0,ref}\left[exp\left(\frac{q\left(V_{mp,ref} + R_{s,ref}I_{mp,ref}\right)}{a_{ref}kT}\right) - 1\right] - \frac{V_{mp,ref} + R_{s,ref}I_{mp,ref}}{R_{sh,ref}} \quad \text{(Eq.9)}$$

where:

$I_{mp,ref}$ = maximum power point current at reference conditions [A]

$V_{mp,ref}$ = maximum power point voltage at reference conditions [V]

As the fourth equation, the derivative of power with respect to the voltage equal to zero is taken, so that:

$$\frac{I_{mp,ref}}{V_{mp,ref}} = \frac{\frac{I_{0,ref}}{a_{ref}}\, exp\left[\frac{q\left(V_{mp,ref} + R_{s,ref}I_{mp,ref}\right)}{a_{ref}kT}\right] + \frac{1}{R_{sh,ref}}}{1 + \frac{I_{0,ref}R_{s,ref}}{a_{ref}}\, exp\left[\frac{q\left(V_{mp,ref} + R_{s,ref}I_{mp,ref}\right)}{a_{ref}kT}\right] + \frac{R_{s,ref}}{R_{sh,ref}}} \quad \text{(Eq.10)}$$

The last condition regards the temperature coefficient of open-circuit voltage, resulting in:

$$\frac{\partial V_{oc}}{\partial T} = \mu_{Voc} \approx \frac{V_{oc}(T_C) - V_{oc}(T_{C,ref})}{T_C - T_{C,ref}} \quad \text{(Eq.11)}$$

where:

μ_{Voc} = open-circuit voltage temperature coefficient [V/°C]

The shunt resistance R_{sh} is regarded as independent of temperature, but changes with irradiance, as:

$$\frac{R_{sh}}{R_{sh,ref}} = \frac{G_{ref}}{G_{eff}} \quad \text{(Eq.12)}$$

where:

G_{eff} = effective irradiance on a tilted plane [W/m^2]

G_{ref} = reference incidence irradiance [W/m^2]

The series resistance R_s is found to be independent of both temperature and irradiance, so that:

$$R_s = R_{s,ref} \quad \text{(Eq.13)}$$

Ideality factor a on the other hand changes with temperature and is independent of irradiance, so that:

$$\frac{a}{a_{ref}} = \frac{T_C}{T_{C,ref}} \quad \text{(Eq.14)}$$

where:

$T_{C,ref}$ = reference cell temperature [°C]

T_C = actual cell temperature [°C]

In order to determine the values of the five parameters at their reference condition, the equations (from Eq. 7 to Eq.11) need be solved simultaneously, using numerical methods. Once finished, it is possible to calculate the remaining parameters of the model at any operating conditions.

One of them is the photocurrent I_L, which depends on the effective irradiance G_{eff} (obtained through the Perez transposition model), cell temperature T_c and a short-circuit current temperature coefficient.

$$I_L = \frac{G_{eff}}{G_{ref}}\left[I_{L,ref} + \mu_{Isc}\left(T_C - T_{C,ref}\right)\right] \quad \text{(Eq.15)}$$

where:

μ_{Isc} = short-circuit current temperature coefficient [A/°C]

T_C = actual cell temperature [°C]

$T_{C,ref}$ = reference cell temperature [°C]

Lastly, the dark saturation current can be determined I_0 with the below equation

$$I_0 = I_{0,ref}\left(\frac{T_C}{T_{C,ref}}\right)^3 exp\left(\frac{E_g}{kT}\Big|_{T_{C,ref}} - \frac{E_g}{kT}\Big|_{T_C}\right) \quad \text{(Eq.16)}$$

where:

E_g = material's energy bandgap [eV]

To compute it, it is necessary to additionally calculate a temperature dependant material's bandgap E_g. which is temperature dependent. For silicon cells the $E_{g,ref}$ = 1.12eV and C = 0.0002677.

$$E_g = E_{g,ref}\left[1 - C\left(T - T_{C,ref}\right)\right] \quad \text{(Eq.17)}$$

By substituting the results of the above calculations to the main equation of the model (Eq.6) it is possible to calculate the output current and voltage of the PV cell at any operating conditions. Knowing I and V is essential, as they enable the computation of the key parameter – the generated power output.

$$P = IV \quad \text{(Eq.18)}$$

where:

P = generated power [W]

4.5 PV string sizing method

When connecting PV panels to the inverter it is necessary to know the maximum and minimum number of modules that can be connected in series, which is often referred to as a string. As PV module's performance depend on temperature - they generate higher voltage in low temperatures and lower voltage in higher – it is crucial to size the sting in a way that it's working conditions will stay within the operating range of the inverter.

The first limit regards the maximum number of modules connected in series that would keep the maximum PV output voltage below the maximum operating inverter voltage. To test it, both the maximum open-circuit voltage V_{oc} and the MPP voltage V_{mp} are calculated for the lowest winter cell temperatures. Minimal cell temperature $T_{c,min}$ = -10°C is regarded as standard for the systems working in

the Northern Hemisphere [48]. Maximum values of V_{oc} and V_{mp} are given respectively as:

$$V_{oc,max} = V_{oc,ref}\left[1 + \left(T_{c,min} - T_{C,ref}\right)\mu_V\right] \quad \text{(Eq.19)}$$

$$V_{mp,max} = V_{mp,ref}\left[1 + \left(T_{c,min} - T_{C,ref}\right)\mu_V\right] \quad \text{(Eq.20)}$$

where:

μ_V = voltage temperature coefficient [V/°C]

$V_{oc,max}$ = maximum open-circuit voltage of the PV module [V]

$V_{mp,max}$ = maximum voltage at MPP of the PV module [V]

Next, the upper limits of the inverter's DC input voltage $V_{invDC,max}$ and MPPT tracking voltage $V_{invMPPT,max}$ are respectively divided by the values of $V_{oc,max}$ and $V_{mp,max}$, giving a maximum number of modules N_{max}

$$N_{max}(\mathrm{V}_{oc}) = \frac{V_{invDC,max}}{V_{oc,max}} \quad \text{(Eq.21)}$$

$$N_{max}(\mathrm{V}_{mp}) = \frac{V_{invMPPT,max}}{V_{mp,max}} \quad \text{(Eq.22)}$$

where:

$N_{max}(V_{oc})$ = maximum number of modules in a series, calculated for V_{oc} criterion [-]

$N_{max}(V_{mp})$ = maximum number of modules in a series, calculated for V_{mp} criterion [-]

$V_{invDC,max}$ = maximum input DC voltage of the inverter [V]

$V_{invMPPT,max}$ = maximum MPP tracking voltage of the inverter [V]

The maximum number of modules connected in series is the rounded down smaller value of N_{max}.

To compute the minimal string size of the system similar procedure is conducted for summer months. Here, the commonly assumed cell temperature is equal to $T_{c,max}$ = 60°C. Minimum values of minimum open circuit voltage $V_{oc,min}$ and MPP voltage $V_{mp,min}$ are respectively calculated as:

$$V_{oc,min} = V_{oc,ref}\left[1 + \left(T_{c,max} - T_{C,ref}\right)\mu_V\right] \quad \text{(Eq.23)}$$

$$V_{mp,min} = V_{mp,ref}\left[1 + \left(T_{c,max} - T_{C,ref}\right)\mu_V\right] \quad \text{(Eq.24)}$$

where:

$V_{oc,min}$ = minimum open-circuit voltage of the PV module [V]

$V_{mp,min}$ = minimum voltage at MPP of the PV module [V]

Here, the lower limits of the inverter's DC input voltage $V_{invDC,min}$ and MPPT tracking voltage $V_{invMPPT,min}$ are correspondingly divided by the computed values of $V_{oc,min}$ and $V_{mp,min}$, giving a least amount of modules connected in series N_{min}.

$$N_{min}(\mathrm{V}_{oc}) = \frac{V_{invDC,min}}{V_{oc,min}} \quad \text{(Eq.25)}$$

$$N_{min}(\mathrm{V}_{mp}) = \frac{V_{invMPPT,min}}{V_{mp,min}} \quad \text{(Eq.26)}$$

where:

$N_{min}(V_{oc})$ = minimum number of modules in a series, calculated for V_{oc} criterion [-]

$N_{min}(V_{mp})$ = minimum number of modules in a series, calculated for V_{mp} criterion [-]

$V_{invDC,min}$ = minimum input DC voltage of the inverter [V]

$V_{invMPPT,min}$ = minimum MPP tracking voltage of the inverter [V]

The difference is that here, the minimal string size, is found by rounding up the higher value of N_{min}.

4.6 Economic assessment

Solar projects can be optimized with regard to several different production indicators, such as amount of energy available from the rooftop PV system, self-consumption ratio, overall system efficiency, etc.. Yet, from the investor's point of view, most important is the economical attractiveness of the proposed project. For this reason, an economic assessment of each simulated PV system was made to evaluate the feasibility, and profitability of the system. Financial indicators used in this study include: Net Present Value (NPV), Internal Rate of Return (IRR), Discounted Payback Period (DPP) and Levelized Cost of Electricity (LCOE). To take into account the concept of time value of money – meaning that the money available at present moment is worth more than the same amount in the future, owing to its possible earning capacity – a discount rate will be applied to all the cash flows. This will enable to evaluate the present value of the project investment based on the forecasted future cash flows.

There are long debates in the literature of finance about which of the indicators, NPV or IRR, is superior for decision making properties, however most of the literature concludes the supremacy of the NPV [55]. Firstly, because the NPV undertakes that cash inflows will be reinvested at the assumed rate of return, while IRR assumes that inflows of cash will be reinvested at computed IRR. Reinvestment at the required rate of return turns to be more realistic and provides reliable results when comparing mutually exclusive projects. Secondly, if projects are mutually exclusive and different in size, which is a case of this thesis, then NPV is superior, as it selects the option that maximizes the value of the project [56],[57].

As the company is looking for the highest profitability of the investment, the key decisive indicator in this case will be the NPV, which it is a difference between a discounted present values of cash inflows and cash outflows calculated over the project's lifetime. During the project, the goal would be to find a system for which the NPV will be highest, as it translates to highest monetary benefit for the investor. The NPV measures profitability in an absolute manner and as a general rule, only the project with positive NPV should be undertaken [58].

To gain a better understanding of the profitability of the project, an IRR will also be calculated for each case. IRR is a discount rate that would make NPV equal to zero, and is a projection of the rate of growth the project will generate [59]. IRR takes into account the time value of money, and the higher the value of it is, the more desirable the case is. It is important to use IRR in conjunction with NPV, as alone the results may be misleading. For example an investment can have a low IRR and high NPV, which means that although the rate of return is slower, the added monetary value at the end of the project's lifetime will be bigger [58].

DPP is the measure that indicated how long it would take to recover the initial capital expenditure from the present value of the anticipated future cash flows. The shorter the recovery time, the more feasible and attractive the project is. Only projects which DPP is lower than their lifetime should be accepted.

The last parameter to be calculated is the LCOE, which can be defined as discounted lifetime cost of an investment and system operation, divided by produced electricity. LCOE is usually expressed in €/MWh and will be used to compare with each other the simulated system variants [60].

4.6.1 Description of the model for economic assessment

To start with, it is essential to list all the components that build up the investment cost. A common practice is to calculate the gross investment cost per installed Wp of the PV system, as it is the key information needed when applying for the governmental subsidies. It is defined as:

$$c_{gross} = c_{PV} + c_{inv} + c_{inst} + c_{mount} + c_{BOS} + c_{trans} \quad \text{(Eq.27)}$$

where:

c_{gross} = gross investment cost per installed Wp of the PV system [EUR/Wp]
c_{PV} = PV panels cost per installed Wp of the PV system [EUR/Wp]
c_{inv} = inverter cost per installed Wp of the PV system [EUR/Wp]
c_{inst} = installation cost per installed Wp of the PV system [EUR/Wp]
c_{mount} = mounting structure cost per installed Wp of the PV system [EUR/Wp]
c_{BOS} = balance of system cost per installed Wp of the PV system [EUR/Wp]
c_{trans} = transportation cost per installed Wp of the PV system [EUR/Wp]

The amount of the subsidy for the PV system may cover up to 15% of the total investment, with the provision that subsidies will be granted only up to the gross investment cost per Wp equal to 1.4 EUR/Wp [42]. The amount is calculated as:

$$Subsidy = \begin{cases} 15\% \times c_{gross} \times PV_{cap} & if \quad c_{gross} \leq 1.4\, EUR/Wp \\ 15\% \times 1.4 \times PV_{cap} & if \quad c_{gross} > 1.4\, EUR/Wp \end{cases} \quad \text{(Eq.28)}$$

where:

PV_{cap} = installed capacity of the PV system [Wp]

After knowing the amount of subsidy that the system is entitled for, the actual capital expenditures (CAPEX) are calculated according to the formula:

$$CAPEX = PV_{cap} \times (c_{PV} + c_{inst} + c_{mount} + c_{BOS} + c_{trans}) + C_{inv} - Subsidy \quad \text{(Eq.29)}$$

where:

C_{inv} = cost of the inverter(s) [EUR]

Annual operating expenditures (OPEX), that include the costs of regular operation and maintenance (O&M) of the equipment, can be approximately accounted for 1% of the CAPEX [61]. However, as the expected lifetime of a string inverter is of 10-15 years [62], the cost of the OPEX will vary depending on the year. For this study, the worst case was assumed, requiring the replacement on the every 10th year. The cost of operating expenditures in the nth year – $OPEX_n$ – is given as:

$$OPEX_n = \begin{cases} 1\% \times CAPEX & for\ years\ form\ 1st\ to\ 25th\ excluding\ 10th\ and\ 20th \\ 1\% \times CAPEX + C_{inv} & for\ the\ 10th\ and\ 20th\ year \end{cases} \quad \text{(Eq.30)}$$

In order to account for the benefits of electricity generation from the PV installation for each year, several production data must be obtained from the simulations run in the PVsyst. Those parameters are the annual amounts of energy at the nth year of operation: available from the PV system – $E_{avilPV,n}$, consumed

from the PV system by the user, $E_{consPV,n}$, injected to the grid, $E_{inj,n}$, purchased from the grid, $E_{pur,n}$. Additionally, for the Net Metering support scheme amount of energy recovered from the grid, $E_{rec,n,}$ is taken into consideration, and for the Feed-In-Tariff support scheme the amount of energy sold to the grid, $E_{sold,n}$. As those amounts vary each year due to PV system performance, the small letter "n" denotes the year of operation. All of the above parameters are expressed in kWh/year.

As the PV panels are ageing, their performance gradually deteriorates over time. To compute the amount of energy available from the PV system at the nth year of operation, the initial yield in corrected by annual degradation factor:

$$E_{availPV,n} = E_{avail,1} \times (1 - D)^n \quad \text{(Eq.31)}$$

where:

$E_{avail,n}$ = annual amount of available electricity from the PV system in the nth year [kWh/year]

$E_{avail,1}$ = annual amount of available electricity from the PV system in the 1st year [kWh/year]

D = annual degradation factor [%/year]

n = year of the investment [year]

Energy available from the PV system would cover the instantaneous energy demand of the facility, or in case of the surplus this energy would be injected into the grid This surplus amount of electricity is simulated and computed in the PVsyst software by subtracting the hourly production profile from the hourly demand profile.

$$E_{inj,n} = E_{availPV,n} - E_{consPV,n} \quad \text{(Eq.32)}$$

where:

$E_{inj,n}$ = annual amount of electricity injected to the grid in the nth year [kWh/year]

$E_{consPV,n}$ = annual amount of electricity immediately consumed from the PV system by the user in the nth year [kWh/year]

If the PV system works under the **Feed-In-Tariff** (FIT) support scheme, the energy injected to the grid is sold and the quantity of energy needed to cover the demand is purchased from the grid.

$$E_{pur,n(FIT)} = E_{dem,n} - E_{consPV,n} \quad \text{(Eq.33)}$$

where:

$E_{pur,n}$ = annual amount of purchased electricity in the nth year [kWh/year]

$E_{dem,n}$ = annual electricity demand at nth year [kWh/year]

However, if the PV system works under the **Net-Metering** (NM) support scheme, a user can store virtually the surplus energy which was injected into the grid and collect it later, at a reduced amount, to meet the ongoing demand. According to the Polish Energy Law, For the installations with the capacity up to 10 kWp, for each 1 kWh injected into the grid, the prosumer will receive the maximum of 0,8 kWh. In case of the micro-installations between 10 and 50 kWp the ratio is 1 to 0.7 [42].

Amount of the recovered electricity is calculated in a following way:

- for the $PV_{cap} \leq$ 10 kWp:

$$E_{rec,n} = \begin{cases} 0.8 \times E_{inj,n} & if \quad (0.8 \times E_{inj,n} + E_{consPV,n} \leq E_{dem,n} \\ E_{dem,n} - E_{consPV,n} & if \quad (0.8 \times E_{inj,n} + E_{consPV,n} > E_{dem,n} \end{cases} \quad \text{(Eq.34)}$$

- for the 10 kWp $< PV_{cap} \leq$ 50 kWp:

$$E_{rec,n} = \begin{cases} 0.7 \times E_{inj,n} & if \quad (0.7 \times E_{inj,n} + E_{consPV,n} \leq E_{dem,n} \\ E_{dem,n} - E_{consPV,n} & if \quad (0.7 \times E_{inj,n} + E_{consPV,n} > E_{dem,n} \end{cases} \quad \text{(Eq.35)}$$

With a constraint for the maximum amount of annually recovered electricity is:

$$E_{rec,n} \leq E_{dem,n} - E_{consPV,n} \quad \text{(Eq.36)}$$

The annual amount of electricity purchased from the grid in a Net-Metering scheme is then:

$$E_{pur,n(NM)} = E_{dem,n} - E_{consPV,n} - E_{rec,n} \quad \text{(Eq.37)}$$

In the next step, electricity flows will be translated to monetary values, in order to carry out the economical evaluation. The annual cost of purchased electricity is composed of variable part – dependant on the electricity imports, and fixed part. It is calculated as follows:

$$C_{e.pur,n} = \begin{cases} E_{pur,n(NM)} \times p_{e,pur,var} + p_{e,pur,fix} & for\ NM \\ E_{pur,n(FIT)} \times p_{e,pur,var} + p_{e,pur,fix} & for\ FIT \end{cases} \quad \text{(Eq.38)}$$

where:

$C_{pur,n}$ = annual cost of electricity purchased in the nth year [EUR]

$p_{e,pur,var}$ = variable price of the electricity [EUR/kWh]

$p_{e,pur,fix}$ = fixed price of the electricity [EUR]

To assess the profitability of the investment, it is crucial to know how much money does the PV system save, thanks to the mitigated need of purchasing a part of the electricity from the grid. The amount of saved electricity again depends on the support scheme.

For FIT mechanism, the annual profit from the saved electricity is calculated by the equation:

$$C_{e.save,n(FIT)} = E_{consPV,n} \times p_{e,pur,var} \quad \text{(Eq.39)}$$

where:

$C_{e.saved,n}$ = annual mitigated cost of electricity purchase in the nth year [EUR]

Additionally to the saved electricity, in the FIT scheme the user can also sell the surplus energy. The income from the transaction is calculated by the equation:

$$I_{e.sold,n} = E_{inj,n} \times p_{e,sold} \times (1 - tax_{e.sold}) \quad \text{(Eq.40)}$$

where:

$I_{e.sold,n}$ = annual income from the sold surplus electricity in the nth year [EUR]

$p_{e,sold}$ = price at which the grid operator buys the surplus electricity [EUR/kWh]

$tax_{e.sold}$ = income tax on the sold surplus of electricity [%]

In the NM scheme, the annual profit from the saved electricity is calculated by the equation:

$$C_{e.save,n(NM)} = (E_{consPV,n} + E_{rec,n}) \times p_{e,pur,var} \quad \text{(Eq.41)}$$

A cash flow, summarizing the cash inflows and outflows for a FIT support scheme is calculated by:

$$CF_{n(FIT)} = C_{e.save,n(FIT)} + I_{e.sold,n} - OPEX_n \quad \text{(Eq.42)}$$

For Net Metering support scheme, the cash flow for the n[th] year is computed by the equation:

$$CF_{n(NM)} = C_{e.save,n(NM)} - OPEX_n \quad \text{(Eq.43)}$$

As mentioned at the beginning of the chapter, the leading financial parameter, in respect to which the system size will be optimized, is the NPV. Its formula goes as follows:

$$NPV = \sum_{n=1}^{N} \frac{CF_n}{(1+r)^n} - CAPEX \quad \text{(Eq.44)}$$

where:

N = lifetime of the project [years]

r = discount rate [%]

To compute the IRR, one must equal the NPV formula to zero, and solve it for the discount rate.

$$0 = \sum_{n=1}^{N} \frac{CF_n}{(1+IRR)^n} - CAPEX \quad \text{(Eq.45)}$$

To calculate DPP, the below equation must be solved for the year at which the initial investment equals the discounted cumulative cash flow.

$$\sum_{n=1}^{DPP} \frac{CF_n}{(1+r)^n} - CAPEX = 0 \quad \text{(Eq.46)}$$

Lastly, to calculate the LCOE, the lifetime costs of CAPEX and OPEX of the investment are divided by the discounted amount of electricity produced over this period. As the O&M costs are incurred every year, they need to be discounted for the future, in contrary to the CAPEX which is buried only once, at the beginning of the investment.

$$LCOE = \frac{CAPEX + \sum_{n=1}^{N} \frac{OPEX_n}{(1+r)^n}}{\sum_{n=1}^{N} \frac{E_{avail,1} \times (1-D)^n}{(1+r)^n}} \quad \text{(Eq.47)}$$

Chapter 5

Case study – background and preliminary analysis

At the beginning of the chapter background information about the studied facility and the location at which it will be build are presented. Estimation of electricity demand and creation of load profiles is later covered. Next in the chapter, analysis of system's optimal tilt and size is conducted. Lastly, components selection and assumptions for the specific simulations are covered.

5.1 Site analysis

5.1.1 Location

The building on which PV panels will be fitted is located in northern Poland, in the city of Miszewo, with the latitude of 54°24'53.9"N and longitude of 18°22'41.1"E. The location is presented on the map in figure 5.1. The site is situated on a flat plot of an altitude of 120 m above the sea level.

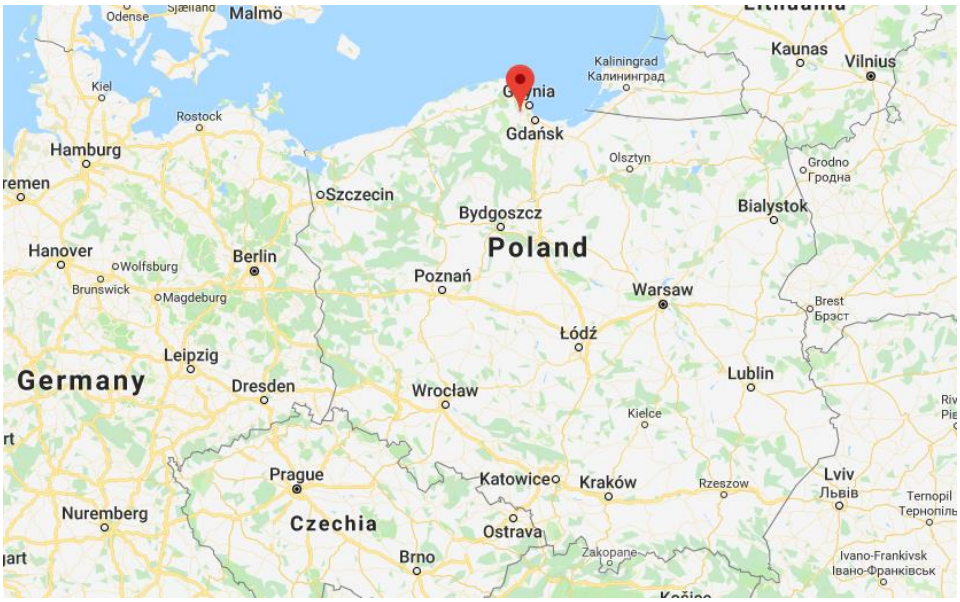

Figure 5.1 Site location. Source: GoogleMaps

5.1.2 Meteorological data

The meteorological data used in this project was obtained from the Meteonorm (version 7.2), which is a database of solar radiation and weather data broadly utilized and acknowledged in the industry of solar energy. The statistics provided from Meteonorm are a synthetical combination of mathematically modelled and real measurements of weather data, that can be presented in a form of monthly, daily or hourly averages. The meteorological information necessary for the project was given as a form of a typical meteorological year format (TMY), which provides an average from years 1991 to 2010 of the following parameters : 3 values of irradiance (extraterrestrial, horizontal global and horizontal diffuse), clearness index, ambient temperature, humidity and wind velocity [63].

As the city of Miszewo, where the warehouse will be located, does not have a meteorological station, the weather data was taken from nearest station, which in this case is the Gdańsk-Rębiechowo airport. The approximation is considered to be accurate enough as the weather station is located merely 7 km from the project's location and the topography of the terrain is similar. The monthly values of weather data are presented in the Table 5.1.

Table 5.1 Monthly weather data values for the city of Miszewo

Monthly Meteo Values Source Meteonorm 7.1 (1991-2010), Sat=100% (Modified by user)

	Jan.	Feb.	Mar.	Apr.	May	June	July	Aug.	Sep.	Oct.	Nov.	Dec.	Year	
Hor. global	16.3	24.2	71.4	123.7	154.7	162.6	159.7	122.0	86.4	46.9	16.5	10.4	994.8	kWh/m².mth
Hor. diffuse	11.8	17.8	37.8	54.5	67.3	88.8	76.6	72.2	46.3	24.3	12.4	7.0	516.8	kWh/m².mth
Extraterrestrial	57.4	96.3	175.0	250.1	324.7	344.7	343.1	288.0	202.1	130.8	68.3	44.9	2325.5	kWh/m².mth
Clearness Index	0.284	0.251	0.408	0.495	0.476	0.472	0.466	0.424	0.427	0.358	0.241	0.232	0.428	
Amb. temper.	-1.0	-0.4	1.9	7.0	12.4	14.9	17.7	17.3	13.1	8.6	4.1	0.6	8.0	°C
Wind velocity	4.2	4.1	3.9	3.2	3.2	3.5	3.1	3.1	3.0	3.3	3.8	3.6	3.5	m/s

5.1.3 Building parameters

At the time of writing this master thesis, the building was still in a design phase. Due to this fact, the information presented below, which were used for designing the generation system, may vary from the final layout chosen by the company.

According to the latest information (September 2019) obtained from the company the warehouse will be built from concreate, on the plan of the rectangle, 18.5 m long and 38m wide. The roof is planned to be single-pitched, with a tilt of 8 degrees, with its higher edge elevated by 9 m from the ground. Total roof area is 703 m^2. However, as the building's rooftop will be equipped with 24 skylights, and the safety mounting distances must be kept, the available area for PV installation will be limited down to around 450m^2. The azimuth of the roof is to be oriented 23 degrees to the West from the South, making it an attractive area for setting up the PV system. The office part will be located in northern side, as the building extension. As its roof is neither suitable for the PV coverage, nor it creates shadow on the building, its dimensions will not be described here. Building's visualization shown in figure 5.2 was created in SketchUp and will later be used for the simulation of shading.

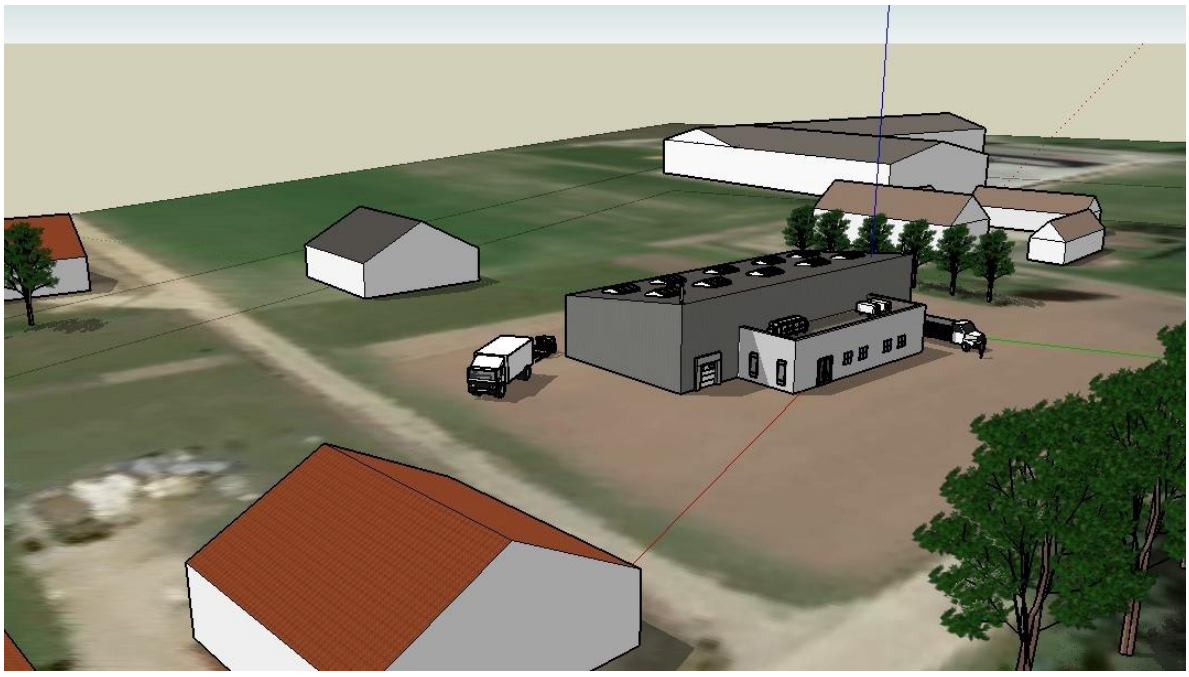

Figure 5.2 Site visualization

5.1.4 Far and near shading

One of the very important elements of the site analysis is determination of shading as it reveals the feasible area for PV installation There are two types of shading that are being distinguished – far and near shading.

The far shading (sometimes called as a horizon shading) is defined as a horizon line that is visible from the PV field. it takes into account objects, such as tall buildings, forests, mountains, etc., that are so far away from the PV system, that their shading effect on the installation is considered in a global way – at the given moment the sun can or cannot be seen from the perspective of the installation. Its determination can be done by either downloading the horizon profile from the Meteonorm digital terrain model – which was done in case of this project – or by taking a panoramic picture on site and running it through horizon analysing software, such as HORIcatcher, HorizON or PanoramaMaster [64].

Near shading is understood as the one casted by neighbouring objects, and in principal is much more complex to treat, as to understand the shade trajectories and analyse potential impacts of shading loss, a detailed 3D visualization of the system and its environment must be made. For this purpose a Sketch Up Pro software was utilized for building a 3D model. Firstly, in order to maintain an appropriate scale between neighbouring buildings and the natural environment, the geo-localization tag was placed on a map. Based on that, a satellite image was downloaded and set as a base layer. Later, after conducting a site visit and noting down the dimensions of the surrounding constructions and vegetation, all of the significant shade creating objects were extruded on the map. Such model was later exported to both PVsyst and PV*SOL, where a simulation of sun pathways at each hour of the year was run.

5.2 Building’s electricity demand

5.2.1 List of appliances and their use

To estimate the building’s electricity consumption, bottom-up method was used. To do so, all electrical appliances were first inventoried. Types, quantities and power ratings of the electrical equipment were obtained through the meetings with the investor and the designers. To get a better comprehension of the labour plan, as well as of the frequency and usage intensity of the electrical appliances, employees working in current warehouse were interviewed, as it is assumed that the working pattern is going to remain similar in the new building. Power rating of several appliances was also done in respect to their operational state. Frequency of use, average usage duration as well as the individual power ratings of the equipment were obtained from the combination of interview process and data from the energy auditing reference handbook for commercial buildings [65].

The gathered information was put in the table 5.2. The appliances were clustered and categorised on the basis of what part of the building they will be located in. The mentioned categories are: office part,

warehouse part and the whole building, in which all the devices that are common for the entire building – such as monitoring, air conditioning unit and outer lighting – were placed.

As some of the devices are going to turned on intermittently (ex. fridge) and the usage of others is of short duration (ex. coffee machines, printers) the total mean energy demand was introduced. It was calculated by multiplying the quantity by the hourly duration, by the individual power ratings and by the demand factor, which is the ratio of the average load to its maximum value. The last column in the table indicates whether the device will only by used during weekdays, or also during the weekends.

Table 5.2 List and specification of electrical appliances

Building part	Equipmnet	Quantity	Mode	Usage density	Individual power, W	Demand factor, h/h	Total mean hourly power demand, W	Weekends
Office	Computers	5	working	during office work time	75	1	375	no
	Printers	4	printing	4 times per hour	40	0,2	32	no
			idle	rest of the time	5	1	20	yes
	Lighting	30	wokring	when needed	35	1	1050	no
	Server	1	wokring	all the time	500	1	500	yes
	Refrigeration	1	working	all the time	120	0,4	48	yes
	Dishwasher	1	working	1 time per day	1200	1	1200	no
	Microwave	1	working	4 times per day	2400	0,1	240	no
	Coffee machine	1	working	20 times per day	750	0,05	37,5	no
Warehouse	Lighting	50	working	during warehouse work time	45	1	2250	no
	Air curtains	4	working	during delivery and shipping	210	1	840	no
	Wrapping machines	1	working	1,5h in the morning and in the evening	2400	1	2400	no
			idle	rest of the time	15	1	15	no
	Electric forklifts charger	2	charging	8h each day, after end of work	625	1	1250	no
			idle	rest of the time	10	1	20	no
Whole building	Outer lighting	8	working	from 1h after the sunset, till 1h before sunrise	100	1	800	yes
	Monitoring	18	working	all the time	12	1	216	yes
	Air heaters	8	heating	winter, during working hours	110	0,35	308	yes
	AC fan motor	1	heating	winter, during working hours	370	1	370	no
		2	cooling	summer, during working hours	370	1	740	no

5.2.2 Load profiles

Meaning and importance

Consumption profiles, or otherwise called energy load profiles are a graphical illustration of aggregated electricity loads and their variations in electricity consumption over a specified time horizon. The data is presented at regular time intervals, typically of one hour, half an hour or 15 minutes, and allows to determine for example: consumption patterns, seasonal changes, maximum power demand and total electricity consumption. This information enables also to estimate the spending on electricity bills, especially for a situation in which a tariff varies depending on a time of a day.

To assess the attractiveness of the investment, a baseline scenario – in which no PVs are installed – must be benchmarked against the electricity savings deriving from the installation and operation of a certain PV system. In order to calculate those savings it is necessary though to compare the PV production profile with the load profile of the facility. By finding the common part of those profiles it is possible to determine the fraction of energy consumed directly from PV and calculate the remaining amount that needs to be purchased from the grid to cover the demand [66]. For this reason, load profiles are a master key in the process of optimal sizing of the solar PV system and calculating its financial benefits.

Main assumptions

For this case study, a bottom-up approach of creating the load profiles was adopted. Knowing, from the interview processes, the usage density and power demand of each device, all appliances were put in a time table that starts at 00:00 and ends at 23:00, with half-an-hour time intervals. Such input data resolution was considered to be the most reasonable for two reasons. Firstly, it was the shortest common time interval available to be later uploaded and processed in the PV simulation software. Secondly, 30 min time interval reflects well the very organized labour plan and still leaves some time margin for day-to-day fluctuations.

As the building is not in operation yet, it is only possible the create a prediction of the load profiles In order to model the consumption demand and stay within sensible limits of precision, a set of simplifications were introduced. The main assumptions include:

- It was assumed that energy consumption on individual days of the month does not differ significantly, so instead of modelling each day independently, a monthly estimation will be conducted, based on an “average working day of the month” and an “average weekend day of the month”. This will result in modelling separately 12 average working days and 12 average weekend days – one of each per each month.
- Weekly profiles were created by taking 5 times the average working day and adding to it twice the average weekend day. Monthly profiles were assembled from the weekly profile. This operation was done for each month of the year.
- Working hours of the office are going to be between 8 am to 5:30 pm, including an hour lunch break in the middle. Working hours of the warehouse will stretch between 6:30 am to 6 pm.
- Electric forklifts are going to be charged every night of the working day, after the closure of the warehouse.
- Outer lighting is going to be turned on 1h after the sunset and turned off 0,5h before the sunrise. The time of the sunset and sunrise was taken for a middle day of each month.
- Intensity of inner lighting is corelated with the amount of available daylight, to reduce the energy consumption. The energy demand was modelled to vary throughout the day and was also linked with the times of a sun rise and sun set.
- To compare in the PV simulation software, the electricity consumed by the building with the electricity harvested from the PV panels, a CSV file representing the yearly energy needs was created. The timestep of data entry is half an hour, and combined they represent the changes

in power demand throughout the year. At this point a simplification had to be made, by assuming that the load profile will remain unchanged in the next years. At the moment of writing this master thesis, neither of the software allowed to alter this input information. The yearly consumption data will be treated as a typical load profile of this building and will be used in the simulations that will cover the time horizon of 25 years.

A small part of the 30 min time step load table is presented in table 5.3. The data represents the average power demand on the average working day in April, between 5AM and 12AM.

Power demand of each electrical appliance was assigned to the specific time slots based on the conducted interviews about the labour patterns and usage habits of the employees.

The transition of colours from grey to yellow at the top part of the table indicate the monthly average hour of the sun-rise and similarly at the later part of the day for a sun-set. As mentioned in the assumptions, those hours are linked with switching on and off the outer lighting.

Table 5.3 Part of a load demand table for an average working day in April

equipmnet	mode	total mean power, W	5:00	5:30	6:00	6:30	7:00	7:30	8:00	8:30	9:00	9:30	10:00	10:30	11:00	11:30	12:00
computers	working	375	0	0	0	0	0	0	375	375	375	375	375	375	375	375	375
printers	printing	32	0	0	0	0	32	32	32	32	32	32	32	32	32	32	32
printers	idle	20	20	20	20	20	0	0	0	0	0	0	0	0	0	0	0
lighting	working	1050	0	0	0	0	0	0	1050	1050	1050	1050	1050	1050	1050	525	525
server	working	500	500	500	500	500	500	500	500	500	500	500	500	500	500	500	500
refrigeration	working	48	48	48	48	48	48	48	48	48	48	48	48	48	48	48	48
dishwasher	working	1200	0	0	0	0	0	0	0	0	0	0	0	0	0	0	0
microwave	working	240	0	0	0	0	0	0	0	0	0	0	0	0	0	0	240
coffee machine	working	37,5	0	0	0	75	0	0	150	75	0	0	0	75	0	0	150
lighting	working	2250	0	0	0	2250	2250	2250	2250	2250	2250	2250	2250	2250	2250	2250	2250
air curtains	working	840	0	0	0	840	840	840	840	0	0	0	0	0	0	0	0
wrapping machines	working	2400	0	0	0	0	0	0	0	0	2400	2400	2400	0	0	0	0
wrapping machines	idle	15	15	15	15	15	15	15	15	15	0	0	0	15	15	15	15
electric forklifts charger	charging	1250	0	0	0	0	0	0	0	0	0	0	0	0	0	0	0
electric forklifts charger	idle	20	10	10	10	10	10	10	10	10	10	10	10	10	10	10	10
outer lighting	working	800	800	800	0	0	0	0	0	0	0	0	0	0	0	0	0
monitoring	working	216	216	216	216	216	216	216	216	216	216	216	216	216	216	216	216
air heaters	heating	308	0	0	0	308	308	308	308	308	308	308	308	308	308	308	308
AC fan motor	heating	370	185	185	185	370	370	370	370	370	370	370	370	370	370	370	370
AC fan motor	cooling	740	0	0	0	0	0	0	0	0	0	0	0	0	0	0	0

Data presentation

To have a better comprehension of the gathered tabularised data, several graphs demonstrating electricity demand figures were created. The first one, figure 3.3, illustrates how the power demand of the average day of the month changes during the day. The hourly plot shows clearly that there is a strong correlation between the time of the year and the electricity consumption profile. During the winter months the demand is higher than during the summer months.

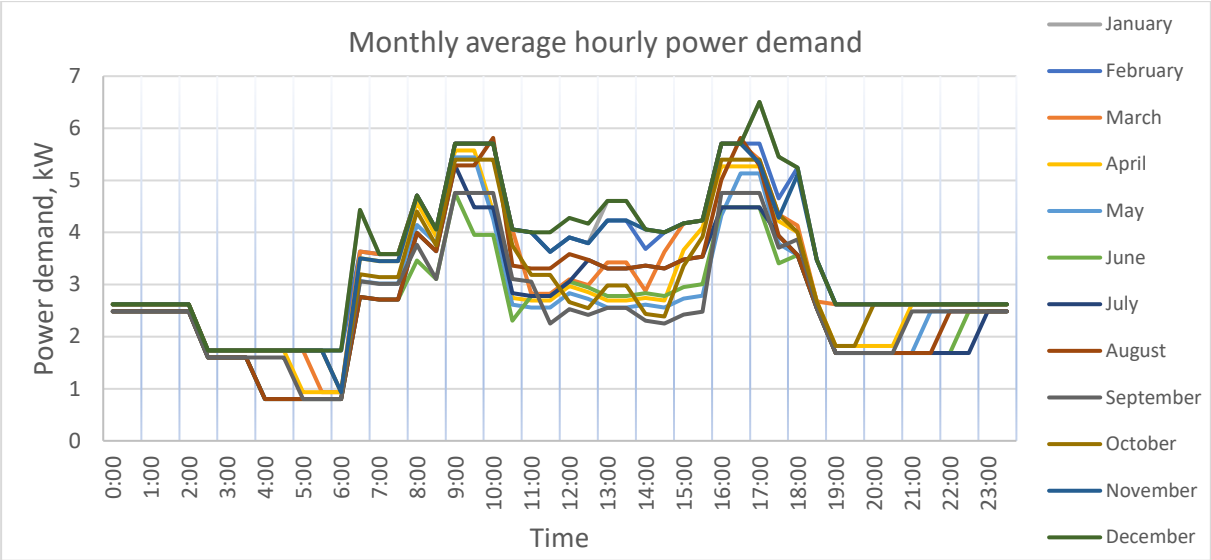

Figure 5.3 Average daily electricity consumption – profiles of all months

To observe better the difference in power demand, the graph in figure 5.3 was filtered down to two most abject months, June and December, and presented in figure 5.4. In addition, a yearly average was plotted as a reference point. The biggest discrepancy can be observed during the midday, when the difference in the power can be of around 2kW. The graph explains also one of the key difficulties associated with the power generation from PV, that is the incoherency between the demand, which is highest in winter, and the production, that is highest in summer.

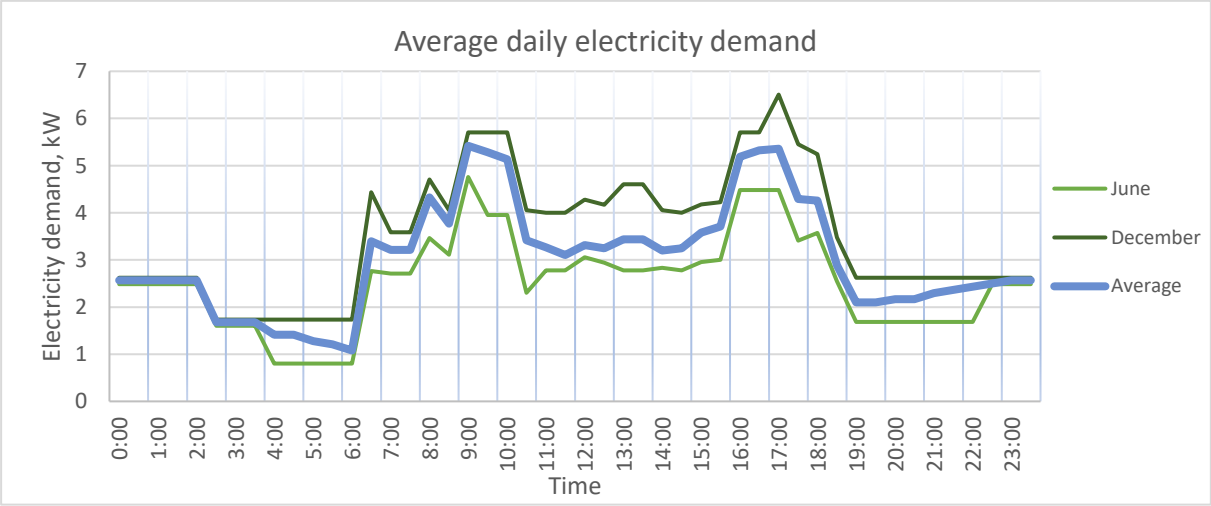

Figure 5.4 Monthly average hourly power demand – selected months

As the building has been initially divided into three functional parts, it has been analysed how the power demand is shaped by the facility section. The annual trend has been plotted on figure 5.5.

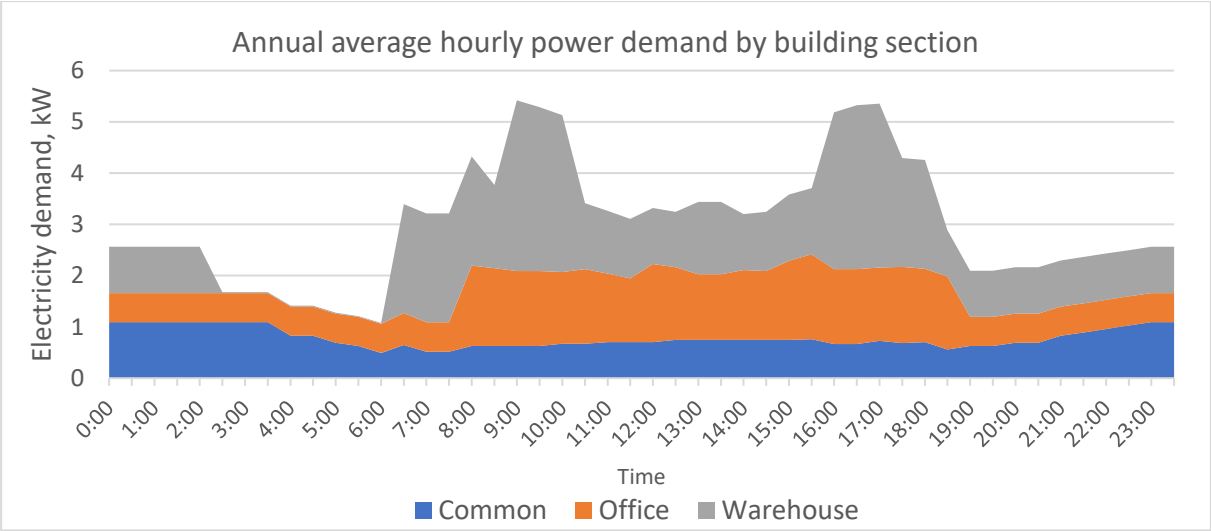

Figure 5.5 Annual average hourly power demand by building section

A conclusion can be drawn that the consumption of the common part varies modestly during the day, with the small decrease during the typical working hours.

As for the office, two clear and levels of consumption can be observed. During the office working hours, this part mostly has a consistent power demand of around 1,5 kW, with the exception of a small peak during the lunch time. After the operational hours, the demand for electricity drops down to around 500 W, which shall be associated with the power needs of a server, which is on 24/7.

The power demand inside the storage part is the most abrupt. Between 2am and 6am it does not consume electricity at all, and outside those hours it is its biggest consumer. Around 9am and 5pm the power demand skyrockets, crating 2 significant power peaks.

To complement the analysis, an annual average hourly area chart, stacked by the type of electrical appliance has been created, and labelled as figure 5.6.

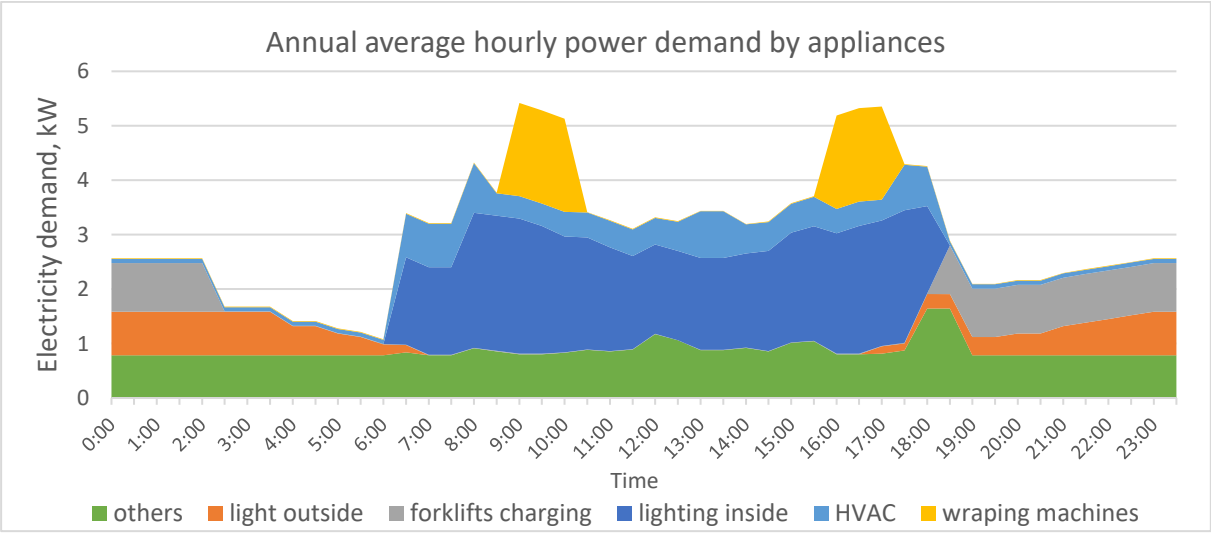

Figure 5.6 Annual average hourly power demand by appliance type

It can be seen that at 6am, when the warehouse opens, a sharp rise of demand is observed, which shall

be associated with the lights and the HVAC system being turned on. The peak at 8am indicates the beginning of the office work, and additional inside lighting being turned on. The power demand during the working hours of the facility changes drastically. Majority of the power is consumed by inside lighting, which is mostly needed in the storage part of the building. The wrapping machines, located in the warehouse part are by far the biggest disruptors of consumption. They are responsible for the two energy peaks at the beginning and at the end of the working hours, that lifts up the momentary demand by nearly 2,5kW. After the operating hours of the facility, the biggest power consumer are chargers of electrical forklifts, that are plugged in to charge from 6pm to 2am. The second biggest power consumer at night is the outside lighting. Power demand of other devices is mostly at a steady level of 1 kW.

The last chart, figure 5.7, presents the electricity consumption on the aggregated level of each month.

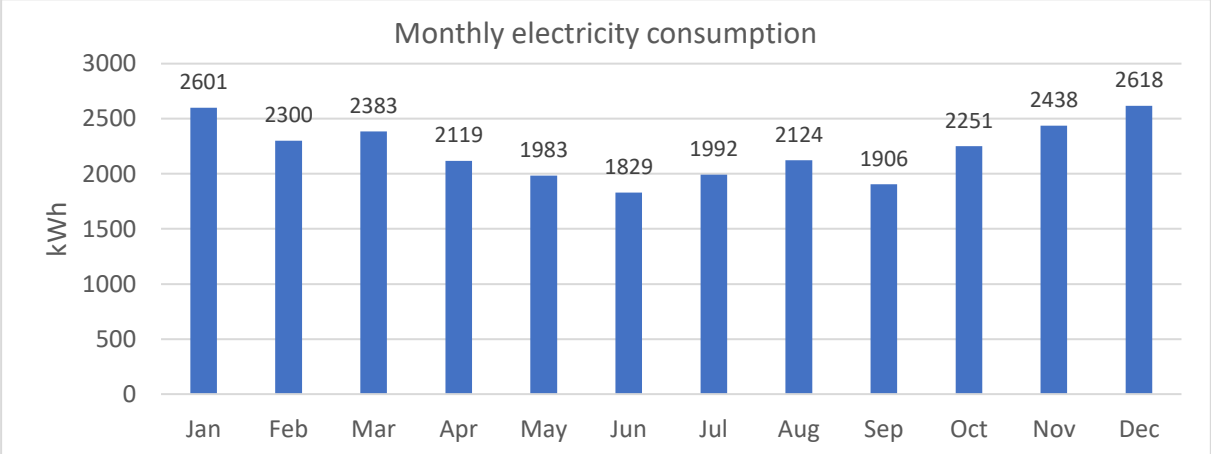

Figure 5.7 Average daily electricity demand

The monthly electricity consumption has a profile of a flat “V”. The consumption decreases steadily from January and hits it low in June. From then on, the tendency is reversed, with the exception of September, when a slight drop is observed. This is due to a weather transition period and the use of HVAC – air conditioning is not working anymore, and the heating season has not started yet. On average, the monthly electricity consumption is at the level of around 2200 kWh/month. Yearly electricity demand is of around 27.3 MWh

5.3 Preliminary design

Before committing to a specific design of the system, a preliminary design was done. This step allowed to determine the most suitable tilt of the PV panels and further, approximate the optimal capacity range of the system, for both Net-Metering and Feed-in-Tariff support schemes. The study also gave a rough idea about the system’s performance and financial benefits.

To save up the computing time, the model applied during the preliminary design uses a monthly averaged value of solar radiation to simulate the performance of a generic PV panels connected to a generic inverter. Moreover, only a monthly averaged values of solar irradiance and a simplified shading

effect (only the attenuation of irradiance is taken into account, without considering the electrical effects) are used during the computations.

Simulations were run for PV system capacities ranging from about 10 kWp to 45 kWp, with increments of around 4 kWp in installed power. Results of the PV performance simulations were later processed in the economic assessment model to find the optimal configuration for each of the support schemes, indicated by the highest value of NPV. For the preliminary design average prices of a PV rooftop system in a capacity range of 10-50 kWp where used in the economic model [46].

Results of the preliminary design are supposed to estimate the range of PV system capacities, within lies the optimum. Later on during the specific design, optimal system configuration based on real components will be sought within those ranges.

5.3.1 Optimal tilt

Due to the fact that ideal tilt of the PV panels depend on the sun position on the sky which changes every second, each mounting angle will have some benefits and shortcomings. A common practice for a fixed-tilt panels is to optimize the tilt in respect to the season. For the application where summer production is prioritized, PV panels will be mounted with less inclination, as the sun pathways are positioned higher on the horizon. Due to low tilt, the distance between the arrays can be smaller, as the effect of mutual shading is decreased. Winter optimization on the other hand will be characterized by much steeper profiles and larger distances between rows. For projects that are expected to deliver the greatest annual yield, an in-between tilt should be used [64].

For each of the selected capacities, an iterative simulation of finding the optimal tilt for the azimuth of 23° was performed. The tilt configurations were tested for each of the selected system capacities in a range between 30° to 55° in respect to the horizontal plane. The optimal tilts for a given capacity and support scheme where found in respect to the maximum economic benefit, indicated by the highest NPV. Optimization results were plotted on the figure 5.8. For all of the computations, electricity demand of the facility remained unchanged.

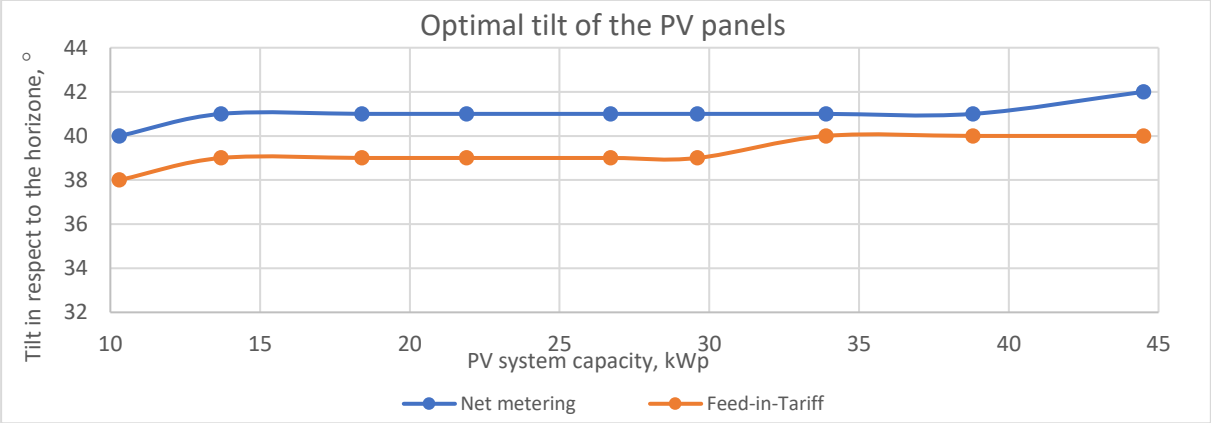

Figure 5.8 Optimal tilt of the PV panes

Results of the simulation shown that with the growing system capacity, the optimal tilt slightly sharpens.

For most cases, the best tilt for the studied system, that would work in the NM scheme, would be to install the PV panels at 41° in respect to the horizontal plane, which can be translated to 33° in respect to the roof, which has a slop of 8°. Under the FIT option the PV panels should be less steep - on average by 2° less in respect to the ones working in the NM option.

5.3.2 Source of energy to cover the demand

The effects of increasing system capacity on the level of self-consumption were also investigated for both FIT and NM, and shown respectively in figures 5.9 and 5.10. Results of the simulations indicate that with the increased size of the PV based generation system, depicted by the blue bars, the share of energy consumed directly from PVs doesn't change substantially. In fact, only a small increase can be noticed up until the PV system capacity of around 27 kWp, and later on the differences are marginal.

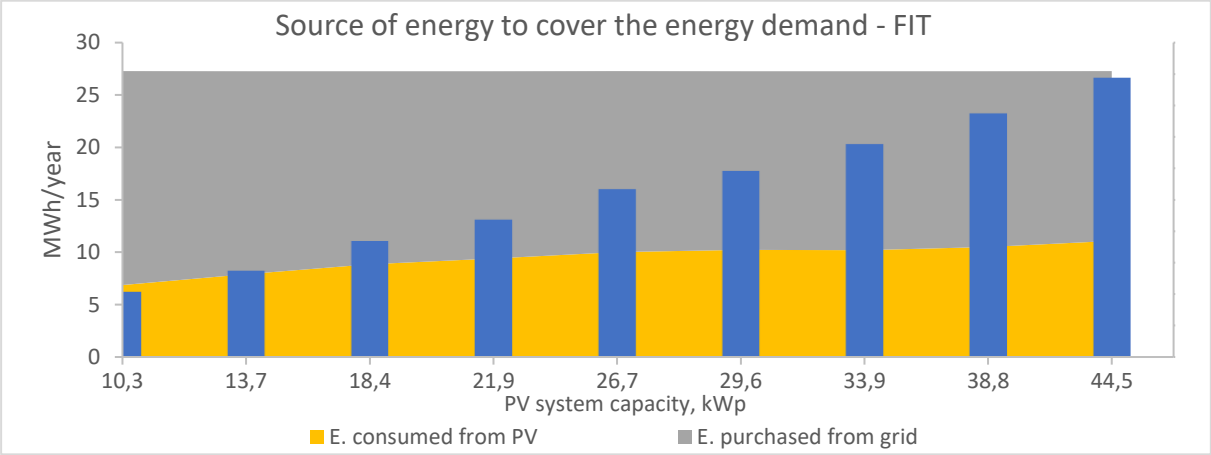

Figure 5.9 Breakdown of energy sources covering up the demand vs. system capacities - FIT

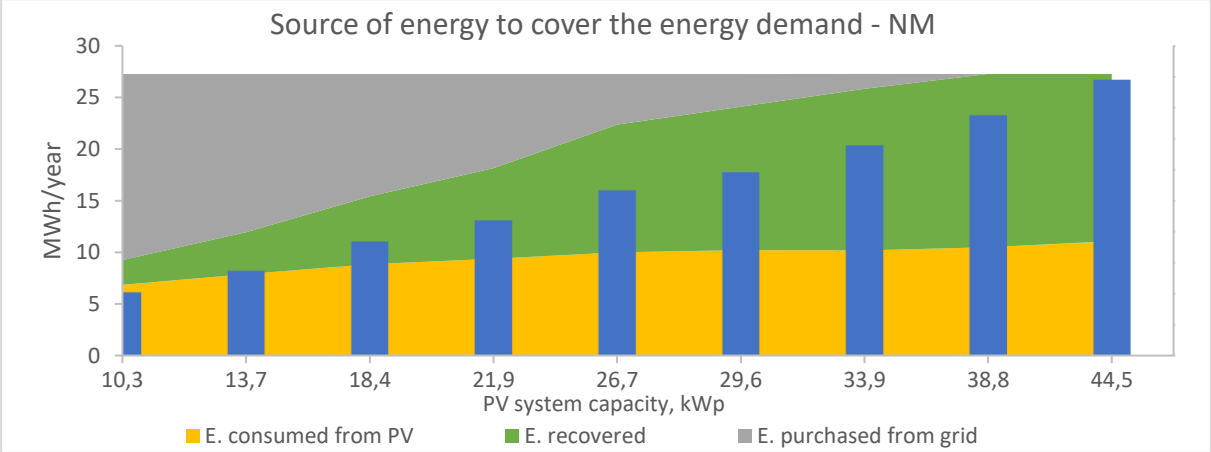

Figure 5.10 Breakdown of energy sources covering up the demand vs. system capacities – NM

For the system working under the NM scheme, it is worth noting that with the increased capacity of the PV system, amount of energy recovered from the grid (max. 70% of what was previously injected) rises steadily. For the capacity of around 40 kWp the net imports of electricity from the grid are equal to zero, which may indicate that somewhere around this point lies the optimal capacity.

5.3.3 NPV and IRR vs. PV system capacity

Referring to what has been discussed before in the economic section, the leading financial measure of profitability for the studied case is the NPV, as it shows best the monetary benefits of this investment. For this study a discount rate of 4%, the project's lifetime of 25 years, and the selling price of electricity in FIT model of 0.053 EUR/kWh was assumed. As during the preliminary design only selected capacities were tested, results of below simulations indicate only the range in which lies the optimal capacity of the PV system. Boundaries of the solution are determined by the two point, adjacent to the point with the highest NPV. The range in which the maximum NPV should be sought for is marked with a red line in the figure 5.11.

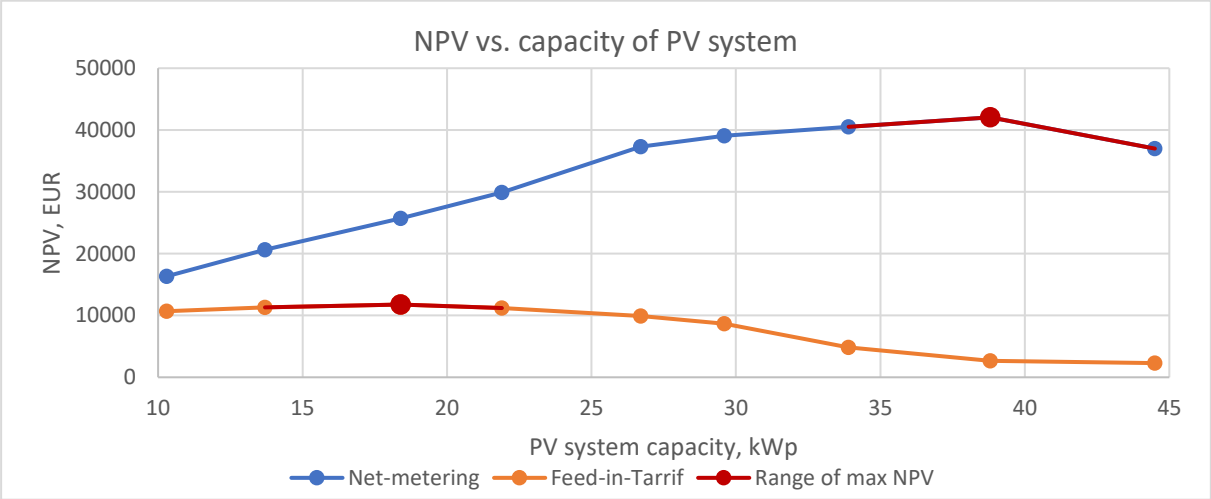

Figure 5.11 NPVs of various PV system's capacities and support models

Results of the preliminary simulations show that for a scenario in which:

- the legislation will change so that the **NM support mechanism** will also cover the companies, the optimal capacity is somewhere within the range of **34 kWp to 44 kWp**
- the legislation remains unchanged, offering the **FIT support mechanism** to the companies, the optimal capacity is somewhere within the range of **13 kWp to 22 kWp**

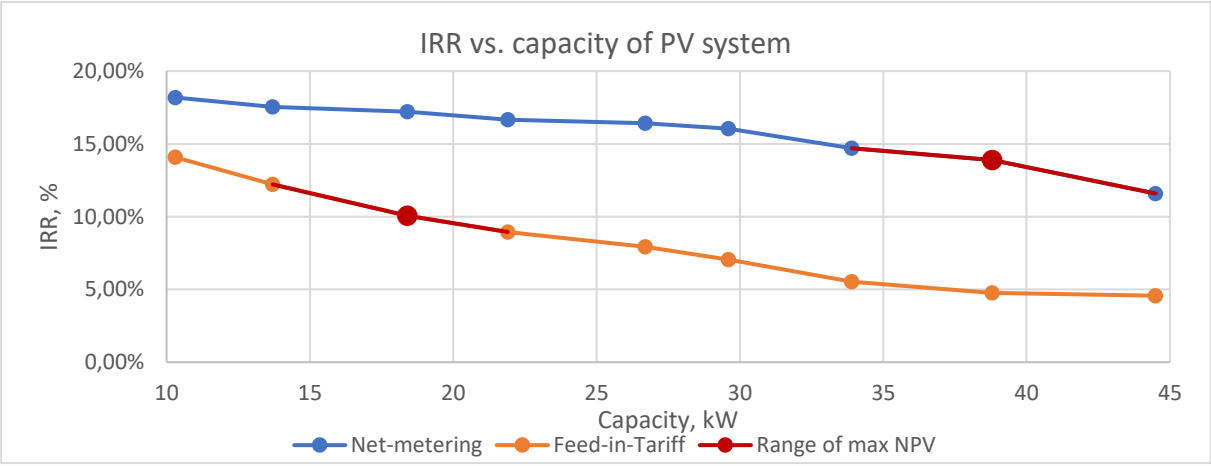

Figure 5.12 IRRs of various PV system's capacities and support models

It can be seen from the figure 5.12, that the ranges of the highest NPVs do not match the highest IRRs. The underlying reason for this conflict is that the sequence of cash flows. IRR is calculated with an assumption that the cash flow can be reinvested at the internal rate of return. Such an theory is problematic, as there is no guarantee that equal chances will be available for reinvesting each time the cash flow occurs. Such phenomena is called reinvestment risk. On the contrary, NPV does not suffer from this problem, as it assumes that the reinvestment happens at the cost of capital which is much more realistic.

Moreover, NPV is stated in an absolute measure and ranks higher an option which adds more monetary value during the lifespan of the project, regardless of the initial investment required. IRR is a relative measure, and it will rank higher the projects that offer best investment returns regardless of the total value added. In case of the conflict of NPV and IRR, the option with higher NPV should be chosen [57].

5.3.4 Annual cost structure

In addition, a lifetime average annual cost of covering the facility's electrical demand was computed. In the baseline option, with no PVs, the average discounted annual electricity expenditures would be of around 4000 EUR. The base case is benchmarked against various capacities of the PV system, showing the cost structure and the annual cost saving ratio.

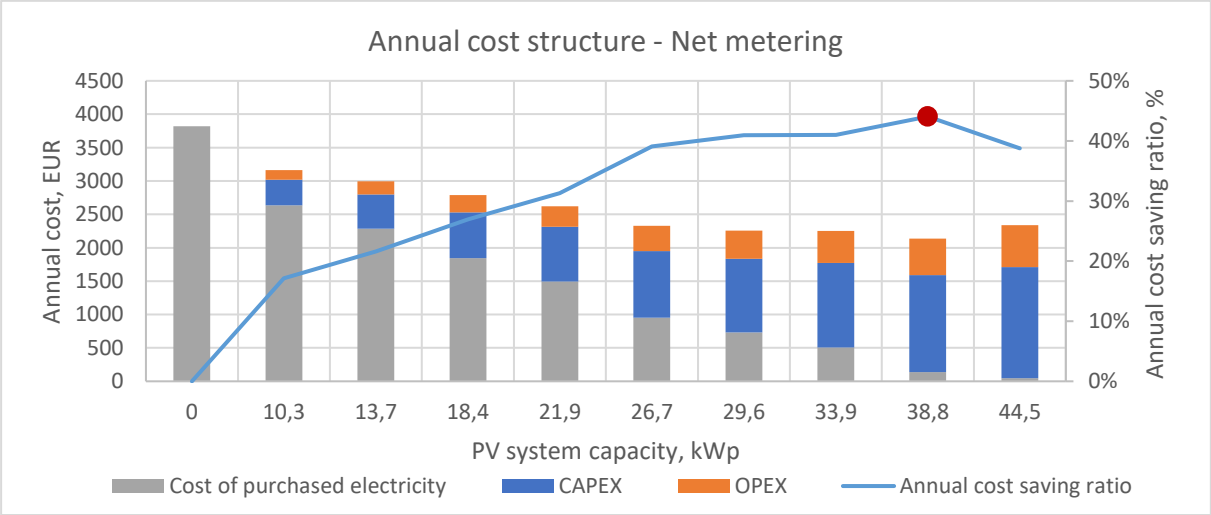

Figure 5.13 Annual cost structure of different PV system capacities – case of NM

It can be seen from figure 5.13 that the for NM option, the lowest annual cost is achieved for the tested capacity, of 38.8 kWp, however the optimal option, giving even lower costs, may be somewhere within the range of 33.9 to 44.5 kWp, what is in line with the results indicated by the NPV study. The annual cost saving ratio can be expected at the levels close to 50%.

Results for FIT are demonstrated in figure 5.14. The annual costs of CAPEX, OPEX and the costs of purchased electricity are reduced by the profit from the electricity sold to the grid. The annual costs will be lowest for a capacity that is between 13.7 to 21.9 kWp, similarly to the NPV study. Annual cost saving ratio is expected to be around 12%.

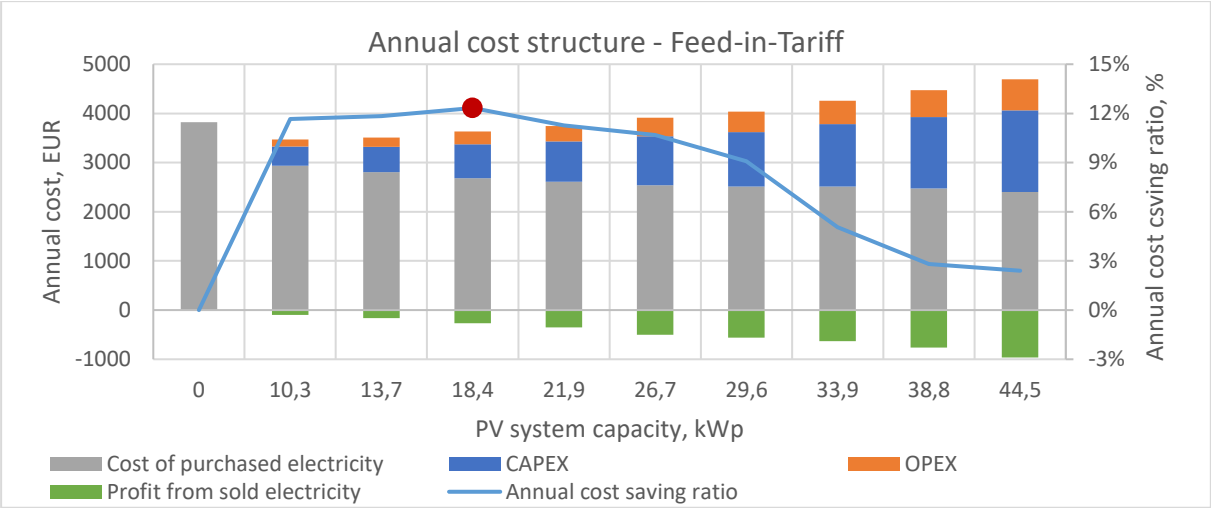

Figure 5.14 Annual cost structure of different PV system capacities – case of FIT

5.4 Components selection

In order to start simulations of the investment's bankability, components selection must be made. After studying the photovoltaic market, local retailers were requested for updated quotas of the system components. All of the pre-selected components were chosen bases on their price competitiveness, proven quality and the satisfying warranty conditions. During the specific design, components' match and performance were tested.

5.4.1 PV modules

For the specific design 5 PV panels were selected – 2 polycrystalline silicone and 3 made in a monocrystalline silicone technology. Their short specification is presented in the table 5.4. Full characteristics of the selected panels are included in the Annex.

During the selection, a special attention was paid to choose panels that:

- were ranked as Tier 1 or Tier 2 category
- have rated power not smaller than 260Wp, due to space restrictions
- have high efficiency – at least 16%
- have positive power tolerance, which guarantees that the achieved power will be not smaller than nominal
- have at least 10 years product warranty

Table 5.4 Shortened characteristics of the selected PV panels

Manufacturer	JA Solar	Talesun	Boviet	Bruk-Bet Solar	LG Electronics
Model	JAP6-60/275/4BB	TP660P - 280	BVM6610M-300 W	BEM 300	LG330N1C-A5
Technology	polycrystalline Si	polycrystalline Si	monocrystalline Si	monocrystalline Si	monocrystalline Si
Panel efficiency	16.5	17.1	18.4	18.44	19.3
Rated power PMPP (Wp)	275	280	300	300	330
Rated voltage VMPP (V)	31.4	29.4	32.2	32.5	33.7
Rated current IMPP (A)	8,75	7.04	9.32	9.25	9,8
Open-circuit voltage (V)	38.45	36	39.5	38.8	40.9
Short-circuit voltage (A)	9.26	7.49	9.84	9.85	10.45
Power tolerance	-0/+5W	-0/+5W	-0/+5W	-0/+5W	-0/+10W
NOCT (◦C)	45	44	45	43	45
Temp. coeff. of PMPP (%/◦C)	-0.41	-0.4	-0.4	-0.39	-0.37
Warranty	10 years limited product warranty, 25 years power output warranty: first year > 97,5%, at 10 years 91,2%, and by the 25th year, no less than 80%	10 years product warranty, 25 years power output warranty: first year 97%, after 1st year 0.5% annual degradation, at 25 years 85%	12 years limited product warranty, 25 years power output warranty: first year 97,5%, after 1st year 0.7% annual degradation, at 25 years 80%	15 years product warranty, 25 years power output warranty: first year 97%, after 1st year 0.6% annual degradation, at 25 years 83%	25 years product warranty, 25 years power output warranty: first year 98%, after 1st year 0.5% annual degradation, at 25 years 86%
Price (EUR)	102,0	120,0	128,0	149,5	209,5
Price/Wp (EUR)	0,37	0,43	0,43	0,50	0,63

5.4.2 Inverters

As the results of the preliminary study were indicating a wide range of system capacities, 5 inverters of several nominal powers were chosen from the offers provided by the local retailers. Their simplified specifications are listed in table 5.5. Full characteristics of the selected panels are included in the Annex.

Table 5.5 Shortened characteristics of the selected inverters

Manufacturer	KACO	SMA	KACO	KACO	KACO
Model	Blueplanet 8.6 TL3	Sunny Tripower 15000TL	Blueplanet 20.0 TL3	Powador 36.0 TL3	Blueplanet 15.0 TL3
Max DC power	8 800 W	15 330 W	24 000 W	30 000 W	18 000 W
MPPT voltage range	400 V - 800 V	240 V - 800 V	515 V -800 V	200 V - 800 V	420 V - 800 V
Operating voltage range	200 V - 1000 V	150 V - 1000 V	200 V - 1000 V	200 V - 1000 V	200 V - 1000 V
Number of MPP trackers / max strings per MPPT	2 / 2	2 / 3	2 / 2	3 / 4	2 / 2
Rated AC power	8 600 W	15 000 W	20 000 W	30 000 W	15 000 W
AC voltage/frequency	230V / 50Hz	230V / 50Hz	230V / 50Hz	230V / 50Hz	230V / 50Hz
Euro Efficiency	98.1%	98%	98.1%	97.8%	97.7%
Circuity topology	transformerless	transformerless	transformerless	transformerless	transformerless
Warranty	5 years	5 years	5 years	5 years	5 years
Price (EUR)	1505	2510	2712	3719	2221
Price/Wp (EUR)	0.175	0.167	0.136	0.149	0.148

The minimal requirements for the selected inverters were the following:

- They should have a 3-phase 230/400 V AC output and be comparable with Polish 50Hz grid,
- The euro efficiency not be lower than 97%,
- They should have an integrated Maximum Power Point (MPP) tracker,
- Minimum 5 years manufacturer warranty,
- They must have an anti-islanding protection.

5.5 Specific design

For the specific design results obtained from the preliminary design will be used as a starting point for the detailed simulations. Based on the optimal ranges found before, various configurations of PV panels and inverters will be studied. Performance simulations will be conducted starting from the smallest nominal powers of the PV systems. The system's power will be gradually increased, by adding more panels to it. The increases will be done by adding possibly smallest amount of PV panels that will be in the operating range of the inverter.

System's performance will be analysed through detailed hourly simulations. The model applied for it utilizes hourly meteorological data and a full electrical shadowing effect is taken into account.

Economic indicators will be later calculated for each simulation in order to find the optimal configuration for each of the support schemes, indicated by the highest value of NPV. Results of this part will be presented and discussed in the next chapter.

5.5.1 Effects of snow cover on soiling loss and albedo

As discussed in the literature overview, modelling the snow cover is agreed to be an extremely difficult task. For these reasons certain simplification and assumptions were taken to adjust the model. As the snow starts to fall in the studied region of Poland from mid-December and ends around February, soiling from snow and values of albedo were adjusted accordingly. It has been assumed that the PV panels will be covered under snow for 50% of time in January, and for 30% in December and February. Following the suggestions from the PVsyst software manual, values of albedo were set for 0.8 for the months were snow is present and 0.2 for the times when it is not [49]. The monthly setting are demonstrated in table 5.6.

Table 5.6 Monthly values of albedo and soiling from snow

Month	Jan	Feb	Mar	Apr	May	Jun	Jul	Aug	Sep	Oct	Nov	Dec
Soiling from snow	50%	30%	0%	0%	0%	0%	0%	0%	0%	0%	0%	30%
Albedo	0.8	0.8	0.2	0.2	0.2	0.2	0.2	0.2	0.2	0.2	0.2	0.8

Chapter 6

Results and discussion

In this chapter results of the detailed simulations of selected PV modules and inverters are presented. Next, the optimal configurations of the PV generation systems for both NM and FIT support mechanisms are summarized. Lastly, performance of each system is discussed.

6.1 Results of the detailed simulations conducted in the ranges from the preliminary design

Based on the optimal ranges found in the preliminary design, a detailed performance simulations of the selected components were carried out in the PVsyst software. Based on them, economics of each configuration were computed and plotted on the below graphs. Results illustrate the relationship between financial indicators (NPV, IRR, DPP, LCOE) and the nominal power of the PV system. Each point on the charts represents an individual system configuration of the PV panel and the inverter.

As the NPV is the key indicator, the configuration that offers the highest NPV, was indicated by the red marker. The marker is also visible on the graphs of IRR, DPP and LCOE to indicate the optimal configuration in respect to the highest system's NPV.

6.1.1 Results for the system ranges working under the NM

Results of the simulations, presented in figure 6.1, show that the among the studied configuration, the one bases on the JA Solar JAP6-60/275/4BB PV panel and a KACO Powador 36.0 TL inverter is financially the most attractive. The PV system of 36,3 kWp will bring the highest Net Present Value over the 25 year lifetime of the investment. Surprisingly, even though the LG panels offer the best efficiency and the lowest degradation, due to their high price they are the least financially attractive option.

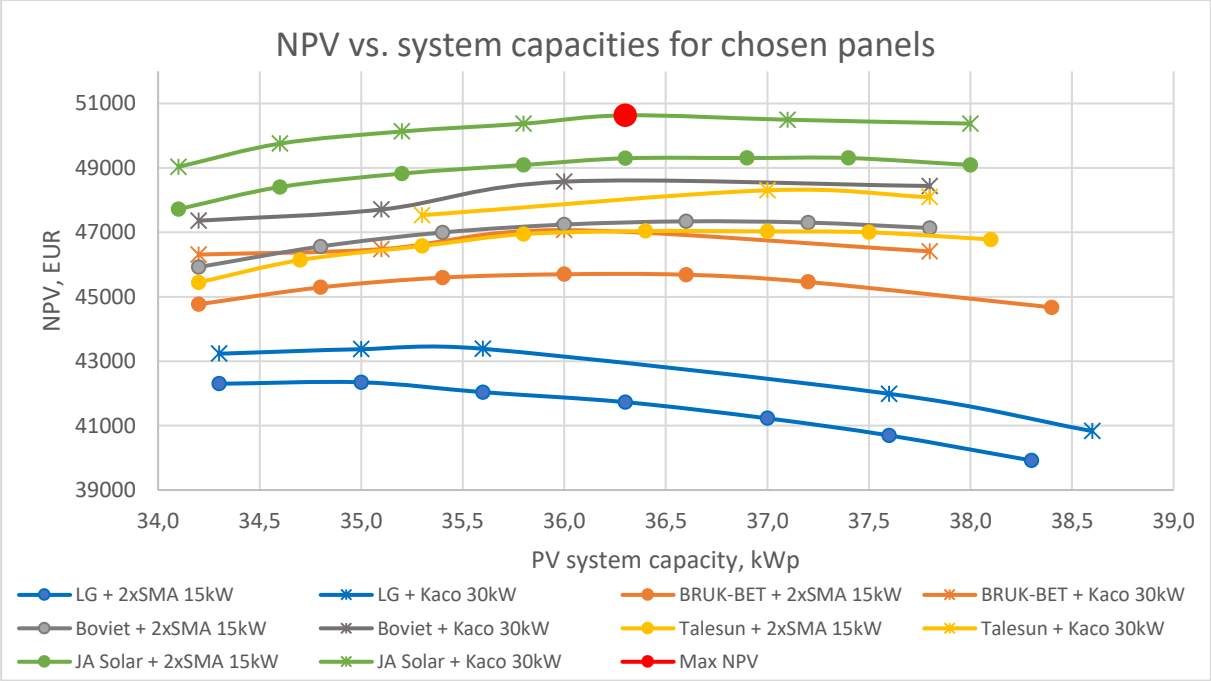

Figure 6.1 NPV vs. system capacities - for NM support scheme

It can be seen on the below figure 6.2, that there is a conflict between the highest NPV and the highest IRR. As mentioned in the chapter regarding economic assessment, such situation is common for a mutually excluding options, which is the case. This means that even though the internal rate of return is slower, the added monetary value by the end of the project's lifetime will be bigger.

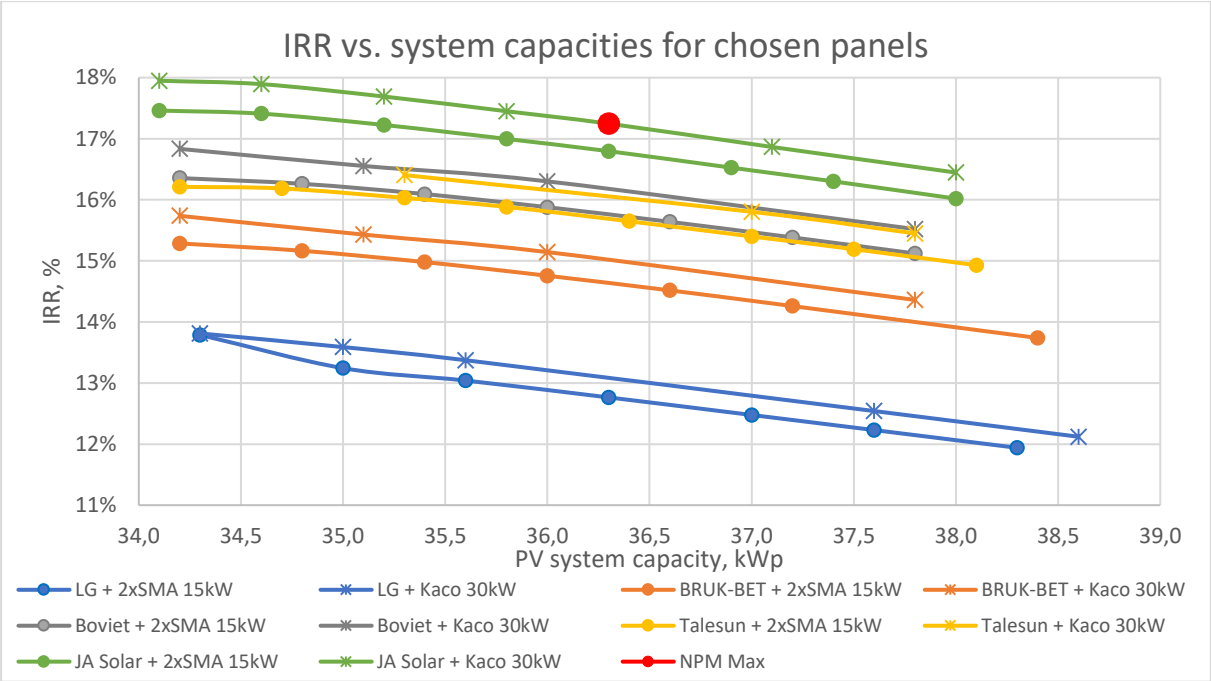

Figure 6.2 IRR vs. system capacities - for NM support scheme

The DPP varies considerably for the studied capacities. As can be seen in the figure 6.3, the shortest payback period is for the JA Solar + KACO set, and takes around 6 years for the system to pay off, whereas for the most expensive option it could take even 9 years.

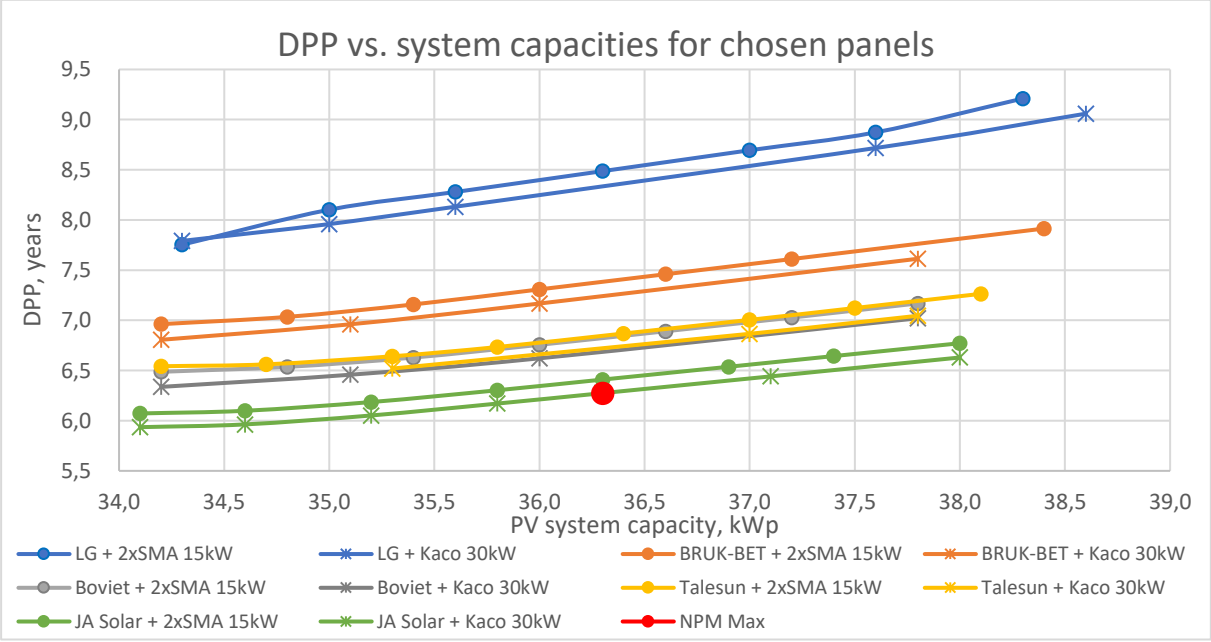

Figure 6.3 DPP vs. system capacities - for NM support scheme

Similarly to the IRR, a conflict can be seen between the optimal system size in terms of the DPP and NPV. The reason being, that even though the system will take longer time to pay itself off, the financial benefits will be grater over the lifetime of the project.

As presented in figure 6.4, LCOE of the most optimal configuration is of around 0.048 EUR/kWh making it a competitive option.

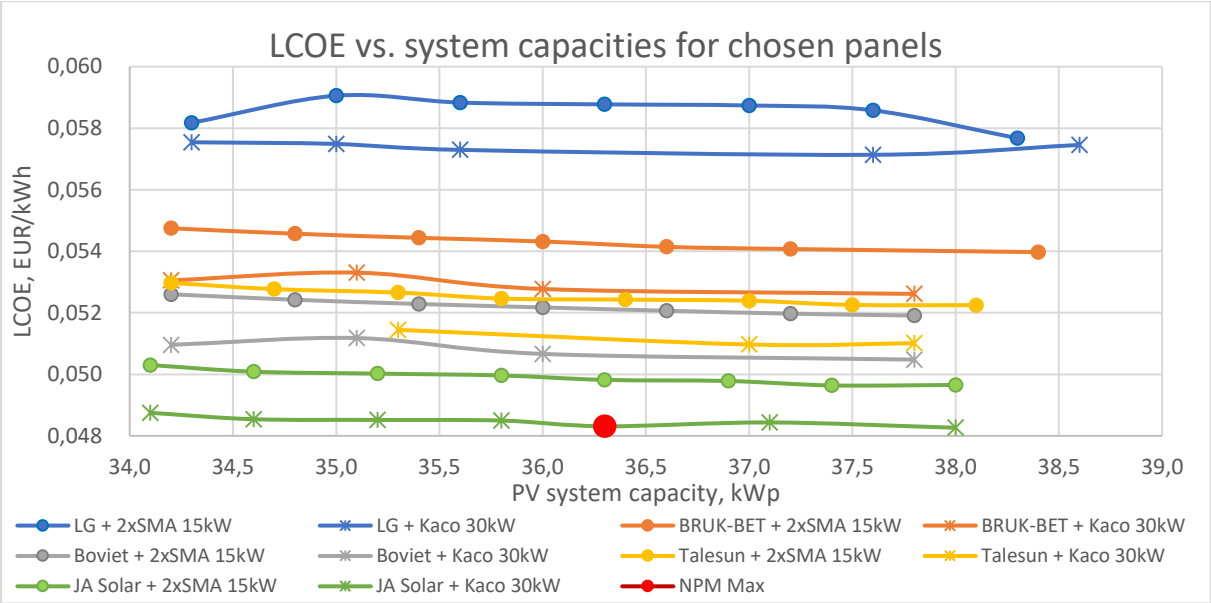

Figure 6.4 LCOE vs. system capacities - for NM support scheme

6.1.2 Results for the system ranges working under the FIT

Results of the simulations for FIT support, presented in figure 6.6 indicate that the optimum system should be one bases on the JA Solar JAP6-60/275 PV panels and a KACO Blueplanet 20.0 TL3 inverter. The optimal PV system, marked with the red dot, has 21.4 kWp of nominal power, as it will bring the highest Net Present Value over the 25 year lifetime of the investment. It can be noticed that the NPVs for the FIT option are around 3 to 4 times smaller than the configurations working under NM scheme.

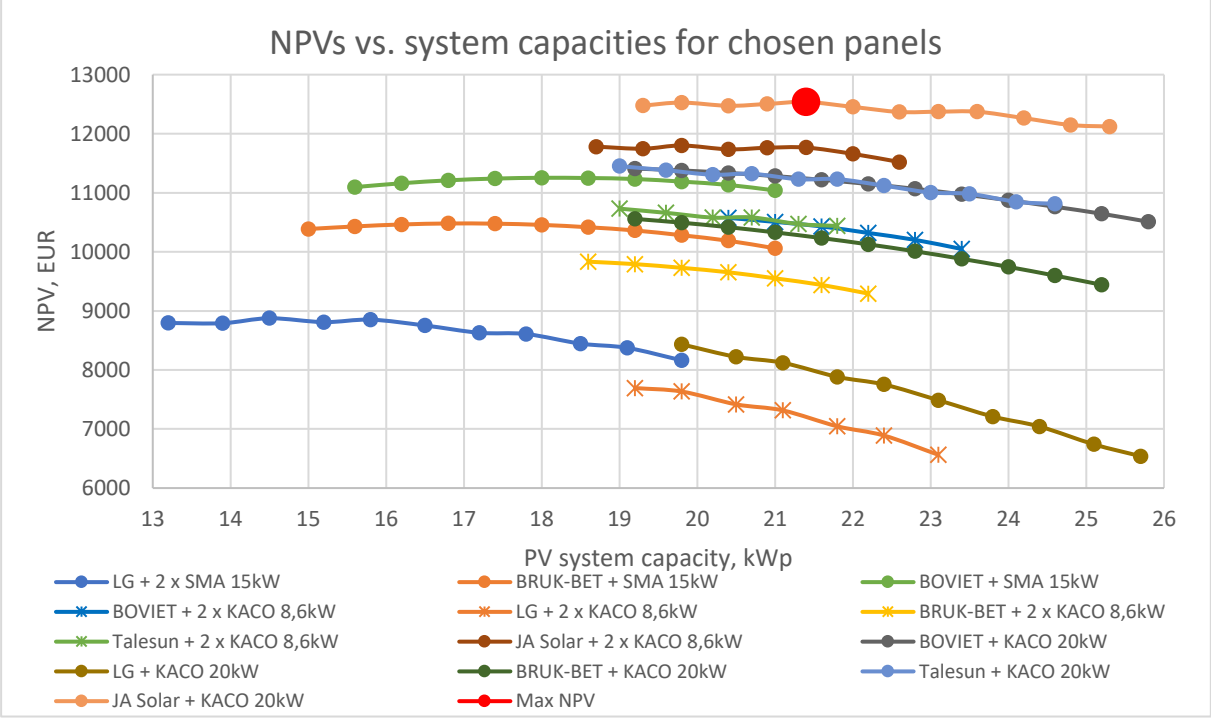

Figure 6.5 NPV vs. system capacities - for FIT support scheme

When it comes to IRR, the same conflict as before is noticed – the highest IRR value and the highest

NPV are not matching. The explanation is as previously, meaning that accumulated monetary value over the lifetime of the project is more important than the rate of return. Values of IRR are smaller than the ones in NM option, making the investment under this legislation less profitable and attractive.

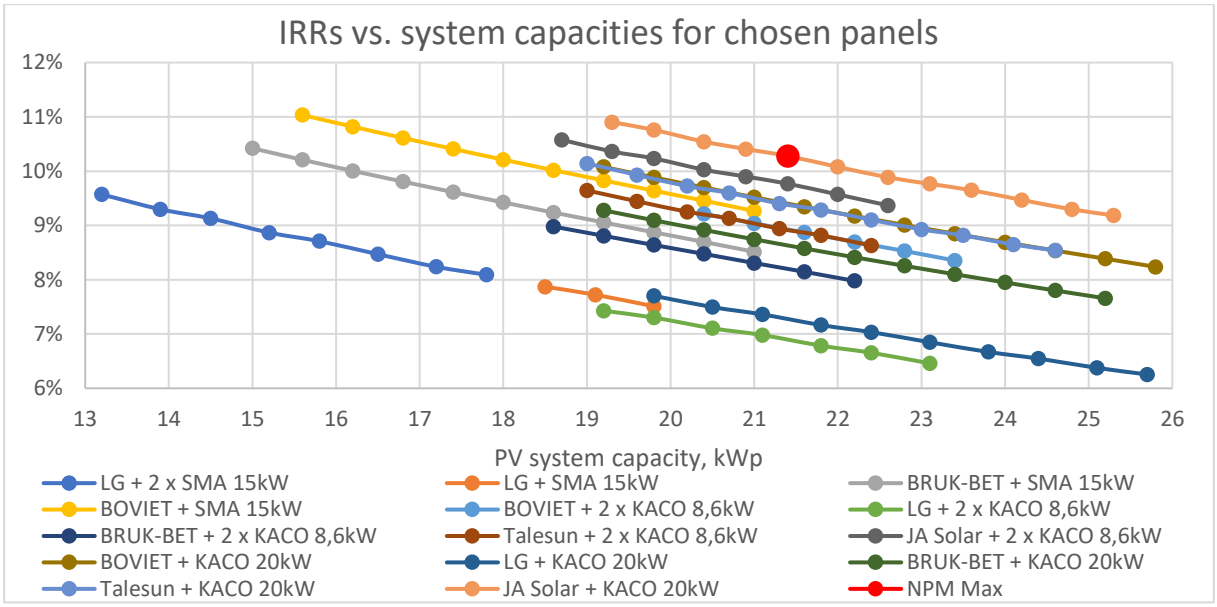

Figure 6.6 IRR vs. system capacities - for FIT support scheme

From the figure 6.7 for the FIT support mechanism it can be seen, that it takes around 11 years for the optimal configuration to pay back, which is around twice longer than for the NM. The DPPs of the studied configurations, ranges from 10.5 to 17 years.

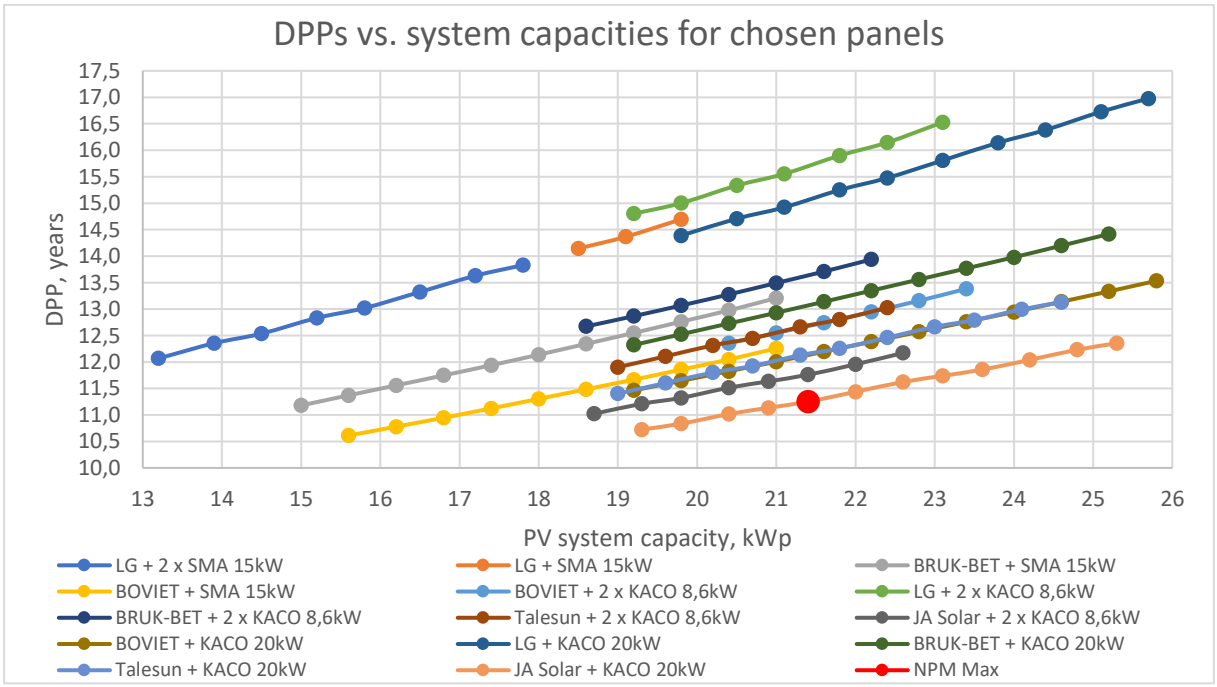

Figure 6.7 DPP vs. system capacities - for FIT support scheme

Even though the previous indicators of the economic analysis were looking less attractive for the FIT, the LCOE of the optimal system, shown in figure 6.8, is nearly the same. Regardless of the support scheme, the levelized cost of electricity is of around 0.048 EUR per installed kWh.

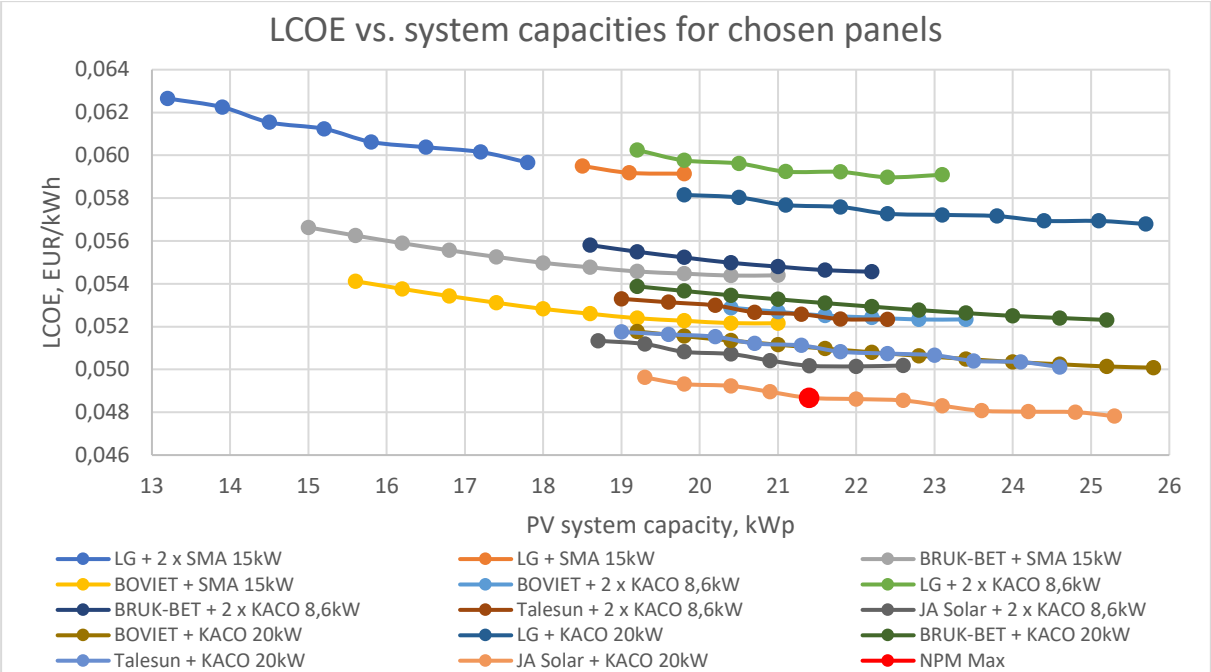

Figure 6.8 LCOE vs. system capacities - for FIT support scheme

6.2 Optimal system for the NM support mechanism

The PV system configuration optimized for NM support mechanism, presented in table 6.1, should be composed of 132 PV panels from JA Solar, inclined at 41° in respect to the horizon.

Table 6.1 Optimal PV system for NM support scheme - Configuration

PV modules	
Manufacturer	JA Solar
Model	JAP6-60-275/4BB
Nominal PV module power	275 Wp
Number of modules	132
Modules area	216 m2
Inclination in respect to the horizon	41°
Nominal PV system power	36.3 kWp
Inverter	
Manufacturer	KACO New Energy
Model	Powador 36 TL3 XL
Nominal power	30 kWac
Number of MPPTs	3
Number of inverters	1
Pnom ratio	1.21
MPPT string configurations	
MPPT 1:	2x22
MPPT 2:	2x22
MPPT 3:	2x22

The optimal PV system, would have a nominal power of 36.3 kWp, and would be linked with a 30 kWac KACO inverter into 3 MPP tracers. Each tracker will receive a string of 2 panels in parallel and 22 in series. The ratio of PV panels nominal power ratio to the inverter nominal power is 1.21. System's layout on the roof, as well as the shading analysis is presented in the Annex.

Table 6.2 gathers the results of the system's production and financial performance. The designed system will have a specific annual yield of 1017 kWh/kWp in the annual bases, resulting in the 36,9 MWh of produced electricity during the first year. The amount surpasses the electricity demand, however due to the NM, the surplus electricity injected into the grid was later partially recovered. This allowed to achieve a staggering 96.88% of solar fraction, being the percentage share of the electricity provided from PV in the total project's lifetime electricity consumption. Performance ratio is estimated for a 85.7%

Table 6.2 Optimal PV system for NM support scheme – Performance results

System performance (at a 1st year)	
Nominal PV system power	36.3 kWp
Specific annual yield	1017 kWh/kWp/year
PV system production	36.9 MWh/year
Electricity demand	27.3 MWh/year
Electricity covered immediately from PV system	10.8 MWh/year
Electricity recovered from the grid	16.5 MWh/year
Electricity purchased from the grid	3.9 MWh/year
Solar fraction	96.88%
Performance ratio	85.70%
Financial performance (over 25 years)	
CAPEX	31 165 EUR
OPEX	312 EUR/year
Avg. Annual cost	1 788 EUR/year
NPV	50 632 EUR
IRR	17.25%
LCOE	0.048 EUR/kWh
DPP	6.3 years

From the financial side, the initial investment would be of around 31 000 EUR, and the average discounted running costs of the system close to 300 EUR/year. The system will offer substantial energy savings – the average annual cost is projected to be around 1800 EUR/year in comparison to the baseline 3800 EUR/year where no PVs are installed. Over the 25 years the accumulated NPV of the investment will be of around 50 000 EUR, with the IRR at the level of 17%. Under those performance conditions, the system will pay off in a little bit over 6 year. The LCOE of the system is 0.048 EUR/kWh.

When looking at the monthly bars of electricity balances from figure 6.9, it can be seen that the production is largest during summer months, when the amount of available sun light is the biggest. Due to the mismatch between production and consumption, even during the summer months, the electricity demand is not fully covered directly from the installation. However, thanks to the Net Metering, the missing electricity demand is covered from the recovered electricity which was previously injected into the grid.

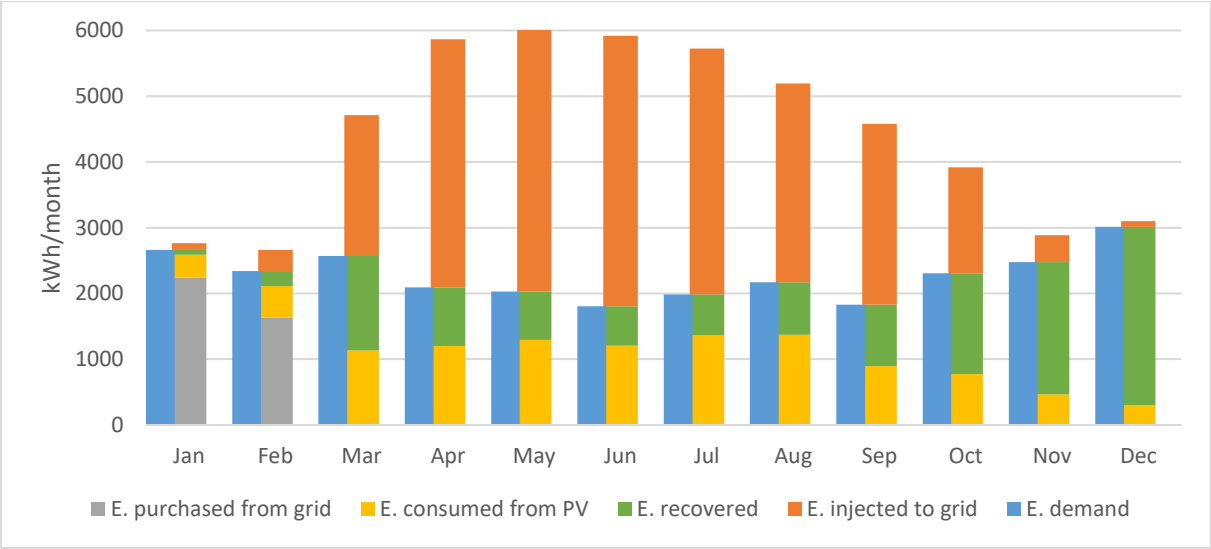

Figure 6.9 Monthly values of electricity balances – NM

From the figure 4.10, regarding the normalized production per installed kWp, it can be seen that the biggest collection losses of the PV array occur during summer months. This should be associated with the higher ambient temperatures which affect negatively the power output of the PV cells. The effect is due to reduction of a semiconductor band gap with the increase of temperature. The parameter mostly affected in the PV cell is the open-circuit voltage, which drops rapidly with the increase of temperature.

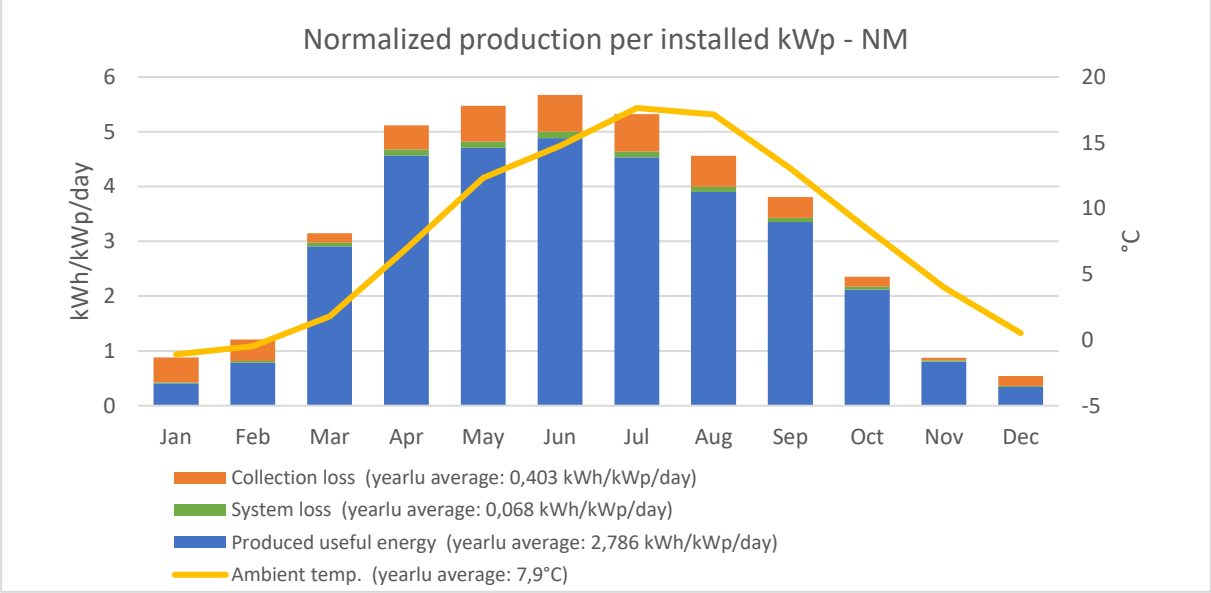

Figure 6.10 Monthly normalized production per installed kWp for and a temperature - NM

To better visualize the efficiency of production, a performance ratio (PR) of the PV installation was evaluated. PR is the ratio of the actual and theoretical outputs of the PV generation system, commonly measured over the period of one year. The formula for manual calculations of PR is given as [54]:

$$PR = \frac{E_{AC}}{\bar{H} \times A \times \eta} \times 100\% \quad \text{(Eq.48)}$$

where:

E_{AC} = AC electrical output of the PV system, measured over a given time period [kWh]

$\bar{H}$ = average solar irradiation intensity, measured over a given time period [kWh/m^2]

A = generator area of the PV system [m^2]

η = rated efficiency of the PV modules [%]

The PR is a measure of the quality of the PV installation, as it shows the proportion of the actually available energy after deducing all the system's energy losses. PR is stated in %, and the closer the PR gets to 100%, the higher is the system's performance. High-performance systems are expected to have a yearly level of PR of around 80-85%. As the measure is largely independent of the PV set orientation and incident solar irradiation, it is commonly used for comparing systems in different locations [67].

The monthly variations of PR for the studied PV set optimized for NM, are shown in figure 6.11. The annual average PR is of 85.7%, indicating high performance of the designed system. It can be observed that from March to November the PV system works close to the theoretical output with the PR close to 90%. The decrease in PR observed from December to February is due to the snow layer covering the photovoltaic cells.

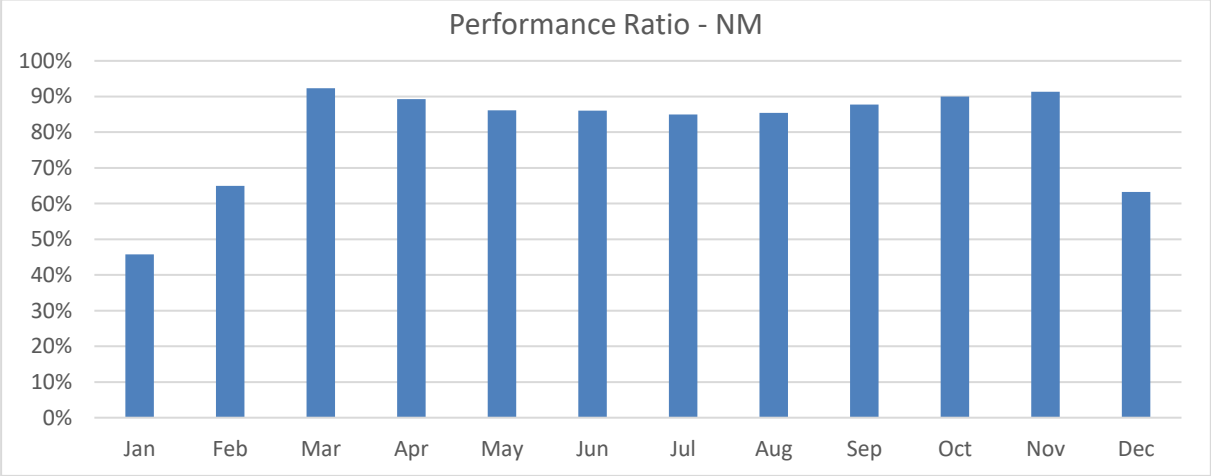

Figure 6.11 Performance Ratio - NM

6.3 Optimal system for the FIT support mechanism

The configuration for the system optimized for FIT is shown in table 6.3. It should be composed of 78 PV panels from JA Solar, inclined at 39° in respect to the horizon. The 21.4 kWp PV system should be linked with a KACO Blueplanet 20 kWac inverter which has 2 MPP tracers. The first tracker will receive a string of 2 panels in parallel and 19 in a series, and the second one 2 in parallel and 20 in a series The ratio of PV panels nominal power to the inverter nominal power is 1.09. Layout of the system and analysis of shading are presented in the Annex.

Table 6.3 Optimal PV system for FIT support scheme - Configuration

PV modules	
Manufacturer	JA Solar
Model	JAP6-60-275/4BB
Nominal PV module power	275 Wp
Number of modules	78
Modules area	127.5 m2
Inclination in respect to the horizon	39°
Nominal PV system power	21.4 kWp
Inverter	
Manufacturer	KACO New Energy
Model	Blueplanet 20.0 kW TL3
Nominal power	20 kWac
Number of MPPTs	2
Number of inverters	1
Pnom ratio	1.09
MPPT string configurations	
MPPT 1:	2x19
MPPT 2:	2x20

Production performance of the system optimized for NM, as well as its lifetime financial results are aggregated in table 6.4.

The designed system produces 21.8 MWh of electricity per year with a specific annual yield of 1016 kWh/kWp. The amount is lower than the 27.3 MWh electricity demand, as FIT doesn't allow for recovering surplus electricity in ejected into the grid. Under this legislation, the surplus is sold to the grid at the average market price of electricity from the previous quarter. Those prices are however much lower than the purchasing prices for the consumers. For this reason the designed system is smaller than the one for NM option. As a consequence, the solar fraction is much smaller, covering approximately 32% of electricity demand directly from the PV system. The remaining part is bought in this case from the grid. Performance ratio is slightly smaller, averaging 80.9%.

The initial investment would be of a little over 18 000 EUR, and the average discounted running costs of the system close to 180 EUR/year. The system will offer a slight reduction energy savings – the average annual cost is projected to be around 3300 EUR/year in comparison to the baseline 3800 EUR/year where no PVs are installed. Over the 25 years the accumulated NPV of the investment will be of around 12 500 EUR, which is nearly 4 times less than for the NM option. The IRR is projected at the level of 10%. Under those performance conditions, the system will pay off in a little bit over 11 year. The LCOE of the system is 0.049 EUR/kWh.

Table 6.4 Optimal PV system for FIT support scheme -- Performance results

System performance (at a 1st year)	
Nominal PV system power	21.4 kWp
Specific annual yield	1016 kWh/kWp/year
PV system production	21.8 MWh/year
Electricity demand	27.3 MWh/year
Electricity covered from PV system	9.4 MWh/year
Electricity sold to the grid	12.4 MWh/year
Electricity purchased from the grid	17.8 MWh/year
Solar fraction	31.83%
Performance ratio	80.96%
Financial performance (over 25 years)	
CAPEX	18 280 EUR
OPEX	183 EUR/year
Avg. Annual cost	3 312 EUR/year
NPV	12 538 EUR
IRR	10,28%
LCOE	0.049 EUR/kWh
DPP	11.3 years

When looking at the monthly bars of electricity balances from the figure 6.12, it can be seen that the production is largest during summer months, however the difference between production and consumption is much smaller, owing to the smaller capacity of the system. The highest rates of self-consumption are observed between May and June, whereas during winter nearly all electricity must be purchased from the grid.

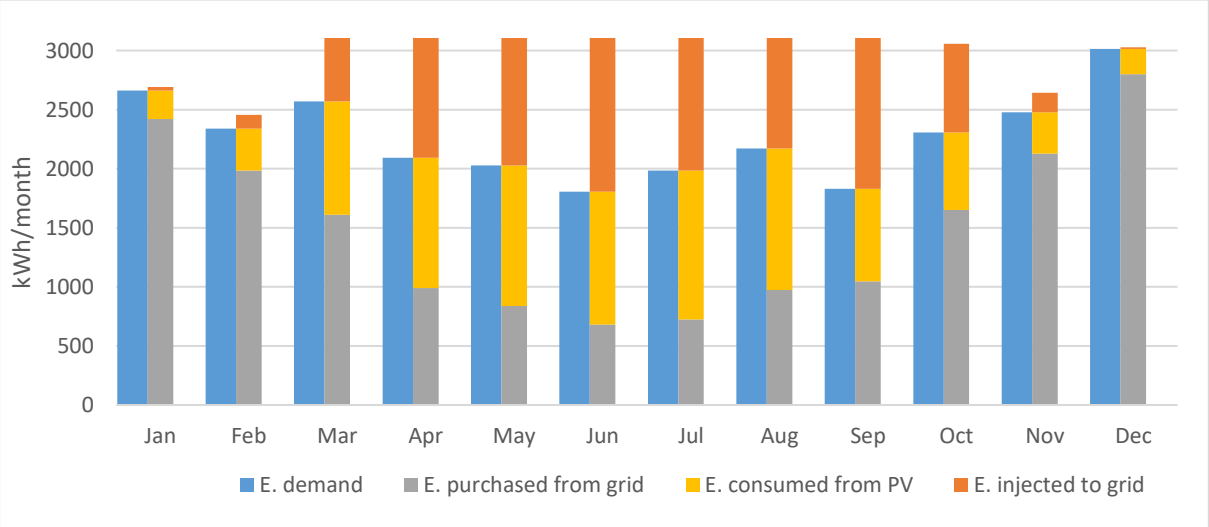

Figure 6.12 Monthly values of electricity balances - FIT

Bar chart with normalized production per installed kWp is presented in figure 6.13. Identically as for NM, the biggest nominal collection losses of the PV array occur during summer months, which should be associated with the negatively temperature effect on the power output of the PV cells.

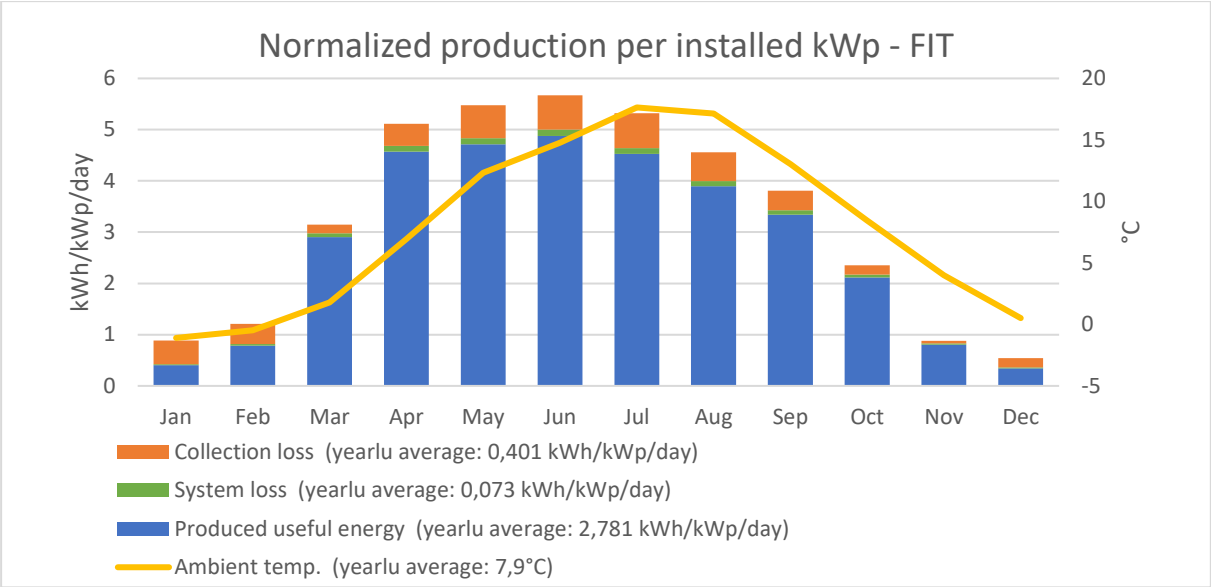

Figure 6.13 Monthly normalized production per installed kWp for and a temperature

Monthly variations of PR can be seen in figure 6.14. Similarly as for NM, it can be observed that from March to November the PV system works close to the theoretical output with the PR close to 90%. The decrease in PR observed from December to February is due to the snow layer covering the photovoltaic cells.

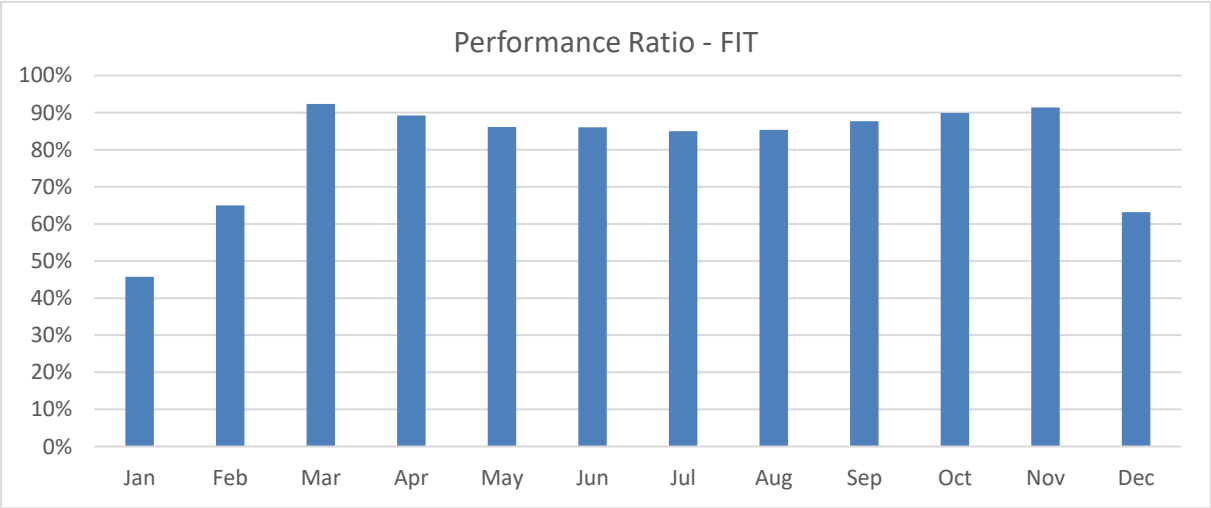

Figure 6.14 Performance Ratio - FIT

6.4 Comparison of energy profiles

To capture the essential difference between NM and FIT support schemes, it is worth comparing the energy profiles of the studied facility for both scenarios. 2 first years of PV system's operation were plotted in figure 6.15, assuming that the installation will start operating in January 2020.

The first figure presents the case of NM. It can be seen that during the first two months of operation, it will be necessary to purchase additional electricity from the grid to cover the demand. However, later, due to the appropriate sizing of the installation, energy shortages will be covered with energy recovered from the grid.

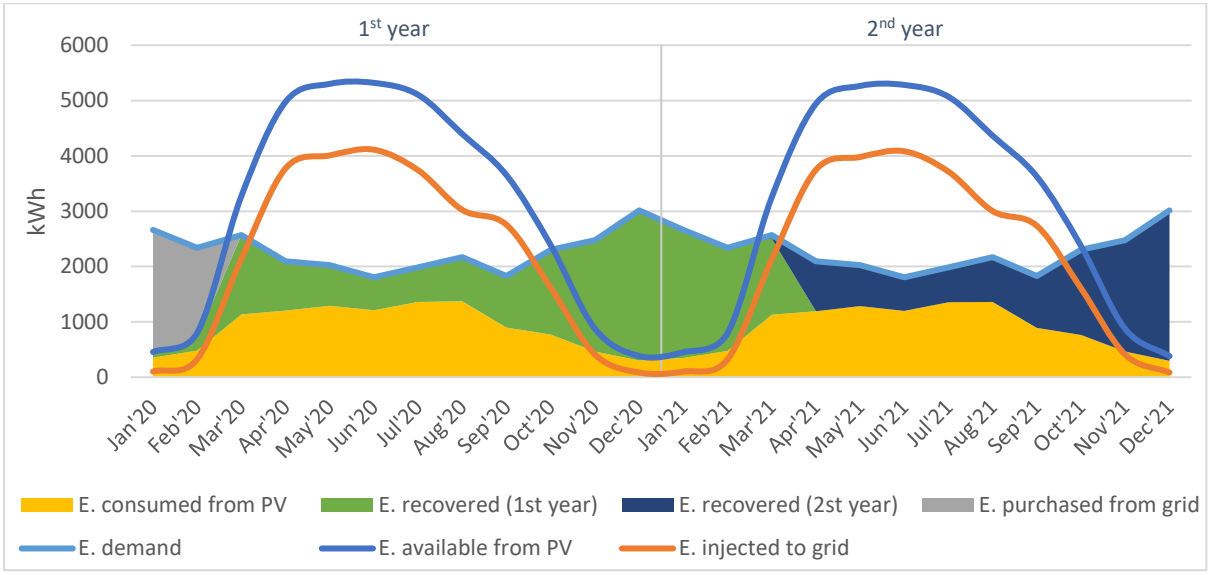

Figure 6.15 Energy profile of the facility - NM

Net-metering regulations state that it is possible to recover energy stored in the grid within 365 days from the date of its injection. Hence, the shortages of electricity in April 2020 will still be covered from the energy produced in 2019.

In contrast, as seen from figure 6.16, the system working under FIT support scheme will require purchases of electricity from the grid in every month. In fact, in this case we can only talk about the reduction in electricity spending, which is highest during summer months. The surplus electricity injected into the grid can only be sold to the grid, not stored in it.

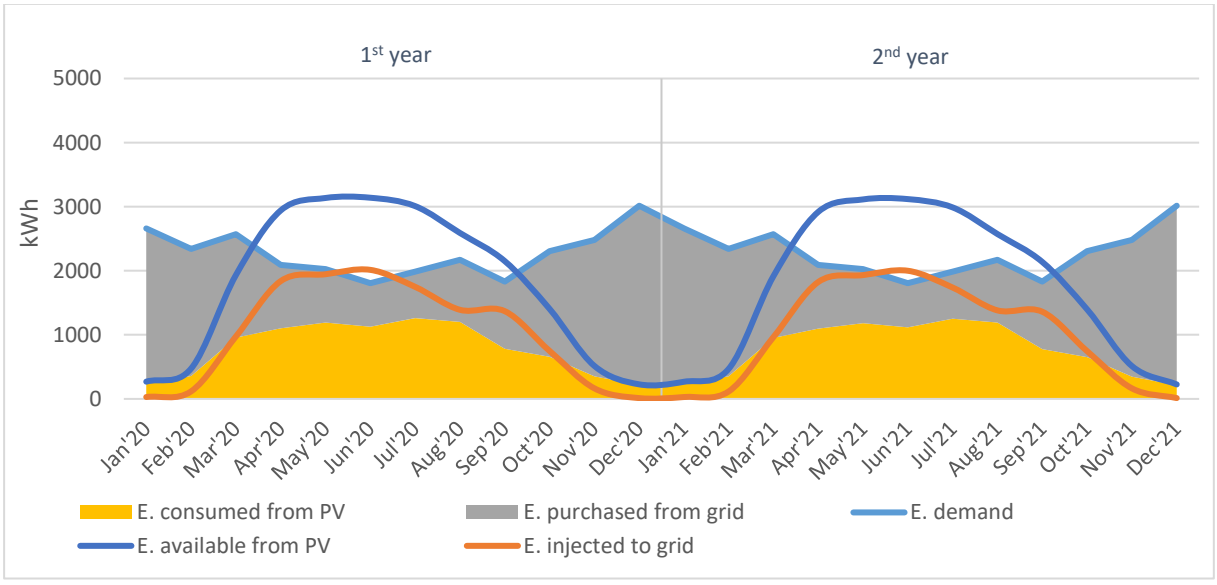

Figure 6.16 Energy profile of the facility – FIT

6.5 Comparison of produced and consumed energy

The pie charts in figure 6.17 present the aggregated values of energy that the systems will produce over the period of 25 years. The 36.3 kWp solar system optimised for NM will produce a total of 851 MWh. Around 29% of it will be immediately consumed and the remaining 71% will be injected into the grid. The 21.4 kWp system optimised for FIT will produce proportionally less – 501 MWh over its lifetime. Even though the system is nearly twice smaller, the nominal amount of energy consumed immediately from the PV set is just a bit smaller – 217 MWh in comparison to 249 MWh of the NM system. This is due to the inability of matching the momentary energy production with its demand. In result, the rate of self-consumption changes disproportionately with the increasing capacity. The effect was well depicted during the preliminary analysis.

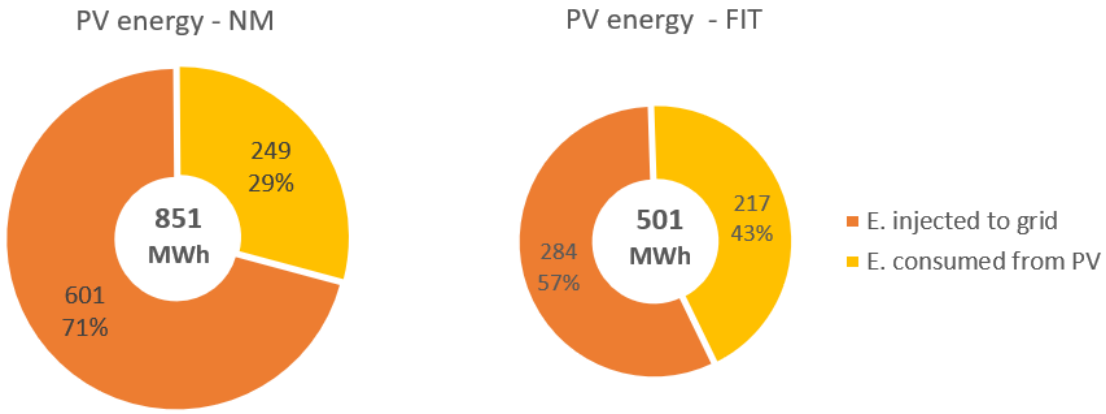

Figure 6.17 Comparison of the energy produced from the PV system during 25 years of operation

The below pie charts present the share of sources from which the facility's electricity demand will be covered. Both circles are of the same size, as the demand is constant, equalling 682 MWh in 25 years. It is predicted that the system optimised for NM will require only around 3% of consumed electricity to by purchased from the grid, whereas for the FIT system a staggering 68% will be bought. As discussed before, this not as much due to the difference in the system's capacity, but mostly thanks to the possibility of recovering part of surplus energy injected to the grid in the NM scheme. Owing to this feature, system optimised for NM satisfies 60% of its demand from the energy recovered from the grid, achieving a 97% self-consumption rate.

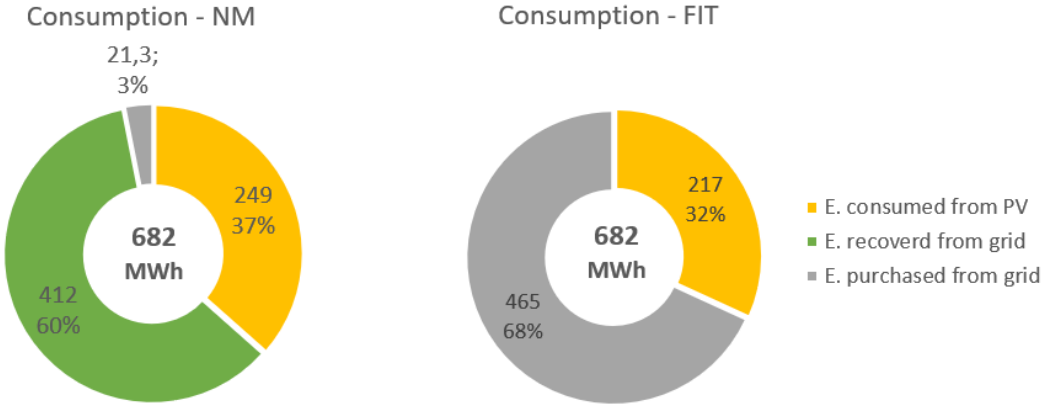

Figure 6.18 Comparison of the energy consumption during 25 years of operation

6.6 Comparison of cashflows and discounted payback time

In order to visualise the financial performance of two scenarios, cashflows of the systems optimized for both FIT and NM were respectively plotted on figures 6.19 and 6.20. Red bars indicate a negative, discounted cumulative CF and the green bars a positive one. The final bar, in year 25th represents the final NPV of the system. An orange line depicts the changes in each year net present value of the CF. Both charts begin at year 0, in which all capital expenditure is incurred. System optimised for NM costs around 31 000 EUR, whereas the one optimised for FIT slightly over 18 000 EUR. The NM system will pay off between 6th and 7th year, while the system working under FIT will take around 5 years more to break even. Lower NPVs in the 10th and 20th, visible as the small dents in the orange line, result from the increased O&M costs, deriving from the need for inverter(s) replacement. By the end of the assumed 25 year lifecycle, the FIT system is expected to reach the NPV of around 12 500 EUR. In contrary, the system optimised for NM would generate the NPV of around 50 500 EUR, making it a much more financially attractive option.

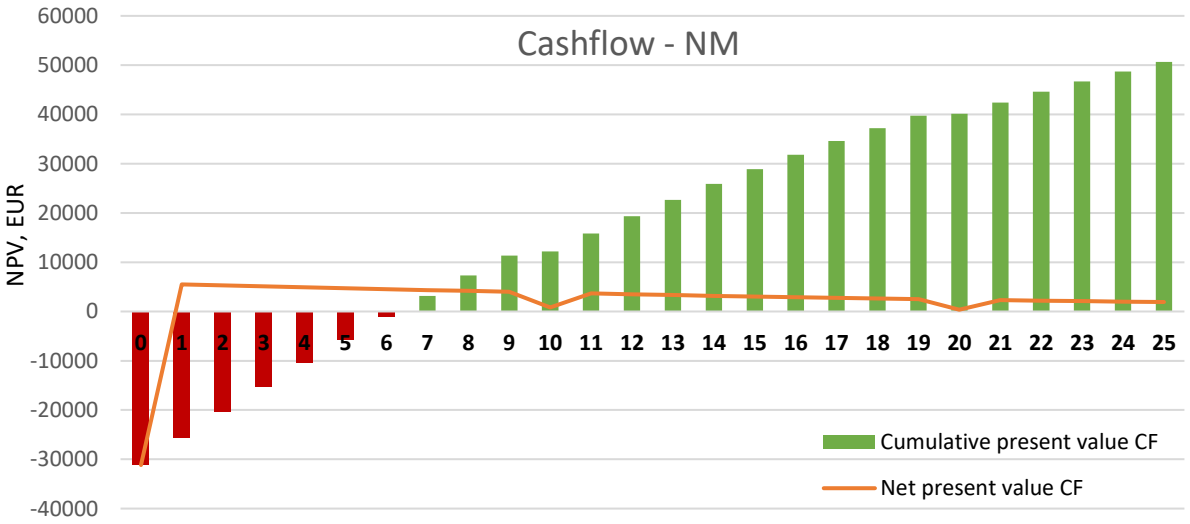

Figure 6.19 Cashflows for the PV system optimised for NM

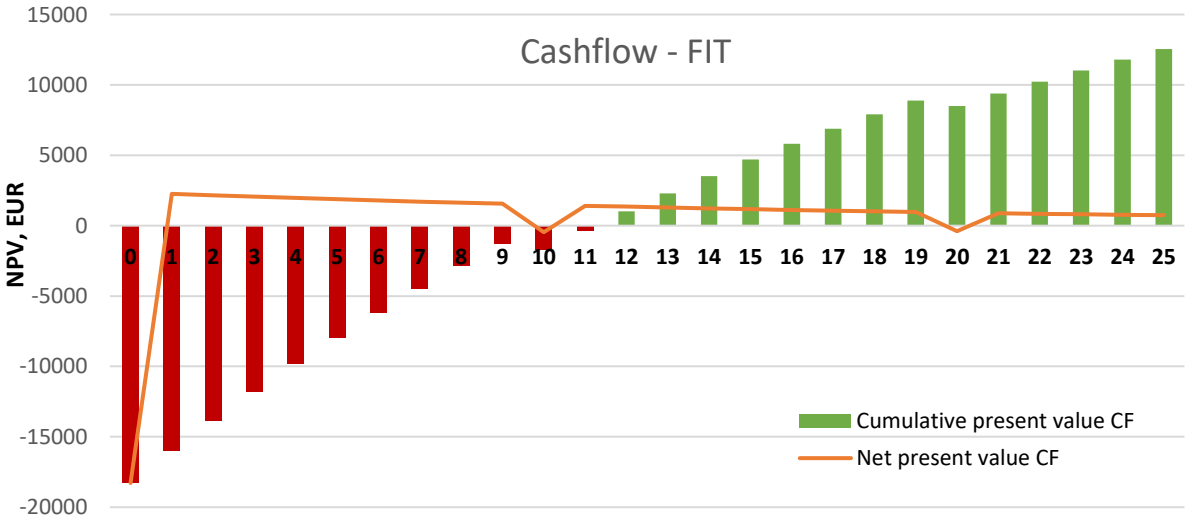

Figure 6.20 Cashflows for the PV system optimised for FIT

6.7 Sensitivity analysis

In order to determine how changes of individual variables could affect the two most important for the investor financial indicators of the model – NPV and DPP, a local sensitivity analysis was conducted. A one-at-a-time technique was used, in which only one parameter at a time has been changed and the rest was kept constant. The chosen parameters were changed in the range of ±20% with a step of 5% points. Variables selected for the analysis that were common for both systems were: CAPEX, OPEX, electricity demand, price of purchased electricity and a discount rate. Additionally, a net metering ratio (a maximum ratio of the energy recovered from the grid to the energy previously injected – currently 0.7) was tested for NM option, and an influence of the price of sold electricity and the income tax were analysed for FIT scenario.

6.7.1 Sensitivity analysis of the system optimised for NM

Sensitivity analysis on NPV and DPP were plotted respectively on figures 6.21 and 6.22. By analysing them, it can be noted that the most influential variable is the price of purchased electricity. With the 20% increase of electricity prices, the NPV would grow by 35%, and the DPP would fall from 6.3 to 5.1 years.

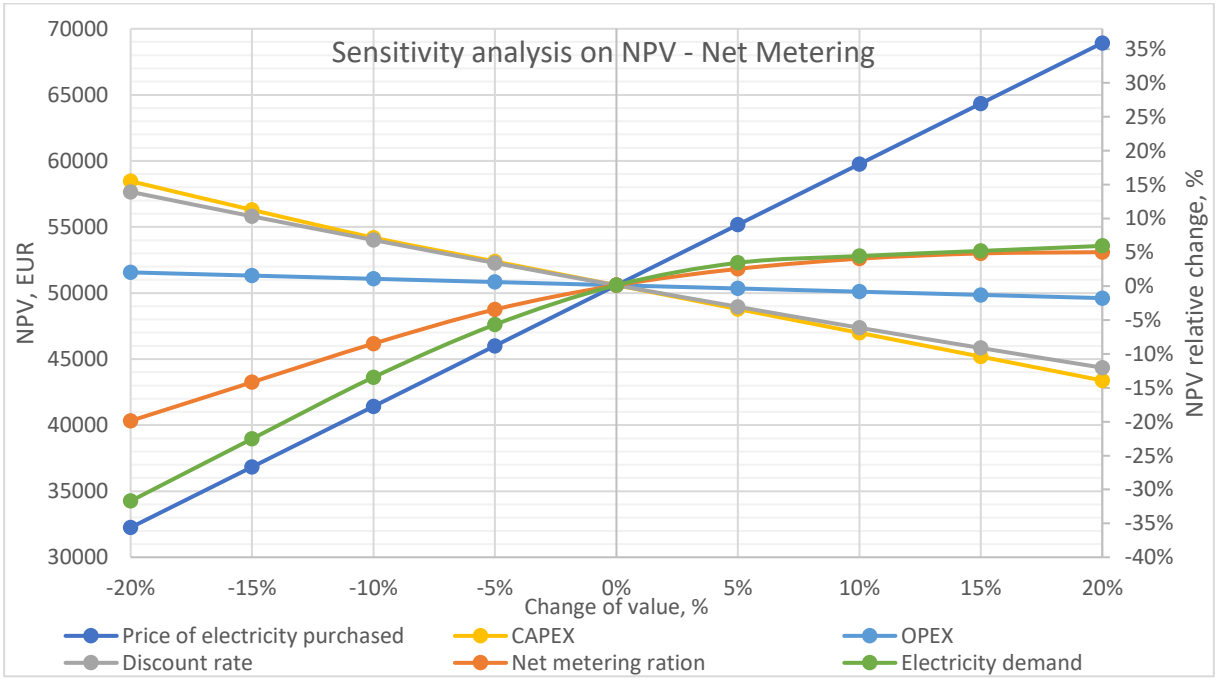

Figure 6.21 Sensitivity analysis on NPV for the system optimised for NM

The reason for such a strong dependence may be surprising, especially since the system optimised for NM is expected to purchase just 3% of its total energy demand from the grid. Yet, it is crucial to remember that the level of investment's attractiveness, here expressed by the NPV, is always benchmarked against the baseline scenario. This means that in a situation in which the electricity prices would fall, the savings resulting from having a PV installation, and with them the NPV, would also decrease. Following the global trends, the prices of electricity will rather increase in the future [2], leading to a higher NPVs, which is a positive information for the investor.

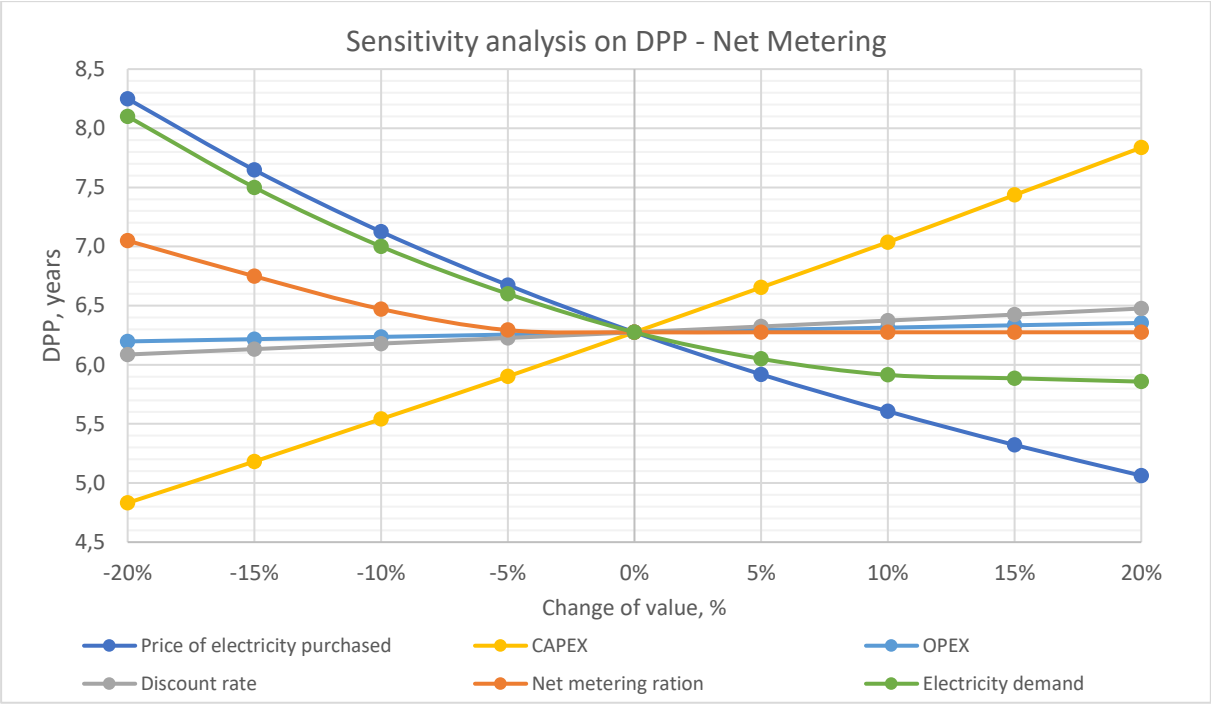

Figure 6.22 Sensitivity analysis on DPP for the system optimised for NM

The second variable that is likely to positively influence the NPV is the decrease of CAPEX. Over the last decade the prices of solar PV system components were falling, and the tendency is likely to continue for at least some time [68]. According to the sensitivity analysis, every 5% drop in CAPEX would increase the NPV by approximately 4% and reduce the DPP by roughly half a year.

Influences of changes in electricity demand and on the net metering ratio depend on the direction of a change. With the 20% increase of both, the NPV will slightly grow, by just 5%, and the DPP will decrease by half a year. However, if the percentage of the energy that can be recovered from grid will decline in the future the effects will be much more pronounced. Same stands true for the decline of facility's energy demand, although the effects will be even more noticeable on both NPV and DPP. It is hard to assess the risk connected to the change of those parameters, as it is difficult to estimate the direction in which they will possibly shift in the future.

Additional simulations were performed to determine what change in individual parameters would turn the investment's NPV to 0. One case that would make it happen, would be a 55% decrease in energy demand to the level of 11 900 kWh/year. Also if the price of electricity would drop below 0.1 EUR/kWh, the investment would not be able to pay itself off. The last instance, under which the NPV would become negative, would be caused by decrease of NM recovery ratio from the current 70% to below 6%. This in practice means that in the absence of NM support scheme, the designed PV system would not be financially viable.

6.7.2 Sensitivity analysis of the system optimised for FIT

Looking at the range of NPV relative change, shown in figure 6.23, it can be concluded that the system optimised for FIT is more vulnerable to changes of the selected variables. The ±20% variations of electricity purchase price would change the NPV in a range of ±50%. As the tendency indicates that the electricity prices will grow, it is likely that the final NPV of the system will be higher than predicted at the moment. In such case, judging from the figure 6.24, it is possible that the DPP will be less than 10 years, especially when looking at the influence of CAPEX.

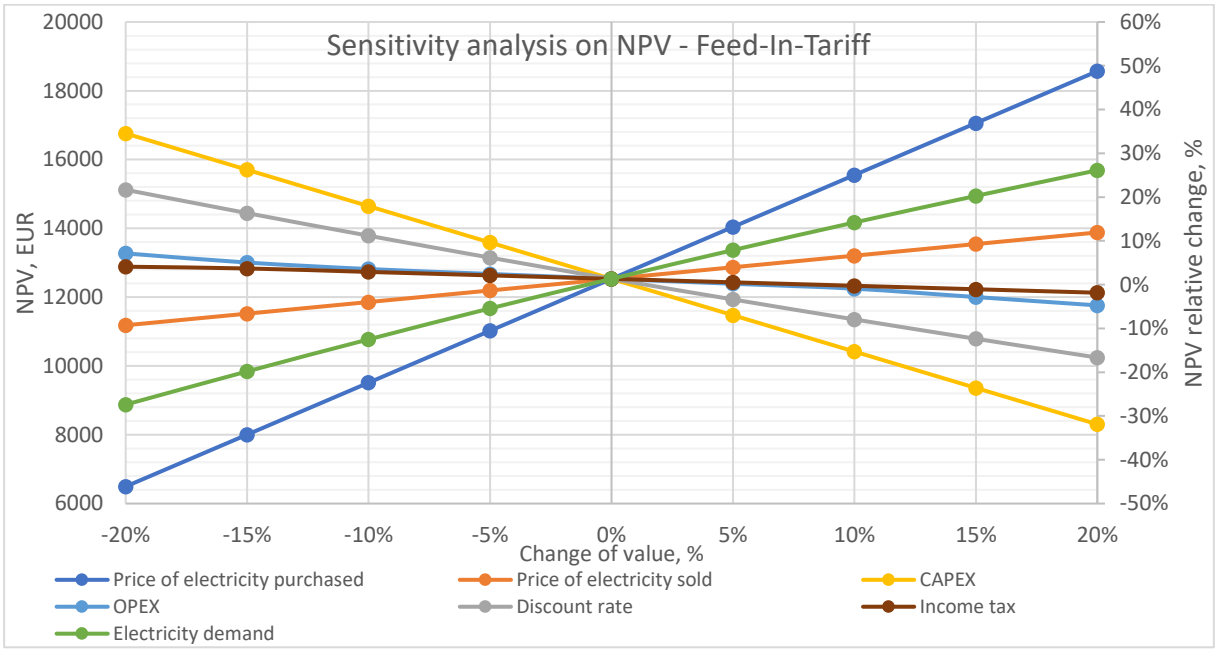

Figure 6.23 Sensitivity analysis on NPV for the system optimised for FIT

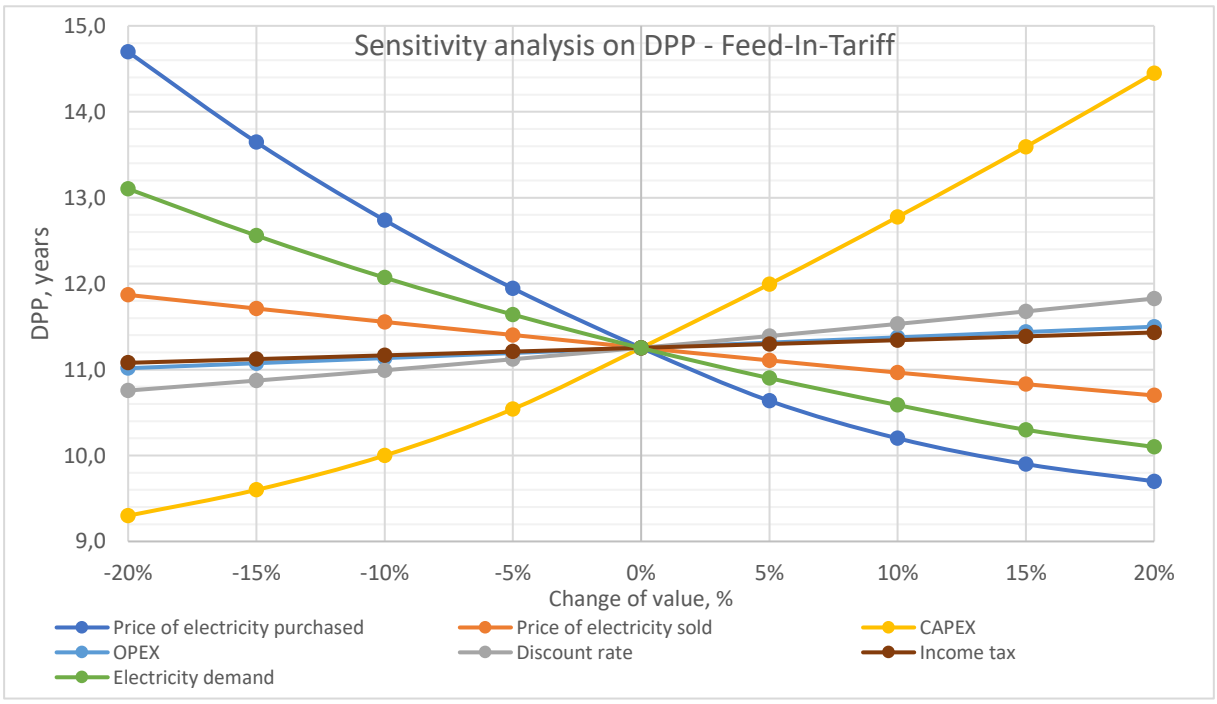

Figure 6.24 Sensitivity analysis on DPP for the system optimised for FIT

Only through the decrease of initial capital expenditure by 10%, the system optimised for FIT would pay off 1.5 years earlier. This would also increase the NPV by 20%.

The increases of both facility's electricity demand and the prices of electricity sold to the grid have a positive, linear influence on the system's attractiveness. However, as the line of electricity demand is steeper than the one of the selling price, it can be concluded that the prior has a more significant influence on the system's NPV.

The analysis also shows that the increase of both OPEX and income tax negatively affects the financial performance, though the influences are marginal.

Similarly as for NM, additional simulations were carried out for the FIT system to determine under which conditions the NPV of the investment would equal 0. It turned out that if the facility's energy demand drops by 70%, to around 7 800 kWh/year, the investment will end with a negative NPV. Another case could be a drop in electricity prices below 0.13 cents/kWh. Simulations have shown, that even if the FIT support system was terminated, and the utility would not offer any compensation for the energy injected into to grid (price of sold electricity would equal 0 cents/kWh), the designed system would still be financially viable. In such pessimistic case, the cumulative NPV after 25 years of operation would reach approximately 6 000 EUR – slightly less than a half of that is forecasted for when the FIT support mechanism stays unchanged.

Chapter 7

Conclusions and recommendations

This chapter finalises this work, by summarising its content and drawing conclusions. Recommendations for the future actions are also included.

The purpose of this thesis was to find the optimal configuration of the rooftop PV generation system for the warehouse located in the northern part of Poland. The system has been optimized in terms of the highest expected financial benefits, expressed by the NPV, generated over the 25 years of the project's lifetime. Due to the current alterations in the Polish energy law regarding support for the solar installations, and the still uncertain direction of those changes, optimization of the studied system has been done in respect to the two possible regulatory outcomes – continuation of the Feed-In-Tariff support scheme or adoption of the Net-Metering support mechanism.

Designing and optimization of the PV system was a complex and time-consuming task. The main challenges encountered during this thesis were:

- Estimation of building's electricity demand is a daunting task, if neither historical measurements of the consumption are present, nor smart-metering devices are in place. This was the issue of the case study, and it required utilizing the bottom-up method for the estimation. The challenge in this approach was to make the inventory of all major electrical devices to be found in the building, especially as it hasn't been commissioned yet. Even more difficult task was to predict the patters of their use - how frequently, at what time, and for how long. The interviews conducted with the employees, designers and the investor proved to be very helpful in determining those usage patterns,
- Although there is quite a lot of software to simulate the production of a PV system, none of them was suitable for conducting a thorough economic analysis in terms of the specifics of the Polish system. As a result, it was necessary to build an extensive calculation model which would combine results from the PV simulation software regarding the amounts of energies produced, demanded, consumed, sold, purchased and recovered from the grid, with the provisions of the energy policies and economics, which was a demanding and complex task,
- Simulating the performance of various PV system configurations was extremely time-consuming due to the inability to automate the process. The reason for this was the need to manually make configuration adjustments and export the results from the PVsyst software, for each of the numerous iterations
- Due to the abundance of PV modules and inverters available on the market, their selection can be overwhelming.

One of the essential parts of this thesis was conducting a preliminary study, based on generic components. Results obtained during this step were valuable, as they narrowed down the search range for the optimal PV system size. Simulations indicated that for NM the optimal capacity lies somewhere within a range of 34 kWp to 44 kWp, with the NPV of around 45 000 EUR. The optimal installed power of the FIT system lies between 13 kWp and 22 kWp, with a predicted NPV close to 12 000 EUR.

Results of the preliminary study also showed the scale of influence which policy has on the system's NPV. Comparing installations with the same nominal power, the NM supported system generated significantly larger NPVs. For the capacity of 20 kWp the NM system generated twice higher NPV than the installation supported by FIT, and for the capacity of 40 kWp the difference was 5-fold bigger. At their optimal configurations, the annual cost saving ratio would be close to 45% for the NM case, and

maximally of around 12% for the system optimized for FIT.

It was also interesting to notice that the level of self-consumption for the system supported by FIT mechanism was not increasing proportionally with the rise of nominal power of the PV system. A small surge was observed for PV system capacities between 10 kWp and 27 kWp, however later, until 45 kWp the level of self-consumption remained unchanged. On contrary, the share of energy demand covered by PV was rising linearly with the growing capacity of the system supported by NM.

Results of the detailed simulation pointed out the optimal setups of the PV generation system. In case the Polish lawmakers decide to stay with the FIT support mechanism, the optimal system should be composed of 78 PV modules from JA Solar, connected into 2 MPP trackers of the 20 kWac inverter from KACO New Energy. The nominal power of the PV installation would be of 21,4 kWp and the modules should optimally be inclined by 39° in respect to the horizon. With such system, on average, 32% of facility's electricity consumption would be covered from PVs. The initial investment of around 18 000 EUR would be paid off in a little over 11 years, generating over 25 years of operation an NPV of 12 500 EUR, at an internal rate of return close to 10%. However, if the upcoming amendments in the energy law adapt the NM support mechanism, then the optimal installation would be nearly twice as big. Precisely, it should have a nominal power of 36.3 kWp, based on 132 JA Solar modules connected into 3 MPP trackers of the 30 kWac KACO New Energy inverter. The optimal inclination of the modules in respect to the horizon would be 41°. With such system the facility would cover nearly 97% of its electricity demand from solar energy. Initial investment would be of around 31 000 EUR, and by the end of the project's lifetime the system would generate an NPV of around 50 500 EUR, at the IRR of 17.25%

Comparing the optimal configuration with the estimates drawn during the preliminary study, it can be concluded that the optimal capacities fall within the predicted range, and the forecasted NPVs differed just by around 10%, which makes the model reliable.

Results of the detailed simulations showed that regardless of the support mechanism, PV module from JA Solar are economically most attractive. Surprisingly, the model from LG, which outruns the selected competitors in terms of efficiency, degradation rate and overall performance, due to the moderately higher price, turned out be the financially the least attractive option.

Sensitivity analysis showed that the three parameters that most affect the NPV of the tested PV systems are: prices of electricity, facility's electricity demand and CAPEX. With the rise of the first two parameters and the fall of the third one, the NPV increased. The global trends suggest, the prices of electricity will most likely rise in the future. As the amount of electrical devices around us grows continuously, the building's need for electricity is also presumably keep growing. During the last 10 years, the prices of PV modules and inverters have fallen significantly and are expected to fall further. If the above predictions prove to be true, systems NPV will be higher than currently estimated. This reduces the risk of investment, positively influencing the moods of investors and hopefully encouraging them to expand more extensively their PV systems portfolio.

Considering that the decision on the direction of legal changes regarding the micro-PV installations support system is soon to come, to mitigate the risk associated with the investment, the author of the works suggests to wait with the purchasing the PV system until the legal situation is certain.

References

[1] International Energy Agency (IEA), “World Energy Outlook 2018,” 2018.

[2] International Renewable Energy Agency (IRENA), *Global Energy Transformation: A Roadmap to 2050*. 2018.

[3] P. Moriarty and D. Honnery, “What is the global potential for renewable energy?,” *Renew. Sustain. Energy Rev.*, vol. 16, no. 1, pp. 244–252, Jan. 2012.

[4] Interstate Renewable Energy Council, “Field Inspection Guideline for PV Systems,” Vacaville, 2010.

[5] S. Barak and S. S. Sadegh, “Forecasting energy consumption using ensemble ARIMA–ANFIS hybrid algorithm,” *Int. J. Electr. Power Energy Syst.*, vol. 82, pp. 92–104, Nov. 2016.

[6] J. K. Gruber, S. Jahromizadeh, M. Prodanović, and V. Rakočević, “Application-oriented modelling of domestic energy demand,” *Int. J. Electr. Power Energy Syst.*, vol. 61, pp. 656–664, Oct. 2014.

[7] L. Chuan and A. Ukil, “Modeling and validation of electrical load profiling in residential buildings in Singapore,” in *2015 IEEE Power & Energy Society General Meeting*, 2015.

[8] L. G. Swan and V. I. Ugursal, “Modeling of end-use energy consumption in the residential sector: A review of modeling techniques,” *Renew. Sustain. Energy Rev.*, vol. 13, no. 8, pp. 1819–1835, Oct. 2009.

[9] M. Sepehr, R. Eghtedaei, A. Toolabimoghadam, Y. Noorollahi, and M. Mohammadi, “Modeling the electrical energy consumption profile for residential buildings in Iran,” *Sustain. Cities Soc.*, vol. 41, no. March, pp. 481–489, 2018.

[10] J. V. Paatero and P. D. Lund, “A model for generating household electricity load profiles,” *Int. J. Energy Res.*, vol. 30, no. 5, pp. 273–290, Apr. 2006.

[11] N. Heidari, J. Gwamuri, T. Townsend, and J. M. Pearce, “Impact of Snow and Ground Interference on Photovoltaic Electric System Performance,” *IEEE J. Photovoltaics*, vol. 5, no. 6, pp. 1680–1685, Nov. 2015.

[12] E. Andenæs, B. P. Jelle, K. Ramlo, T. Kolås, J. Selj, and S. E. Foss, “The influence of snow and ice coverage on the energy generation from photovoltaic solar cells,” *Sol. Energy*, vol. 159, no. September 2017, pp. 318–328, 2018.

[13] D. K. Perovich, “Light reflection and transmission by a temperate snow cover,” *J. Glaciol.*, vol. 53, no. 181, pp. 201–210, Sep. 2007.

[14] R. W. Andrews, A. Pollard, and J. M. Pearce, “The effects of snowfall on solar photovoltaic performance,” *Sol. Energy*, vol. 92, no. April 2013, pp. 84–97, 2013.

[15] A. Orioli and A. Di Gangi, “Review of the energy and economic parameters involved in the effectiveness of grid-connected PV systems installed in multi-storey buildings,” *Appl. Energy*, vol. 113, pp. 955–969, 2014.

[16] J. L. Bernal-Agustín and R. Dufo-López, “Economical and environmental analysis of grid connected photovoltaic systems in Spain,” *Renew. Energy*, vol. 31, no. 8, pp. 1107–1128, Jul. 2006.

[17] A. Audenaert, L. De Boeck, S. De Cleyn, S. Lizin, and J. F. Adam, “An economic evaluation of photovoltaic grid connected systems (PVGCS) in Flanders for companies: A generic model,” *Renew. Energy*, vol. 35, no. 12, pp. 2674–2682, 2010.

[18] L. Dusonchet and E. Telaretti, “Economic analysis of different supporting policies for the production of electrical energy by solar photovoltaics in eastern European Union countries,” *Energy Policy*, vol. 38, no. 8, pp. 4011–4020, Aug. 2010.

[19] L. Dusonchet and E. Telaretti, “Comparative economic analysis of support policies for solar PV in the most representative EU countries,” *Renew. Sustain. Energy Rev.*, vol. 42, pp. 986–998, Feb. 2015.

[20] M. T. García-Álvarez, L. Cabeza-García, and I. Soares, “Assessment of energy policies to promote photovoltaic generation in the European Union,” *Energy*, vol. 151, pp. 864–874, May 2018.

[21] A. Poullikkas, “A comparative assessment of net metering and feed in tariff schemes for residential PV systems,” *Sustain. Energy Technol. Assessments*, vol. 3, pp. 1–8, Sep. 2013.

[22] G. C. Christoforidis, A. Chrysochos, G. Papagiannis, M. Hatzipanayi, and G. E. Georghiou, “Promoting PV energy through net metering optimization: The PV-NET project,” *Renew. Energy Res. Appl.*, pp. 1117–1122, 2013.

[23] P. Pereira da Silva, G. Dantas, G. I. Pereira, L. Câmara, and N. J. De Castro, “Photovoltaic distributed generation – An international review on diffusion, support policies, and electricity sector regulatory adaptation,” *Renew. Sustain. Energy Rev.*, vol. 103, no. December 2018, pp. 30–39, 2019.

[24] E. D. Mehleri, P. L. Zervas, H. Sarimveis, J. A. Palyvos, and N. C. Markatos, “Determination of the optimal tilt angle and orientation for solar photovoltaic arrays,” *Renew. Energy*, vol. 35, no. 11, pp. 2468–2475, Nov. 2010.

[25] I. H. Rowlands, B. P. Kemery, and I. Beausoleil-Morrison, “Optimal solar-PV tilt angle and azimuth: An Ontario (Canada) case-study,” *Energy Policy*, vol. 39, no. 3, pp. 1397–1409, Mar. 2011.

[26] A. Malara, C. Marino, A. Nucara, M. Pietrafesa, F. Scopelliti, and G. Streva, “Energetic and Economic Analysis of Shading Effects on PV Panels Energy Production,” *Int. J. Heat Technol.*, vol. 34, no. 3, pp. 465–472, 2016.

[27] J. Bany and J. Appelbaum, “The effect of shading on the design of a field of solar collectors,” *Sol. Cells*, vol. 20, no. 3, pp. 201–228, Apr. 1987.

[28] J. K. Copper, A. B. Sproul, and A. G. Bruce, “A method to calculate array spacing and potential system size of photovoltaic arrays in the urban environment using vector analysis,” *Appl. Energy*, vol. 161, pp. 11–23, Jan. 2016.

[29] N. N. Castellano, J. A. Gázquez Parra, J. Valls-Guirado, and F. Manzano-Agugliaro, “Optimal displacement of photovoltaic array’s rows using a novel shading model,” *Appl. Energy*, vol. 144, pp. 1–9, Apr. 2015.

[30] A. K. Ioannou, N. E. Stefanakis, and A. G. Boudouvis, “Design optimization of residential grid-connected photovoltaics on rooftops,” *Energy Build.*, vol. 76, pp. 588–596, 2014.

[31] J. D. Mondol, Y. G. Yohanis, and B. Norton, “Optimal sizing of array and inverter for grid-connected photovoltaic systems,” *Sol. Energy*, vol. 80, no. 12, pp. 1517–1539, Dec. 2006.

[32] G. Notton, V. Lazarov, and L. Stoyanov, “Optimal sizing of a grid-connected PV system for various PV module technologies and inclinations, inverter efficiency characteristics and locations,” *Renew. Energy*, vol. 35, no. 2, pp. 541–554, 2010.

[33] X. Gong and M. Kulkarni, “Design optimization of a large scale rooftop photovoltaic system,” *Sol. Energy*, vol. 78, no. 3, pp. 362–374, Mar. 2005.

[34] H. Ren, W. Gao, and Y. Ruan, “Economic optimization and sensitivity analysis of photovoltaic system in residential buildings,” *Renew. Energy*, vol. 34, no. 3, pp. 883–889, 2009.

[35] A. Kornelakis and Y. Marinakis, “Contribution for optimal sizing of grid-connected PV-systems using PSO,” *Renew. Energy*, vol. 35, no. 6, pp. 1333–1341, Jun. 2010.

[36] “Moc zainstalowana (MW) - Potencjał krajowy OZE w liczbach - Urząd Regulacji Energetyki.” [Online]. Available: https://www.ure.gov.pl/pl/oze/potencjal-krajowy-oze/5753,Moc-zainstalowana-MW.html. [Accessed: 10-Jun-2019].

[37] R. Macuk, “Transformacja energetyczna w Polsce,” Warszawa, 2019.

[38] G. Wiśniewski, A. Curkowski, A. Więcka, B. Pejas, and J. Zarzeczna, “Annual Report on

Photovoltaic Market in Polad - 2018," Warszawa, 2018.

[39] "Legal sources on renewable energy," 2019. [Online]. Available: http://www.res-legal.eu/search-by-country/poland/. [Accessed: 01-Jun-2019].

[40] Ministry of Finance, *Taxation forms in case of using renewable energy sources*. Poland.

[41] National Fund for Environmental Protection and Water Management, "Informacje o programie / Prosument-dofinansowanie mikroinstalacji OZE (2015-2020)." [Online]. Available: https://www.nfosigw.gov.pl/oferta-finansowania/srodki-krajowe/programy-priorytetowe/prosument-dofinansowanie-mikroinstalacji-oze/informacje-o-programie/. [Accessed: 01-Jun-2019].

[42] *Act on Renewable Energy Sources*. Poland: Journal of Laws of the Republic of Poland, 2019.

[43] PAP, "Standing Committee of the Council of Ministers confirms to expands the prosumer's status for enterprises." [Online]. Available: https://www.cire.pl/item,181279,1,0,0,0,0,0,mpit-staly-komitet-rm-za-projektem-rozszerzajacym-status-prosumenta-o-male-i-srednie-firmy-.html. [Accessed: 03-Jun-2019].

[44] "Energa S.A - Tariff offer for small and medium companies. C11 Tariff details." [Online]. Available: https://www.energa.pl/dla-firmy/oferta-taryfowa-dla-firmy/male-i-srednie-firmy#c11. [Accessed: 19-Jun-2019].

[45] "©Fraunhofer ISE: Photovoltaics Report, updated: 14 March 2019."

[46] "Ile kosztuje instalacja fotowoltaiczna - GLOBEnergia," 2019. [Online]. Available: https://globenergia.pl/ile-kosztuje-instalacja-fotowoltaiczna/. [Accessed: 10-Jun-2019].

[47] J. A. Duffy and W. A. Beckman, *Solar Engineering of Thermal Processes*, 4th ed. Hoboken: John Wiley & Sons, Inc., 2013.

[48] A. Luque and S. Hegedus, *Handbook of Photovoltaic Science and Engineering*. Wiltshire: John Wiley & Sons Inc, 2003.

[49] A. A. Mermoud and B. Wittmer, *PVsyst Users Manual*, no. January. 2016.

[50] R. Perez, P. Ineichen, R. Seals, J. Michalsky, and R. Stewart, "Modeling daylight Availability and Irradiance Components from Direct and Global Irradiance," *Sol. Energy*, vol. 44, no. 5, pp. 271–289, 1990.

[51] "Calculation methods and models used in the PV*SOL®." [Online]. Available: https://help.valentin-software.com/pvsol/calculation/. [Accessed: 03-Oct-2019].

[52] R. A. Messenger and J. Ventre, *Photovoltaic Systems Engineering*, 2nd ed. CRC Press, 2004.

[53] A. R. Jordehi, "Parameter estimation of solar photovoltaic (PV) cells: A review," *Renew. Sustain. Energy Rev.*, vol. 61, no. July, pp. 354–371, 2016.

[54] T. Ma, H. Yang, and L. Lu, "Solar photovoltaic system modeling and performance prediction," *Renew. Sustain. Energy Rev.*, vol. 36, pp. 304–315, 2014.

[55] A. Arshad, "Net Present Value is better than Internal Rate of Return," *Interdiscip. J. Contemp. Res. Bus.*, vol. 4, no. 8, pp. 221–219, 2012.

[56] M.-T. Bosch, J. Montllor-Serrats, and M.-A. Tarrazon, "NPV as a Function of the IRR: The Value Drivers of Investment Projects," *J. Appl. Financ.*, vol. 17, no. 2, pp. 41–45, 2007.

[57] M. Mowen, D. Hansen, and L. Heitger, *Fundamental Cornerstones of Managerial Accounting*, 4th ed. Manson: Cengage Learnings, 2012.

[58] M. Zeraatpisheh, R. Arababadi, and M. S. Pour, "Economic Analysis for Residential Solar PV Systems Based on Different Demand Charge Tariffs," *Energies*, vol. 11, no. 3271, pp. 1–19, 2018.

[59] "Corporate Finance & Accounting - Definition of the Internal Rate of Return (IRR)." [Online]. Available: https://www.investopedia.com/terms/i/irr.asp. [Accessed: 27-Aug-2019].

[60] F. M. Camilo, R. Castro, M. E. Almeida, and V. F. Pires, "Economic assessment of residential PV systems with self-consumption and storage in Portugal," *Sol. Energy*, vol. 150, pp. 353–362, 2017.

[61] N. Renewable Energy Laboratory, S. National Laboratory, S. Alliance, and S. National Laboratory Multiyear Partnership, “Best Practices for Operation and Maintenance of Photovoltaic and Energy Storage Systems; 3rd Edition,” 2018.

[62] “How Long Do Solar Inverters Last? (2019 Guide),” 2019. [Online]. Available: https://thosesolarguys.com/how-long-do-solar-inverters-last/. [Accessed: 16-Oct-2019].

[63] J. Remund, S. Muller, C. Studer, and R. Cattin, “Meteonorm Handbook part II : Theory Global Meteorological Database Version 7 Software and Data for Engineers , Planers and Education,” no. October, 2018.

[64] Deutsche Gesellschaft Für Sonnenenergie (Dgs), *Planning and Installing Photovoltaic Systems: A Guide for Installers, Architects and Engineers*. London: Routledge, 2013.

[65] C. Steve Doty, PE, *Commercial Energy Auditing Reference Handbook*, 3rd ed. Lilburn: The Fairmont Press, Inc., 2016.

[66] F. Issi, “The Determination of Load Profiles and Power Consumptions of Home Appliances,” *Energies*, vol. 11, no. 607, pp. 1–18, 2018.

[67] “Performance ratio - Quality factor for the PV plant.”

[68] A. Korfiati *et al.*, “Estimation of the Global Solar Energy Potential and Photovoltaic Cost,” *Int. J. Sustain. Energy Plan. Manag.*, vol. 09, pp. 17–30, 2016.

Annex

A.1 Full characteristics of selected PV modules and inverters

Table A.1.1 Full characteristics of the selected PV panels

Manufacturer	JA Solar	Talesun	Boviet	Bruk-Bet Solar	LG Electronics
Model	JAP6-60/275/4BB	TP660P - 280	BVM6610M-300 W	BEM 300	LG330N1C-A5
Technology	polycrystalline Si	polycrystalline Si	monocrystalline Si	monocrystalline Si	monocrystalline Si
Panel efficiency	16,5	17,1	18,4	18,44	19,3
Rated power PMPP (Wp)	275	280	300	300	330
Rated voltage VMPP (V)	31,4	29,4	32,2	32,5	33,7
Rated current IMPP (A)	8,75	7,04	9,32	9,25	9,8
Open-circuit voltage (V)	38,45	36	39,5	38,8	40,9
Short-circuit voltage (A)	9,26	7,49	9,84	9,85	10,45
Power tolerance	-0/+5W	-0/+5W	-0/+5W	-0/+5W	-0/+10W
NOCT (◦C)	45	44	45	43	45
Temp. coeff. of PMPP (%/◦C)	-0,410	-0,4	-0,4	-0,39	-0,37
Temp. coeff. of VOV (%/◦C)	-0,330	-0,3	-0,31	-0,31	-0,27
Temp. coeff. of IMP (%/◦C)	+0,058	+0,06	+0,06	+0,03	+0,03
Dimensions (mm)	1650 x 992 x 40	1640 x 991 x 35	1640 x 992 x 40	1640 x 992 x 40	1686 x 1016 x 40
Weight (kg)	18,2	18,5	18,4	18,3	18
Warranty	10 years limited product warranty, 25 years power output warranty: first year > 97,5%, at 10 years 91,2%, and by the 25th year, no less than 80%	10 years product warranty, 25 years power output warranty: first year 97%, after 1st year 0.5% annual degradation, at 25 years 85%	12 years limited product warranty, 25 years power output warranty: first year 97,5%, after 1st year 0.7% annual degradation, at 25 years 80%	15 years product warranty, 25 years power output warranty: first year 97%, after 1st year 0.6% annual degradation, at 25 years 83%	25 years product warranty, 25 years power output warranty: first year 98%, after 1st year 0.5% annual degradation, at 25 years 86%
Price (PLN)	439	516	549	643	900
Price (EUR)	102,1	120,0	127,7	149,5	209,3
Price/Wp (PLN)	1,60	1,84	1,83	2,14	2,73
Price/Wp (EUR)	0,37	0,43	0,43	0,50	0,63
Origin	China	Thailand	Vietnam	Poland	South Korea
Retailer	Soltech, Poland	Sonneko, Poland	Sonneko, Poland	Bruk-Bet, Poland	Recost, Poland

Table A.1.2 Full characteristics of the selected inverters

Manufacturer	KACO	SMA	KACO	KACO	KACO
Model	Blueplanet 8.6 TL3	Sunny Tripower 15000TL	Blueplanet 20.0 TL3	Powador 36.0 TL3	Blueplanet 15.0 TL3
Max DC power	8 800 W	15 330 W	24 000 W	36 000 W	18 000 W
MPPT voltage range	400 V - 800 V	240 V - 800 V	515 V -800 V	200 V - 800 V	420 V - 800 V
Operating voltage range	200 V - 1000 V	150 V - 1000 V	200 V - 1000 V	200 V - 1000 V	200 V - 1000 V
Max input current	2 x 11 A	2 x 33 A	2 x 20 A	2 x 34 A	2 x 20 A
Number of MPP trackers / max strings per MPPT	2 / 2	2 / 3	2 / 2	3 / 4	2 / 2
Load distribution on MPPT	symmetrical / asymmetrical	symmetrical / asymmetrical	symmetrical / asymmetrical	symmetrical / asymmetrical	symmetrical / asymmetrical
Rated AC power	8 600 W	15 000 W	20 000 W	30 000 W	15 000 W
AC voltage/frequency	230V / 50Hz	230V / 50Hz	230V / 50Hz	230V / 50Hz	230V / 50Hz
Euro Efficiency	98,1%	98%	98,1%	97,8%	97,7%
Night consumption	1,5 W	1 W	1,5 W	1,5 W	1,5 W
Connection phases	3	3	3	3	3
Circuity topology	transformerless	transformerless	transformerless	transformerless	transformerless
Dimensions	52 x 36 x 25 cm	66 x 68 x 26 cm	69 x 42 x 20 cm	136 x 84 x 35 cm	69 x 42 x 20 cm
Weight (kg)	30 kg	61 kg	47 kg	151 kg	47 kg
Warranty	5 years	5 years	5 years	5 years	5 years
Price (PLN)	6472	10793	11660	15990	9550
Price (EUR)	1505	2510	2712	3719	2221
Price/Wp (PLN)	0,753	0,720	0,583	0,640	0,637
Price/Wp (EUR)	0,175	0,167	0,136	0,149	0,148
Origin	Germany	Germany	Germany	Germany	Germany
Retailer	Soltech, Poland	Sonneko, Poland	Soltech, Poland	Soltech, Poland	Soltech, Poland

A.2 Visualization of the shadding simulations

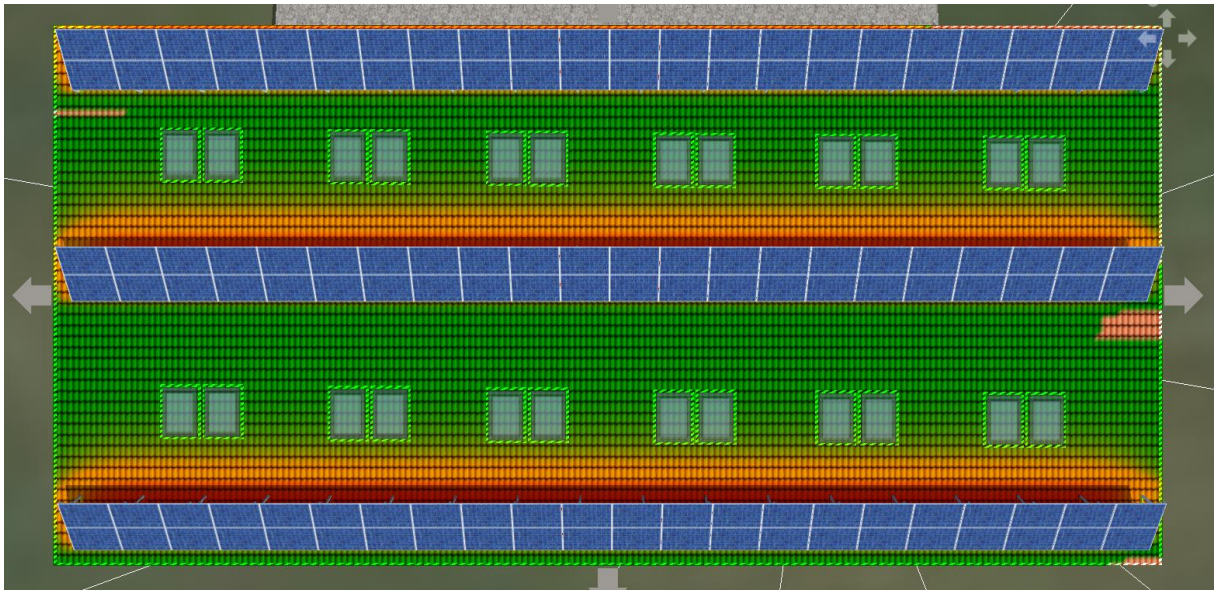

Figure A.2.1 Visualization of shading for the system optimized for NM

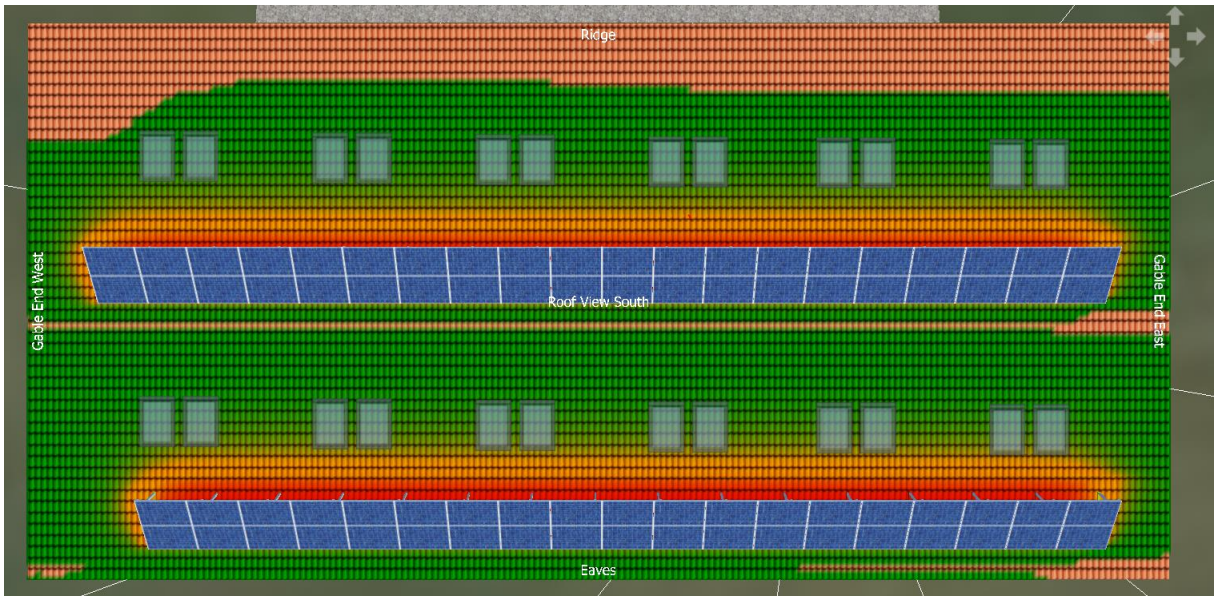

Figure A.2.2 Visualization of shading for the system optimized for FIT

A.3 PV systems layout on the building's roof

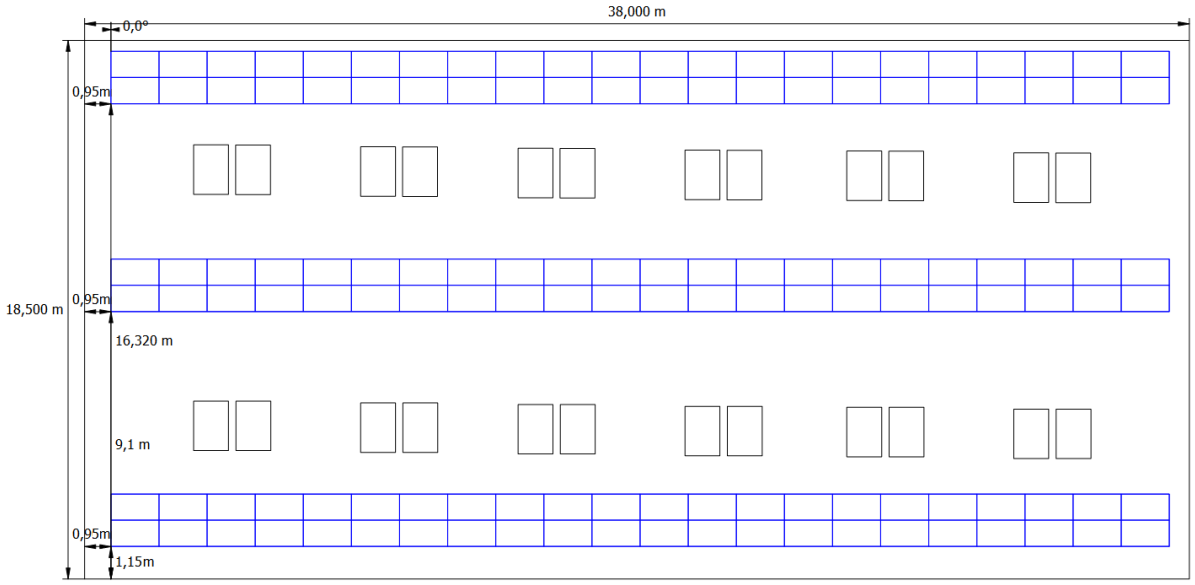

Figure A.3.2 Top view with dimensions of the PV system optimized for NM

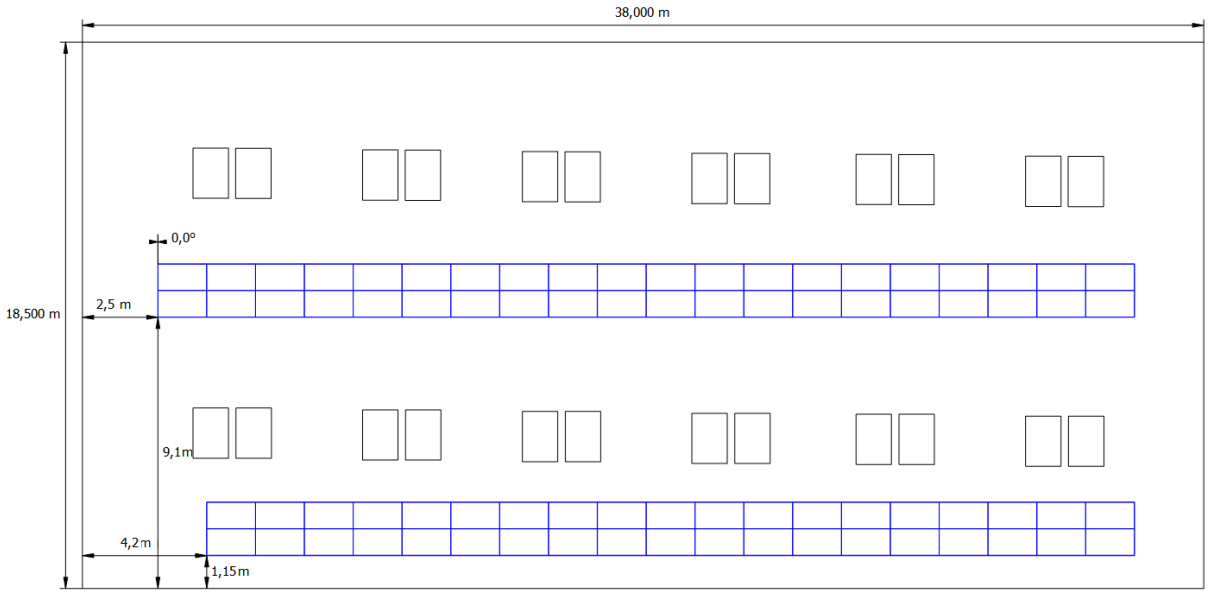

Figure A.3.2 Top view with dimensions of the PV system optimized for FIT

A.4 PV systems simple diagrams

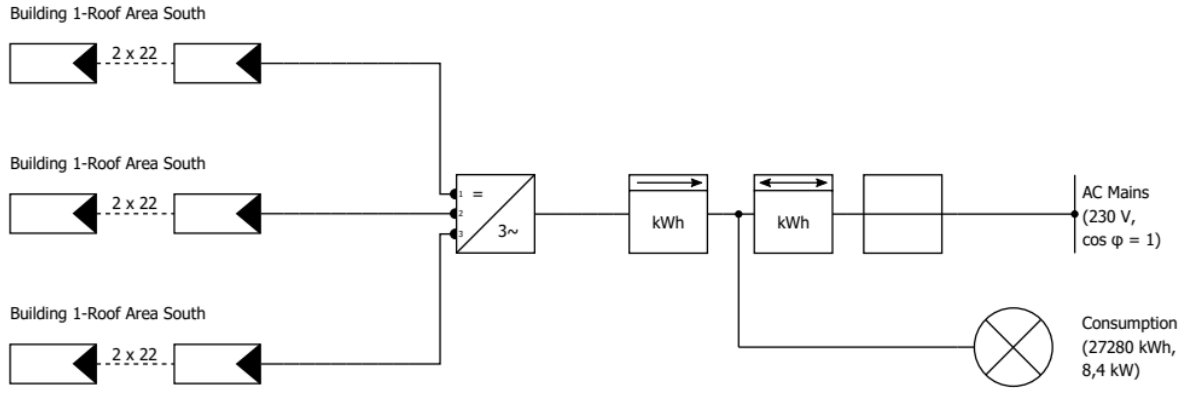

Figure A.4.1 Simple diagram of the PV system optimized for NM

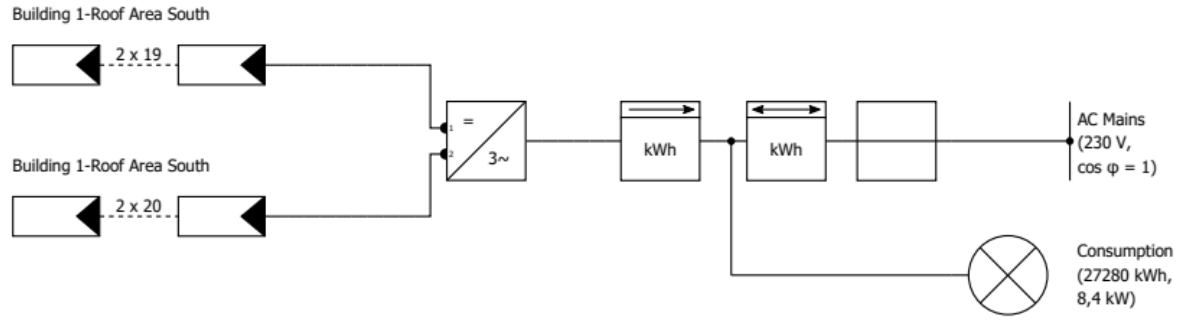

Figure A.4.2 Simple diagram of the PV system optimized for FIT